University of Cambridge
Department of Chemical Engineering and Biotechnology

Selective Cation-exchange Adsorption of the Two Major Whey Proteins

Mayyada El-Sayed
St. Edmund's College

A dissertation submitted for the degree of
Doctor of Philosophy
at the
University of Cambridge

supervised by
Prof. Howard Chase

January 2010

Summary

Whey is a by-product of cheese manufacture, containing a mixture of proteins of commercial value, each having unique attributes for nutritional, biological and food ingredient applications. A tremendous amount of whey, normally treated as a waste product, is produced worldwide each year. This work describes the cation-exchange adsorption of the two major whey proteins, alpha-lactalbumin (ALA) and beta-lactoglobulin (BLG) with the purpose of optimising a process for isolating them from whey. Adsorption of pure BLG and ALA was studied onto SP Sepharose FF using 0.1M acetate buffer. Batch experiments were carried out at various pH values for ALA and BLG, and the relevant Langmuir isotherm parameters, dissociation constant, K_d, and maximum binding capacity, q_m, were determined. The optimum pH for separation was chosen to be pH 3.7. At pH 3.7, both K_d and q_m pertaining to ALA were found to have higher numerical values than those of BLG, implying different characteristics of adsorption of the two proteins on this adsorbent. The K_d for the former protein was almost four times larger than the latter, while q_m was 1.3 times higher. Packed-bed column adsorption was performed using a 1-ml column at pH 3.7, flow rate 1 ml/min and initial concentration of 3 mg/ml for BLG and 1.5 mg/ml for ALA both in 0.1M sodium acetate buffer. The $t_{1/2}$ for the resulting ALA breakthrough was 75% longer than its BLG counterpart. The above results suggest the possibility of the occurrence of competitive adsorption between the proteins when adsorbed simultaneously.

In traditional batch uptake experiments, the kinetic rate constants of ALA and BLG in both the single- and two-component systems were determined using the simple kinetic model. The values so obtained implied that BLG was adsorbed faster than ALA. In the confocal laser scanning microscopy experiments, the different behaviour of ALA and BLG in the single-component system with regard to their penetration within the adsorbent beads suggested that the two proteins have different transport mechanisms governing their adsorption. The two-component system results showed that ALA was able to displace BLG in spite of the lower affinity of the former protein to the adsorbent.

The packed-bed adsorption and elution of a mixture of ALA and BLG were then investigated under the above conditions but using a 5-ml column. BLG breakthrough occurred first, and its concentration in the outlet exceeded its feed value by 1.6 fold before declining to the feed value, followed by the breakthrough of ALA. ALA displaced and eluted all the BLG from the column in a pure form. Pure ALA could then be eluted with good recovery. The single- and two-component breakthrough curves for ALA and BLG were simulated by the simple kinetic model using the isotherm parameters, but the overshoot phenomenon could only be predicted after correcting these parameters.

The evidence of the competitive nature of adsorption observed in binary mixtures was used to develop a facile separation procedure for the two proteins from aqueous solutions of whey concentrate powders. A novel consecutive two-stage separation process was developed to separate ALA and BLG from whey concentrate mixtures. Almost all the BLG in the feed was recovered, with 78% being recovered at 95% purity and a further 20% at 86% purity. In addition, 67% of ALA was recovered, 48% at 54% purity and 19% at 60% purity. The correction factors employed for the pure binary mixture were used to simulate the breakthrough curves of the two proteins in experiments conducted with whey concentrate in each of the two stages of the novel separation process, and there was agreement between the experimental and theoretical results.

Preface

The experimental work presented in this dissertation was carried out in the Department of Chemical Engineering, University of Cambridge between January 2006 and September 2009. The dissertation is a result of my own work and includes nothing which is the outcome of work done in collaboration. No part of the dissertation has been submitted for a degree to any other university. The entire length of the dissertation amounts to 48, 709 words, 15 tables and 70 figures.

Parts of the work in this dissertation were published:

- El-Sayed MMH, Chase HA. Toward separating alpha-lactalbumin and beta-lactoglobulin proteins from whey through cation-exchange adsorption, IAENG Transactions on Engineering Technologies Volume II, American Institute of Physics, New York 2009.
- El-Sayed MMH, Chase HA. Confocal microscopy study of uptake kinetics of alpha-lactalbumin and beta-lactoglobulin onto the cation-exchanger SP Sepharose FF. *J Separation Science* 32 (2009) 18, 3246-3256.
- El-Sayed MMH, Chase HA. Single and two-component cation-exchange adsorption of the two pure major whey proteins. *J Chromatography A* 1216 (2009) 50, 8705-8711.
- El-Sayed MMH, Chase HA. Purification of the two major proteins from whey concentrate using a cation-exchange selective adsorption process. *J Biotechnology Progress* 2009, doi: 10.1002/bp.316.
- El-Sayed MMH, Chase HA. Simulation of the breakthrough curves for the adsorption of alpha-lactalbumin and beta-lactoglobulin to SP Sepharose FF cation-exchanger. *J Biochemical Engineering* 2009, doi: 10.1016/j.bej.2009.12.017.

Some of the work was also presented in conferences:

- M.H.El-Sayed, H.A.Chase, "Ion-exchange adsorption of major whey proteins", book of abstracts, BioProcessUK, Cardiff, Wales, UK, 2007.
- M.H.El-Sayed, H.A.Chase, "Separation of the two major whey proteins using cation-exchange adsorption", WCECS proceedings, UC Berkley, California, US, 2008.
- M.H.El-Sayed, H.A.Chase, "Cation-exchange adsorption of major whey proteins", book of abstracts, PREP symposium, San Jose, California, US, 2008.
- M.H.El-Sayed, H.A.Chase, "Studies on cation-exchange adsorption of major whey proteins", book of abstracts, ISPPP symposium, Baden-Baden, Germany, 2008.
- M.H.El-Sayed, H.A.Chase, "Cation-exchange adsorption of the two major whey proteins", book of abstracts, SPICA symposium, ETH Zurich, Switzerland, 2008.

This four-year study was completely funded by the Egyptian government.

I'd like to take this opportunity to express my deep gratitude to my supervisor, Professor Howard Chase, for his valuable guidance, enlightening advice as well as support and encouragement throughout the course of my study.

Gratitude is due to Dr. Bart Hallmark at the Department of Chemical Engineering and Biotechnology for writing the computer simulation programme for the two-component packed-bed adsorption. Thanks are also due to Dr. Kam Yunus at the Department of Chemical Engineering and Biotechnology for his help in running the confocal microscopy experiments, and Penny Hamlyn from GE Healthcare, UK for her help in setting up the AKTA and FPLC chromatography systems.

I'd also like to thank all my fellow colleagues in 'Cambridge Unit for Bioscience and Engineering' (CUBE), for their support and cooperation. My thanks are also extended to the Electronics Office staff at the Department of Chemical Engineering and Biotechnology for their help in setting up the equipment.

Acknowledgment is also due to the Institute of Chemical Engineers (IChemE), Society of Chemistry and Industry (SCI), Cambridge Philosophical Society, BioProcess UK and St. Edmunds College, Cambridge for providing travel bursaries for attending conferences.

Table of Contents

List of tables

List of figures

Chapter 6

(from the first stage of the consecutive two-stage process) was applied onto an SP Sepharose FF column at pH 3.7 and flow rate 2 ml/min.

Figure 8.14 Size-exclusion analysis on Superdex 200 for the eluted ALA fractions that were collected from the first stage of the consecutive two-stage process and then further purified on a Superdex 200 size-exclusion column, (A) ALA fraction collected in the pH 5.2 eluate; (B) ALA fraction collected in the pH 7.0 eluate.

Figure 8.15 Electrophoretic patterns for the collected ALA peaks shown in Figure 8.14, lane 1: molecular mass marker; lane 2: ALA fraction collected from pH 5.2 eluate; lane 3: ALA fraction collected from pH 7.0 eluate. In this experiment, each well was loaded with 14μl of sample.

Figure 8.16 Flow diagram of the consecutive two-stage process.

Chapter 9

Figure 9.1 Predicted and experimental breakthrough curves for the adsorption of BLG onto a 5-ml packed-bed of SP Sepharose FF at pH 3.7, feed concentration of 3 mg/ml, flow rate of 2 ml/min, and temperature 20^{o}C, using k_1=35*10^{-3}mlmg^{-1}min^{-1}(A), and k_1=55*10^{-3}mlmg^{-1}min^{-1}(B).

Figure 9.2 Predicted and experimental breakthrough curves for the adsorption of ALA onto a 5-ml packed-bed of SP Sepharose FF at pH 3.7, feed concentration of 1.5 mg/ml, flow rate of 2 ml/min, and temperature 20^{o}C, and at flow rate of 2 ml/min using k_1=30*10^{-3}mlmg^{-1}min^{-1} and the equilibrium batch isotherm parameters (A), and after increasing q_m 1.5 times (B).

Figure 9.3 Experimental and predicted profiles for the packed-bed adsorption of a mixture of BLG and ALA onto SP Sepharose FF at pH 3.7, flow rate of 2 ml/min and feed concentrations of 3 and 1.5 mg/ml, respectively. The theoretical profiles were predicted after modifying BLG isotherm parameters such that q'_m = 3.5 (q_m) and K'_d = 600 (K_d).

Figure 9.4 Experimental and predicted profiles for the packed-bed adsorption of a mixture of BLG and ALA onto SP Sepharose FF at pH 3.7, flow rate of 2 ml/min and feed concentrations of 3 and 1.5 mg/ml, respectively. The theoretical profiles were predicted after modifying the isotherm parameters such that for BLG: q'_m = 3.0 (q_m) and K'_d = 600 (K_d), and for ALA: q'_m = 1.5 (q_m).

Figure 9.5 Experimental and predicted profiles for the packed-bed adsorption of BLG and ALA during the first (A) and second (B) stages of the whey purification process. The theoretical profiles were predicted after modifying the isotherm parameters such that for BLG: q'_m = 3.5 (q_m) and K'_d = 600 (K_d).

Figure 9.6 Experimental and predicted profiles for the packed-bed adsorption of BLG and ALA during the second stage of the whey purification process. The theoretical breakthrough curve for ALA was predicted using a modified value for k_1 (90*10^{-3} mlmg^{-1}min^{-1}).

Symbols and Abbreviations

ALA	alpha-lactalbumin
BLG	Beta-lactoglobulin
BSA	bovine serum albumin
CLSM	confocal laser scanning microscopy
DF	Diafiltration
FPLC	fast protein liquid chromatography
GMP	Glycomacropeptide
IEC	Ion-exchange chromatography
IEX	Ion-exchange
Ig	Immunoglobulin
MFGM	Milk fat globule membranes
pI	Iso-electric point
SEC	Size-exclusion chromatography
WP	whey protein powder
WPC	whey protein concentrate
WPI	whey protein isolate

A_A	absolute peak area of ALA, mAu.ml
A_B	absolute peak area of BLG, mAu.ml
A_{tot}	Total absolute peak areas of the two proteins, mAu.ml
C	Bulk fluid protein concentration, mg/ml
C_{AB}	total effluent concentration of ALA and BLG in binary and whey mixtures
C_c	concentration of protein in the collected peak, mg/ml
C_f	Feed bulk fluid protein concentration, mg/ml
C_i	initial concentration of protein in batch solution, mg/ml
C^*	soluble protein concentration at equilibrium, mg/ml
C_o	initial liquid phase batch uptake protein concentration, mg/ml
C	point protein concentration inside the pores, mg/ml
c_i	initial point protein concentration inside the pores, mg/ml
c_R	point protein concentration in equilibrium with q^*, mg/ml
D	effective pore diffusivity, m^2/s
D_{AB}	molecular diffusivity of the protein in free aqueous solution, m^2/s
D_e	dielectric constant of the medium
D_x	coefficient of axial dispersion along the column
ε	porosity of the adsorbent particles
F	Flow rate, ml/min
F_D	amount of feed, mg
F_{ring}	integral fluorescence within the ring, AU
F_s	integral fluorescence within the shell, AU
F^*	Equilibrium integral fluorescence within the shell, AU
k_1	traditional forward rate (adsorption) constant, $mlmg^{-1}min^{-1}$
k_{-1}	traditional backward rate (desorption) constant, min^{-1}

k_1'	confocal forward rate constant, $ml mg^{-1} min^{-1}$
K_d	dissociation constant for the protein-adsorbent interaction, mg/ml
M_A	relative molecular mass of the protein, kDa
q	concentration of protein adsorbed on the adsorbent at any time, mg/ml
q^*	adsorbed protein concentration at equilibrium, mg/ml
q_i	initial concentration of protein adsorbed on the adsorbent, mg/ml
q_m	maximum protein binding capacity of the ion exchanger, mg/ml
Q_{rel}	relative solid-phase capacity, AU/m^3
r_i	inner radius of the fluorescent ring, μm
r_o	outer radius of the fluorescent ring, μm
Δr	thickness of the fluorescent shell, μm
r_t	rate of batch uptake adsorption per volume of solution, $mg.min^{-1}ml^{-1}$
R	ratio of BLG to ALA in binary and whey mixtures
R_F	degree of saturation in terms of fluorescence intensity (F_s/F^*)
R_q	degree of saturation in terms of adsorption capacity (q/q^*)
S_A	slope of the ALA calibration curve, $mAu.ml^2mg^{-1}$
S_B	slope of the BLG calibration curve, $mAu.ml^2mg^{-1}$
$t_{1/2}$	time corresponding to half the maximum concentration ($0.5*C_f$), min
$t_{10\%brkthru}$	time corresponding to 10% of the maximum concentration, min
T	absolute temperature, K
V	volume of solution surrounding the adsorbent, ml
V_b	bead volume, ml
V_c	volume of collected peak, ml
V_f	volume of feed sample loaded onto the column, ml
V_L	volume of column, ml
V_s	volume of original solution before adding the adsorbent suspension
V_w	volume of fluid contained within the adsorbent suspension
v_L	linear velocity, cm/h
V	settled volume of the adsorbent, ml
W	amount of adsorbent, mg
X	distance along the column, m
Z	Charge
μ	viscosity of the protein solution, poise

1 Introduction

Opportunities for the commercial extraction of bioproducts from food waste streams are increasing. Future initiatives to improve the recovery of by-products require additional research to investigate possible uses for valuable waste-stream components and to develop cost-effective techniques for their recovery (Beszedits and Netzer, 1982). One example of a potential field for bioproduct recovery is the extraction of proteins from milk whey using chromatographic techniques (Conrado, 2005).

Whey is a liquid mixture composed of a variety of chemical compounds but are unfortunately present at low concentrations. Because of this, whey has long been considered a waste product of dairy operations rather than a by-product. This very fact has created the problem of utilising whey, a problem which can be further grasped by considering that in the manufacture of cheeses or casein products only 10 to 20% (w/w) of the raw milk is utilised to obtain the final product; 80 to 90% (w/w) of the raw milk yields whey as a waste product. Thus the problem of whey utilisation is that a tremendous amount of whey in the order of 150 million tonnes is produced worldwide each year and this whey is composed of very dilute concentrations of valuable proteins and other biochemicals. There are three main types of whey utilisation: animal feedstocks, lactose production and the production of whey powders and individual whey proteins (Sienkiewicz, 1990).

Whey protein powders (WP), well known for their nutritional value and versatile functional properties, are widely utilised in the food industry. The heterogeneous nature of WP preparations is typical of many commercial food protein preparations. For these products, the observed functionality is the sum of the functionality of individual proteins. The use of WP preparations, rather than the individual proteins, contributes to functional variability among commercially available whey proteins and can limit their applications (Morr and Ha, 1993; Mate and Krochta, 1994). Two main types of WP, whey concentrates which are purified varieties of whey that are concentrated up to a specified percentage of purity (< 90 % (w/w) protein) and whey isolates which are whey concentrate varieties of high purity (90 % (w/w) protein), are used as food additives in the production of a variety of baked goods, dairy products, meats, and beverages (Cayot

and Lorient, 1997). However, the lack of consistency in the gross composition and functionality of these products has limited their acceptance by the food processing industry (Morr and Ha, 1993). Commercial whey protein concentrates can also develop a stale off-flavour due to the presence of lipid and protein impurities (Morr and Ha, 1991). In addition, the unique nutritional, therapeutic, and functional characteristics of the individual whey proteins are largely unrealised in these whey products due to interactions between components and degradation during processing. There has thus been considerable commercial interest in the production of individual (purified) whey proteins with well-characterised functional and biological properties (Zydney, 1998). There is also an increasing need to produce individual whey proteins on a large scale without damaging protein structure or their functional properties.

The present study will focus on the two major whey proteins, alpha-lactalbumin (ALA) and beta-lactoglobulin (BLG), as they constitute in total 75% by weight of the total proteins in whey. In addition, each of these two proteins is of commercial value and has unique attributes for nutritional, biological and food ingredient applications. The uses and applications pertaining to each protein are discussed in detail in Chapter 2.

Several techniques have been proposed for the separation of individual whey proteins. These include selective precipitation, membrane separation and chromatographic techniques. Membrane filtration has proved difficult due to the relatively similar physicochemical properties of the different whey proteins. Good selective separation on the basis of size requires a large difference in molecular weight and would therefore be limited to separating only certain components of whey proteins (Goodall *et al.*, 2008). Chromatographic separation techniques are of singular importance to the biopharmaceutical industry because they can deliver high-purity products, are relatively easy to develop, and can readily be scaled from the laboratory scale to the desired production level (Lightfoot, 1999). Separating proteins on the basis of their isoelectric points gives two distinct groups, namely the major whey proteins: beta-lactoglobulin, bovine serum albumin and alpha-lactalbumin, which are negatively charged at the pH of rennet whey (pH 6.2 to 6.4); and minor whey proteins: lactoferrin and lactoperoxidase that carry a positive net charge at the pH of whey. These distinct properties offer the possibility of selectively separating the groups using ion exchange

chromatography. Ion exchange is probably the most frequently used chromatographic technique for the separation and purification of proteins. The reasons for the success of ion exchange in this regard are its widespread applicability, high resolving power (high selectivity), high capacity, and the simplicity and controllability of the method (Amersham Biosciences, 2001).

In search for a viable facile process for isolating and separating the two major whey proteins, alpha-lactalbumin (ALA) and beta-lactoglobulin (BLG), from whey, it was therefore decided to adopt the ion-exchange adsorption approach. As will be discussed later on, most of the whey purification work has been done using anion-exchange adsorption. Very few studies used cation-exchangers for separating whey proteins, particularly the two major ones. For whey proteins column chromatography, only selective elution has been used for separation by previous workers. Therefore, cation-exchange selective adsorption chromatography was selected for the purpose of this work. This implies that the two proteins must be in the form of cations. Hence, the working pH should be below the lower pI of the two proteins (pI for ALA is 4.2, and for BLG is 5.2). It will be shown that a working pH of 3.7 maximises the adsorption of both proteins. Adsorption took place on the strong cation-exchanger SP Sepharose FF. This type of adsorbent was chosen due to its excellent flow characteristics. It is characterised by having a high degree of cross-linking that greatly improves its physical and chemical stability at high flow rates. Therefore, it allows simple and conventional scale up so that the method established on a small-scale column can be applied more or less directly to the larger column. It is also optically transparent (Stone and Carta, 2007) which enables it to be used for confocal laser scanning microscopy studies.

Very few studies have been devoted to modelling of whey protein purification using adsorption chromatography, most of which were directed to investigating the adsorption of different whey proteins from raw whey solutions. To the best knowledge of the author, no work has been made on the adsorption of pure alpha-lactalbumin and beta-lactoglobulin (major whey components), which forms the underlying foundation for adsorption of whey mixtures as a whole. Understanding the nature of single-component adsorption would enable extension to the binary mixtures and, in turn, to whey mixtures.

Aim of work

The objective of the present work is to investigate the characteristics of the cation-exchange selective adsorption of the two pure major whey proteins, alpha-lactalbumin and beta-lactoglobulin, first as single-components and then in binary mixtures using modelling and simulation tools, with the purpose of developing and optimising a facile process of separating them from whey mixtures. As mentioned earlier, the cation-exchange selective adsorption has been selected because it was not previously used by other workers for whey protein column chromatography. The prime aim of studying the characteristics of adsorption in pure systems is to elucidate the nature of the adsorption process and understand the events underlying the separation of the two proteins, as well as to yield information that could be subsequently exploited in the development and simulation of the whey purification process.

In view of the above objectives, the results and discussion will be organised such that the equilibrium, kinetics and dynamics of adsorption are first studied using batch, batch uptake and packed-bed techniques before embarking on the whey purification process. Hence, the subsequent chapters of the thesis are to be found arranged as follows:

A) A background (Chapter 2) which includes an overview of whey regarding its composition, applications and methods used for its purification. The uses and commercial value of the proteins of interest, ALA and BLG, are discussed in detail. In addition, a background is given to the ion-exchange adsorption method which is the focus of the present study.

B) Theoretical (Chapter 3) which presents the theoretical basis of this work.

C) Experimental (Chapter 4) which discusses the experimental aspects of this work.

D) Equilibrium studies (Chapter 5) to construct the adsorption isotherm and hence obtain the equilibrium parameters, namely the maximum binding capacity of the adsorbent and the dissociation constant for the protein-adsorbent interaction.

E) Kinetic studies (Chapter 6) to determine the rate constant for the adsorption process. The studies will be conducted using the traditional method where the protein uptake profile is obtained indirectly by measuring the change in protein concentration in the bulk liquid phase, and by the direct confocal laser scanning

microscopy measurements where the penetration of the dye-conjugated protein within single adsorbent beads at different times during batch uptake could be visualised.

F) Packed-bed studies (Chapter 7) to obtain the breakthrough curves for the adsorption of pure ALA and BLG in both single- and two-component systems.

G) Chromatographic purification of whey concentrate (Chapter 8) to develop a novel selective adsorption process for isolating ALA and BLG.

H) Simulation of the breakthrough curves of ALA and BLG in pure systems and in whey (Chapter 9) to model the whey purification process.

I) Overall conclusions and outlook (Chapter 10).

It is to be noted that in each of chapters (5, 6, 7 8 and 9), a review of the literature pertinent to the topic under consideration is to be found at the beginning of the chapter; there is no separate chapter totally dedicated to an overall literature survey.

2 Background

2.1 Whey

2.1.1 What is whey?

Whey is a by-product of cheese and casein manufacture that contains about 63 g/l solids, of which 50 g/l is lactose and 6 g/l is protein (Bottomley *et al.*, 1990). It is a multicomponent protein mixture containing proteins of commercial value, each having unique attributes for nutritional, biological, and food ingredient applications (Smithers *et al.*, 1996). Dairy whey is characterised as the water-like liquid or serum that separates from the curds during cheese manufacturing (Kosikowski, 1979). There are two types of whey: sweet and acid. Acid whey is obtained from the manufacturing of cheese in which the caseins or principal milk proteins are removed from milk by precipitation at a pH of 4.6. The proteins and other compounds remaining in the water-like liquid at this pH have a specific composition and the whey is characterized as acidic. Sweet whey is produced when the caseins are enzymatically coagulated using rennet type enzymes at a pH of 5.9 to 6.3 (Dybing & Smith, 1991).

2.1.2 Whey composition

In general whey (sweet or acid) is a dilute solution composed of lactose, a variety of proteins, minerals, vitamins and fat. It contains about 6% (w/w) solids of which 70% (w/w) or more is lactose and about 0.7% (w/w) is proteins (Zall, 1984). These proteins are soluble at pH 4.6 and 20°C including beta-lactoglobulin (0.2-0.4%, w/v, milk), alpha-lactalbumin (0.060-0.17%, w/v, milk), bovine serum albumin (0.04%, w/v, milk) and immunoglobulins (0.040-0.09%, w/v, milk) (Eigel *et al.*, 1984). Minor proteins are also present: lactoferrin, lactoperoxidase, enzymes, protein components of the MFGM (milk fat globule membranes), proteose-peptone components and glycomacropeptide (only found in sweet whey) (Strange *et al.*, 1992). The composition of whey varies according to its production method. There are two types of whey: acid whey and sweet whey. Acid whey is obtained during the making of acid type of cheese such as cottage cheese and is produced by acid coagulation where bacterial cultures of lacto-bacillus are added to the

milk to produce lactic acid. Sweet whey, on the other hand, is manufactured during the making of rennet type hard cheese like cheddar or Swiss cheese and is produced by enzymatic coagulation where rennet (natural complex of enzymes produced in any mammalian stomach to digest the mother's milk) is added to the milk.

2.1.3 Whey protein concentrates and whey protein isolates

In the latest two decades, the evolution of separation technologies, *viz*. those relying on selective, porous membranes, have permitted a number of protein whey components to become widespread additives in food. Whey may indeed be subject to several treatments, thus giving rise to whey products with specific qualitative and quantitative profiles of proteins, minerals, lipids and sugars. The afore-mentioned membrane-based separation technologies include ultrafiltration (UF) to concentrate proteins, or diafiltration (DF) to remove most lactose, minerals and low molecular weight components – and thus produce whey protein concentrates (WPC). Depending on their concentration, there are WPC containing 35%, 50%, 65% and 80% (w/w) protein. When the threshold of 90% (w/w) protein is reached, a whey protein isolate (WPI) is accordingly obtained – which is a protein concentrate of high-quality and purity. Both those products are used as vectors for the promotion of many biological properties (cf. p.8-9) upon addition to foods (Huffman and Harper, 1999).

2.1.4 Individual whey proteins

Table 2.1 shows the composition of the different proteins present in bovine whey together with their isoelectric points and molecular weights of their monomeric subunits.

Table 2.1 Physical characteristics of individual whey proteins (Wong *et al.*, 1996; Cayot and Lorient, 1997).

Protein	Concentration (g/L)	Molecular weight (g/mol)	Isoelectric pH
β-Lactoglobulin (monomer)	2.7	18,362	5.2
α-Lactalbumin	1.2	14,147	4.5–4.8 *
Immunoglobulins	0.65	150,000–1,000,000	5.5–8.3
Bovine serum albumin	0.4	69,000	4.7–4.9
Lactoferrin	0.1	78,000	9.0
Lactoperoxidase	0.02	89,000	9.5
Glycomacropeptide		7000	

* has been also cited as 4.2-4.5 (Gerberding and Byers, 1998). It has to be noted that whey also contains some residual casein whose amount depends on the method of whey storage.

Whey proteins are classified into major and minor proteins.

2.1.4.1 Major whey proteins

2.1.4.1.1 Beta Lactoglobulin (BLG)

Beta-Lactoglobulin is quantitatively the dominant whey protein (58% (w/w)), and was first discovered in 1934 (Madureira *et al.*, 2007). BLG is the major whey protein of cow's milk (~3 g/l), and is also present in many other mammalian species; a notable exception being humans'. When in isolated form, it exhibits a low solubility (despite its globular nature) and a low ionic strength. Synthesised in the mammary gland of ruminants (and other species) and present in milk, this protein has several genetic variants – of which BLG A is the most common (Eigel *et al.*, 1984). Bovine BLG is a small soluble protein that normally exists as a dimer of subunit molecular mass around 18,400 Da. It dissociates to a momomer below about pH 3. Each monomer comprises 162 amino acid residues, with one free cysteine residue and two disulphide bridges. Nevertheless, its native 3D-configuration (Figure 2.1) remains fairly intact at lower pH values, as determined using NMR (Sawyer & Kontopidis, 2000; Uhrinova *et al.*, 2000).

BLG solutions form gels in various conditions when the native structure is sufficiently destabilised to allow aggregation (Bromley *et al.*, 2005). Under prolonged heating at low pH and low ionic strength, a transparent 'fine-stranded' gel is formed, in which the protein molecules assemble into long stiff fibres. BLG is a better foam stabilizer than the other whey proteins, and can be used in the production of confectioneries (Cayot and Lorient, 1997).

BLG plays a role in transfer of passive immunity to the newborn, and in regulation of phosphorus metabolism in the mammary gland (Farrell *et al.*, 1987). The amino acid content of this protein is rather important, because – besides fueling muscle growth – it is a source rich in the essential amino acid cysteine, which is important for synthesis of Glutathione (GSH) antioxidant which protects cells from toxins such as free-radicals (de Wit, 1998).

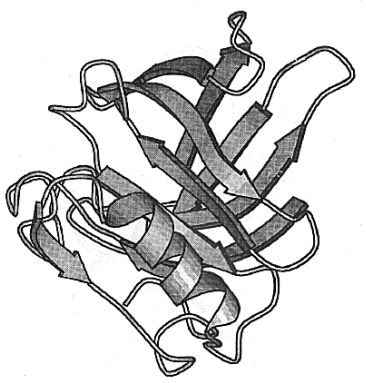

Figure 2.1 Three dimensional structure of beta-lactoglobulin, reproduced from Swaisgood (1996).

2.1.4.1.2 Alpha Lactalbumin(ALA)

Alpha-Lactalbumin is the second major whey protein in cow's milk (~1 g/l) representing about 20% (w/w) of the total whey protein, and is fully synthesized in the mammary gland. It is also present in many other mammalian species. Its molecular weight is 14, 176 Da and it contains 123 amino acid residues with a sequence quite homologous to that of lysozyme. Three genetic variants have already been identified – A, B and C (Fox, 1989). One of the main structural differences with beta-lactoglobulin is that it does not have any free thiol group that can serve as the starting point for a covalent aggregation reaction. As a result, pure ALA will not form gels upon denaturation and acidification (Figure 2.2).

ALA provides an important source of energy for the newborn (de Wit, 1998) and therefore is used in infant formula. It is also used as a nutraceutical (functional food) because of its high tryptophan content. In addition, ALA provides enhanced whippability in meringue-like formulations (Pearce, 1992). The protein was found to have strong affinity for glycosylated receptors on the surface of oocytes and spermatozoids and thus

may have a potential as a contraceptive agent (Maubois and Ollivier, 1997). ALA also contributes to reduce the risk of incidence of some cancers as it constrains cell division, when incubated in distinct mammalian intestinal cell lines (Ganjam *et al.*, 1997).

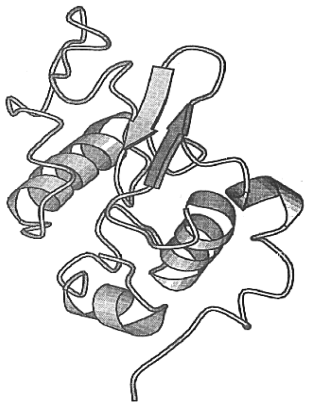

Figure 2.2 Three-dimensional structure of alpha-lactalbumin, Swaisgood (1996).

2.1.4.1.3 Bovine serum albumin (BSA)

Bovine serum albumin is of interest in a number of food and therapeutic applications. It is used as a nutrient in cell and microbial culture. It is also used to stabilise some enzymes during digestion of DNA and to prevent adhesion of the enzyme to reaction tubes and other vessels.

2.1.4.1.4 Bovine Immunoglobulins (Ig)

Immunoglobulins can enhance the immunological properties of infant formula and they can be used therapeutically in the treatment of animal neonates (Zydney, 1998).

2.1.4.2 Minor whey proteins

Whey also contains many proteins present at relatively low concentrations but with important biological activity. Lactoferrin and lactoperoxidase both have strong antibacterial activity and can be used in the development of improved infant formula, "therapeutic"cosmetics, and mouthwash solutions. Lactoferrin also enhances iron absorption in infant formula. In addition, a variety of biologically active peptides with interesting anti-opioid and anti-thrombotic activity can be produced from lactoferrin. Glycomacropeptide (GMP) is a peptide fragment produced by enzymatic cleavage of κ-casein by chymosin. GMP is highly soluble in water and thus remains in the whey

fraction after coagulation of the milk. GMP has been examined for improved lipid digestion, protection against influenza, prevention of tartar adhesion to teeth, and inhibition of *E.coli* attachment to intestinal walls (Maubois and Ollivier, 1997). Whey also contains numerous growth factors, hormones, and a variety of enzymes, many of which have biological activity (Zydney, 1998).

2.1.5 Whey purification

2.1.5.1 Available processes for separation

Several processes have been proposed for commercial-scale production of whey protein fractions. These processes fall into three main categories: (1) **selective precipitation;** (2) **membrane filtration**; and (3) **selective adsorption or selective elution**. Precipitation and membrane separation processes are volume-dependent separation methods, wherein the equipment capacity and cost of manufacture is proportional to the volume of solution processed and not to the mass of product produced. For dilute protein solutions such as whey, large volumes of liquid must be processed to recover a fixed mass of protein. Selective adsorption processes are less volume dependent because adsorbent capacity depends mostly on the mass of protein recovered, not the volume of liquid processed (Doultani *et al.*, 2004), as well as the concentration of the adsorbed species. The following review will be confined to the third type of processes as they are the main interest of this study.

Selective adsorption or selective elution processes include ion exchange chromatography in which polyvalent, charged proteins bind to appropriately charged ion exchangers; affinity chromatography which exploits the specific recognition interactions that can occur between proteins and immobilised ligands; and a more general class normally referred to simply as adsorption chromatography where the mechanism of adsorption is often uncertain. Examples of the latter class include the use of hydroxyapatite where adsorption is due to hydrophilic interactions, and other non-charged adsorbents where hydrophobic interactions are implicated in the adsorption process.

There are many examples of selective adsorption and selective elution processes for whey proteins. In case of *affinity chromatography*, Gurgel *et al.* (2000) used the

immobilized hexapeptide, WHWRKR, for ALA adsorption, while Gambero *et al.* (1997) separated the same protein from bovine milk whey using chemically modified silica with β-Diketoamine groups. For BLG adsorption, Wang and Swaisgood (1993), Noppe *et al.* (1998) and Vyas *et al.* (2002) used immobilised retinal. Puerta *et al.* (2002) studied the adsorption kinetics of beta-lactoglobulin on a polyclonal immunochromatographic support. Konecny *et al.* (1994) used thiophilic chromatography on a T-gel to purify IgG from sweet cheese whey and found this method suitable for large-scale whey IgG isolation.

Using *hydrophobic chromatography*, Chaplin (1986) separated bovine whey proteins and caseins on a fast protein liquid chromatography column, phenyl-superose; Hahn *et al.* (2003) compared different hydrophobic interaction media regarding dynamic binding capacity, recovery and mass transfer properties; and Conrado *et al.* (2005) described the operating parameters related to the use of Streamline®phenyl for the recovery of ALA from cow-milk whey in an expanded-bed adsorption mode of operation using a theoretical model.

Being the focus of this study, ion-exchange chromatography will thus be discussed in more detail in the following subsection. However, the whey purification processes pertaining thereto will be dealt with in a forthcoming chapter dedicated to this topic (cf. Chapter 8).

2.2 Ion-exchange chromatography (IEC)

2.2.1 Historical Background

Separation and purification operations with ion exchange resins involve the reversible interchange of ions between a functionalized insoluble resin (the ion-exchange material) and an ionisable substance in solution (Dechow, 1989). While Thompson (Cuatrecasas *et al*., 1968) reported in 1850 the first ion exchange applications which used naturally-occuring clays, ion exchange resins have only been used in biochemical and fermentation product recovery for the last few decades (Parikh and Cuatrecasas, 1985; Lowe, 1979). In these early studies, biochemicals such as adenosine triphosphate (Scouten, 1981), alcohols (Larson *et al.*, 1983), alkaloids (Colowick *et al.*, 1984), amino

acids (Chaiken *et al.*, 1984), growth regulators (Nishikawa, 1975), hormones (Graves and Wu, 1974), nicotine (Nishikawa *et al.*, 1974), penicillin (Lowe, 1984), and vitamin B-12 (Bottomley *et al.*, 1976) were purified using ion exchange resins.

Ion exchange applications intensified following the work of Moore and Stein (Van Deemter *et al.*, 1956) which showed how very complex mixtures of biochemicals, in this case amino acids and amino acid residues, could be isolated from each other using the ion exchange resin as a column chromatographic separator.

In biotechnology applications, ion exchangers are important in preparing water of the necessary quality to enhance the desired micro-organism activity during fermentation. In downstream processing, ion exchange resins are used to convert, isolate, purify or concentrate the desired product or by-products (Dechow, 1989).

Ionic interactions as the basis for separation and purification of proteins by ion-exchange chromatography have been applied successfully since the late 1940s (Janson and Ryden, 1998). Ion exchange adsorbents have found widespread use in the purification of proteins, both in the laboratory and in the production plant, since the introduction in 1956 of the first ion exchanger specifically designed for proteins (Peterson and Sobers, 1956). This has been highlighted in a study by Bonnerjea *et al.* (1986) which showed that ion exchangers were used in 75% of all the published purification protocols that they examined.

Reasons for the popularity of IEC include its (1) high resolving power, (2) high protein-binding capacity, (3) versatility (there are several types of ion exchangers, and the composition of the buffer and pH can be varied over a wide range), straight forward separation principle (primarily according to differences in charge), and (5) ease of performance (Janson and Ryden, 1998), in addition to relative cheapness and their acceptance by the regulatory authorities in the production of pharmaceutical proteins. This is in contrast to affinity adsorbents which, although they result in good resolution, are limited to one protein or group of proteins, are expensive and their use may be questioned by regulatory bodies (Skidmore and Chase, 1990).

2.2.2 Theory and principles

Separation in ion exchange chromatography depends upon the reversible adsorption of charged solute molecules to immobilised ion exchange groups of opposite charge (Amersham Biosciences, 2001), i.e. IEC separates molecules on the basis of differences in their *net surface charge*. Molecules vary considerably in their charge properties and will exhibit different degrees of interaction with charged adsorbents according to differences in their overall charge, charge density and surface charge distribution. These interactions can be controlled by varying conditions such as ionic strength and pH. The differences in charge properties of biological compounds are often considerable, and since ion exchange chromatography is capable of separating species with very minor differences in properties, e.g. two proteins differing by only one charged amino acid, it is a very powerful separation technique.

In ion exchange chromatography one can choose whether to bind the substances of interest and allow the contaminants to pass through the column, or to bind the contaminants and allow the substance of interest to pass through. Generally, the first method is more useful since it allows a greater degree of fractionation and concentrates the substances of interest.

IEC takes advantage of the fact that the relationship between net surface charge and pH is unique for a specific protein. In an ion-exchange (IEX) separation, *reversible interactions* between *charged* molecules and *oppositely charged* ion-exchange media are controlled in order to favour binding or elution of specific molecules and achieve separation. A protein that has no net charge at a pH equivalent to its *isoelectric point (pI)* will not interact with a charged medium. However, at a pH above its isoelectric point, a protein will be negatively charged and therefore will bind to a positively charged medium or *anion exchanger* and, at a pH below its pI, a protein will bind to a negatively charged medium or *cation exchanger*. In addition to the ion exchange interaction, other types of binding may occur, but these effects are very small and are mainly due to van der Waals forces and non-polar interactions (Amersham Biosciences, 2004).

2.2.3 IEX in practice: Steps in IEX separation

Most ion exchange experiments are performed in five main stages. These steps are illustrated schematically below (Figure 2.3).

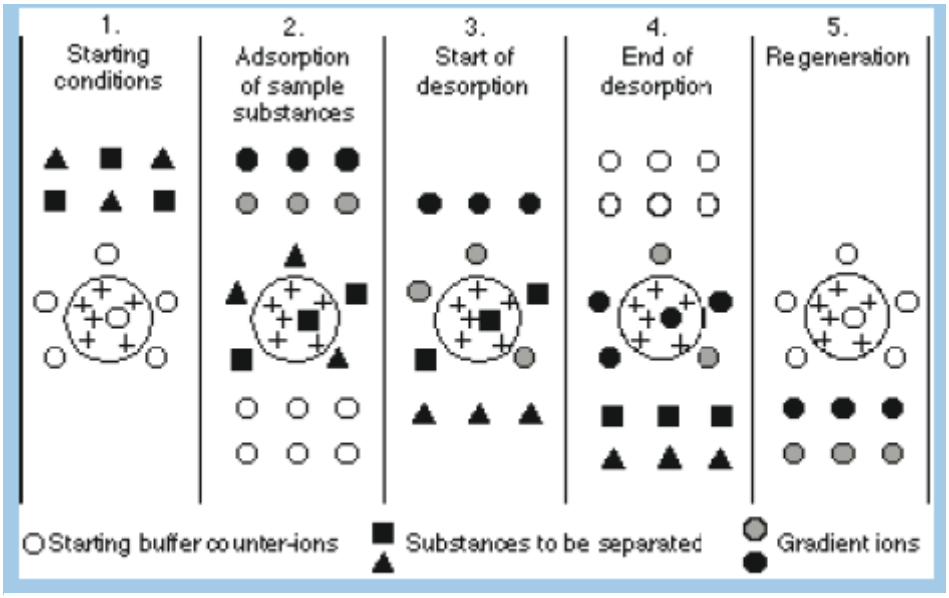

Figure 2.3 Steps of ion-exchange chromatography (Amersham Biosciences, 2001).

The first stage is equilibration in which the ion exchanger is brought to a starting state, in terms of pH and ionic strength, which allows the binding of the desired solute molecules. The exchanger groups are associated at this time with exchangeable counter-ions (usually simple anions or cations, such as chloride or sodium).

The second stage is sample application and adsorption, in which solute molecules carrying the appropriate charge displace counter-ions and bind reversibly to the gel. Unbound substances can be washed out from the exchanger bed using starting buffer.

In the third stage, substances are removed from the column by changing to elution conditions unfavourable for ionic bonding of the solute molecules. This normally involves increasing the ionic strength of the eluting buffer or changing its pH. In Figure 2.3, desorption is achieved by the introduction of an increasing salt concentration gradient and solute molecules are released from the column in the order of their strengths of binding, the most weakly bound substances being eluted first.

The fourth and fifth stages are the removal from the column of substances not eluted under the previous experimental conditions and re-equilibration at the starting conditions for the next purification (Amersham Biosciences, 2001).

2.2.4 The adsorbent (Ion-exchanger)

Ion-exchange media include porous or non-porous matrices, chosen for their physical stability, their chemical resistance to stringent cleaning conditions and their low level of non-specific interaction. The matrices are substituted with functional groups that determine the charge of the medium (Amersham Biosciences, 2004).

2.2.4.1 The matrix

An ion exchanger consists of an insoluble matrix to which charged groups have been covalently bound. The charged groups are associated with mobile counterions. These counter-ions can be reversibly exchanged with other ions of the same charge without altering the matrix.

It is possible to have both positively and negatively charged exchangers (Figure 2.4). Positively charged exchangers have negatively charged counter-ions (anions) available for exchange and are called anion exchangers. Negatively charged exchangers have positively charged counter-ions (cations) and are termed cation exchangers.

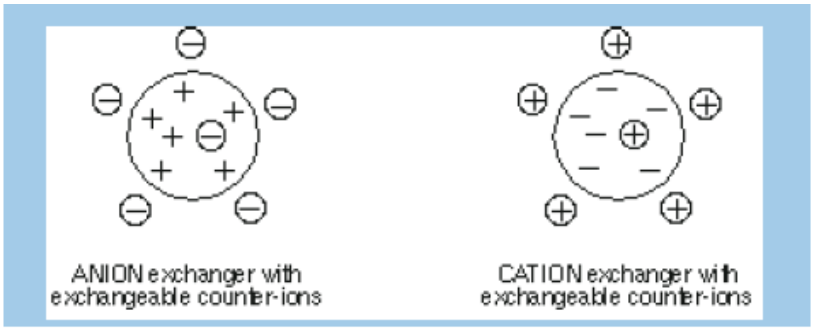

Figure 2.4 Ion-exchanger types (Amersham Biosciences, 2001).

The matrix may be based on inorganic compounds, synthetic resins or polysaccharides. The characteristics of the matrix determine its chromatographic properties such as efficiency, capacity and recovery as well as its chemical stability, mechanical strength and flow properties. The nature of the matrix will also affect its

behaviour towards biological substances and the maintenance of biological activity (Amersham Biosciences, 2001).

Modern ion-exchange media use either polymer or agarose-based matrices to fulfil not only the requirements for high binding capacity as well as chemical and physical stability, but also to generate media with suitable particle sizes for a range of applications (Table 2.2) (Amersham Biosciences, 2004).

Table 2.2 Ion-exchange matrices (Amersham Biosciences, 2004).

	Form	Mean particle size
MiniBeads™	Polystyrene/divinyl benzene	3 µm
MonoBeads™	Polystyrene/divinyl benzene	10 µm
SOURCE 15	Polystyrene/divinyl benzene	15 µm
SOURCE 30	Polystyrene/divinyl benzene	30 µm
Sepharose High Performance	Agarose 6%	34 µm
Sepharose Fast Flow	Agarose 6%	90 µm
Sepharose 4 Fast Flow	Agarose 4%	90 µm
Sepharose XL	Agarose 6%, dextran chains coupled to agarose	90 µm
Sepharose Big Beads	Agarose 6%	200 µm

The second column in the table represents the structure of the adsorbent matrix and the agarose content is expressed in terms of (w/v) %.

2.2.4.2 Functional (charged) groups

The presence of charged groups is a fundamental property of an ion exchanger. The type of group determines the type (in terms of charge of an IEX medium; i.e. a positively-charged anion exchanger or a negatively-charged cation exchanger) and strength of the ion exchanger; while their total number and availability determines the capacity. There is a variety of functional groups which have been chosen for use in ion exchangers; some of these are shown in Table 2.3.

Table 2.3 Functional groups used on ion-exchangers (Amersham Biosciences, 2001).

Anion exchangers		Functional group
Quaternary ammonium (Q)	strong	$-O-CH_2N^+(CH_3)_3$
Diethylaminoethyl (DEAE)*	weak	$-O-CH_2CH_2N^+H(CH_2CH_3)_2$
Diethylaminopropyl (ANX)*	weak	$-O-CH_2CHOHCH_2N^+H(CH_2CH_3)_2$
Cation exchangers		**Functional group**
Sulfopropyl (SP)	strong	$-O-CH_2CHOHCH_2OCH_2CH_2CH_2SO_3^-$
Methyl sulfonate (S)	strong	$-O-CH_2CHOHCH_2OCH_2CHOHCH_2SO_3^-$
Carboxymethyl (CM)	weak	$-O-CH_2COO^-$

Sulphonic and quaternary amino groups are used to form strong ion exchangers; the other groups form weak ion exchangers (as shown in the second column of Table 2.3). The terms strong and weak refer to the extent of variation of ionization with pH and not the strength of binding. Strong ion exchangers are completely ionized over a wide pH range whereas with weak ion exchangers, the degree of dissociation and thus exchange capacity varies much more markedly with pH (Amersham Biosciences, 2001).

There are several advantages to working with strong ion exchangers:

• development and optimisation of separations is fast and easy since the charge characteristics of the medium do not change with pH.

• the mechanism of interaction is simple since there are no intermediate forms of charge interaction.

• sample loading (binding) capacity is maintained at high or low pH since there is no loss of charge from the ion exchanger (Amersham Biosciences, 2004).

Due to their excellent flow characteristics, Sepharose fast flow ion-exchangers were used in the present work, and are therefore described further below.

2.2.4.3 Sepharose Fast Flow ion exchangers

Sepharose Fast Flow ion exchangers are based on 90 μm agarose beads with a high degree of cross-linking that is used to give the media greatly improved physical and chemical stability. This high stability allows the gels to be used at the higher flow rates required for modern laboratory separations as well as meeting the throughput and cleaning-in-place requirements of process scale chromatography. To give a complete range of ion exchange media Sepharose Fast Flow is available with the weak exchanger

groups, DEAE and CM and the strong exchanger groups Q and SP. Figure 2.5 shows the partial structures of these media.

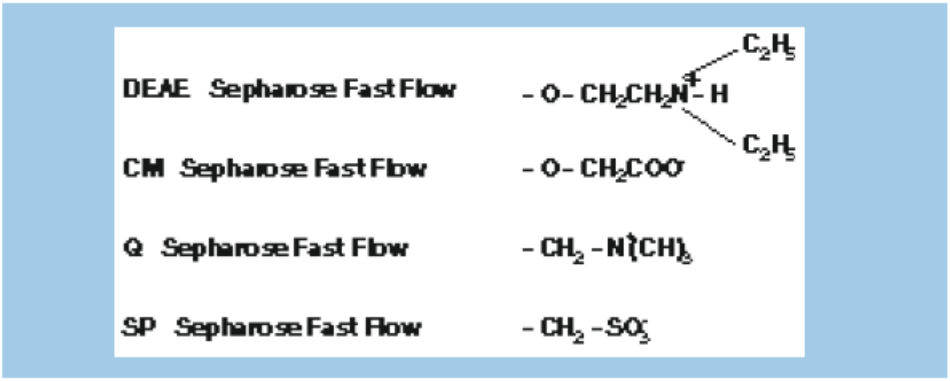

Figure 2.5 Functional groups on different Sepharose Fast Flow ion exchange media (Amersham Biosciences, 2001).

Characteristics of the different ion exchangers based on Sepharose Fast Flow are listed in Table 2.4.

Table 2.4 Characteristics of Q, SP, DEAE and CM Sepharose Fast Flow (Amersham Biosciences, 2001).

Product	Q Sepharose Fast Flow	SP Sepharose Fast Flow	DEAE Sepharose Fast Flow	CM Sepharose Fast Flow
Type of gel	strong anion	strong cation	weak anion	weak cation
Total ionic capacity (µmol/ml gel)	180-250	180-250	110-160	90-130
Recommended working flow rate range (cm/h)	100-300	100-300	100-300	100-300
Approx. mean particle size (µm)	90	90	90	90
Particle size range (µm)	45-165	45-165	45-165	45-165
working pH range*	2-12	4-13	2-9	6-10
pH stability**				
short term	1-14	3-14	1-14	2-14
long term	2-12	4-13	2-13	4-13

* working pH range refers to the pH range over which the ion exchange groups remain charged and maintain consistently high capacity.
** pH stability, long term refers to the pH interval where the gel is stable over a long period of time without adverse effects on its subsequent chromatographic performance.
pH stability, short term refers to the pH interval for regeneration and cleaning procedures.

2.2.4.3.1 Properties

Physical stability

Sepharose Fast Flow ion exchangers are supplied either pre-swollen and ready for packing in a column or already in pre-packed columns. The highly cross-linked nature of the matrix means that the bead size and bed volumes do not change with changes in ionic strength or pH.

Binding Capacity

As is the case with all ion exchangers the capacity is dependent upon the accessibility of the charged groups and their number. Sepharose Fast Flow ion exchangers are highly substituted and have an exclusion limit of approximately 4 x 10^6 giving high capacity for proteins. Q Sepharose Fast Flow and SP Sepharose Fast Flow are highly substituted with strong ion exchange groups. These groups remain charged and maintain consistently high capacities over broad working pH ranges of 2-12 and 4-13 respectively. This allows the selection of a pH value and buffer that best suit the properties of the sample (Amersham Biosciences, 2001).

It is to be noted that throughout this study, the strong cation exchanger SP Sepharose FF will be used for reasons that were discussed above. An electron microscopy image of SP Sepharose FF beads is shown in Figure 2.5. The beads are all regular in shape and the adsorbent has an open structure (Staby *et al.*, 2005).

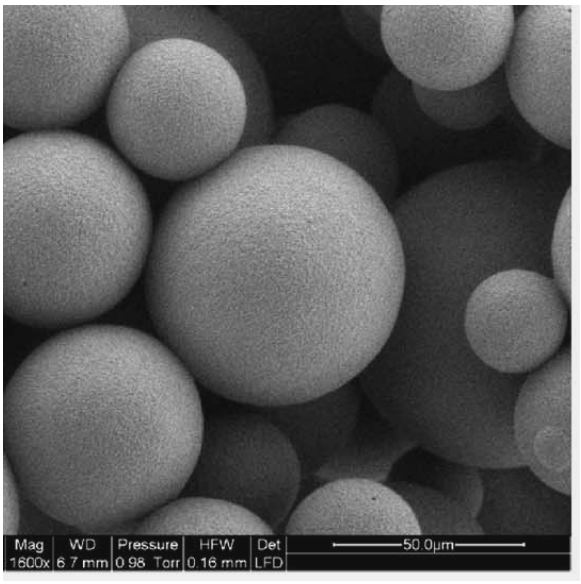

Figure 2.6 Scanning electron microscopy image of SP Sepharose FF beads (reproduced from Staby *et al.*, 2005).The magnification is 1600x.

2.2.5 Factors affecting IEX separation

The interaction between small molecules and ion exchanger depends on the net charge and the ionic strength of the medium. When the concentration of competing ions is low, the ions of interest bind to the ion exchanger, whereas when it is high, they are desorbed. The interaction between a protein and an ion exchanger depends not only on the net charge and the ionic strength, but also on the surface charge distribution of the protein, pH, the nature of particular ions in the solvent, additives such as organic solvents, and properties of the ion exchanger.

The interaction I between two charges Z_a and Z_b separated by a distance r is given by Coulomb's law,

$$I = Z_a Z_b / D_e r^2 \qquad (2.1)$$

where,

D_e = dielectric constant of the medium

From the above equation, it is thus clear that the more charged a protein is, the more strongly it will bind to a given oppositely charged ion exchanger. Similarly, more highly charged ion exchangers (i.e., those with a higher degree of substitution with charged groups) usually bind proteins more effectively than weakly charged ones. Conditions, for

example, pH, that alter the charge on either the protein or the ion exchanger will affect their interaction and may be used to influence the ion-exchange process (Janson and Ryden, 1998).

2.2.5.1 The pH parameter

The pH is one of the most important parameters in determining protein binding, as it determines the charge on both the protein and the ion exchanger.

Since all molecules with ionisable groups can be titrated, their net surface charge is highly pH dependent. In the case of proteins, which are built up of many different amino acids containing weak acidic and basic groups, their net surface charge will change gradually as the pH of the environment changes i.e. proteins are *amphoteric*. Each protein has its own unique *net charge versus pH relationship* which can be visualised as a *titration curve* (Figure 2.7). This curve reflects how the overall net charge of the protein changes according to the pH of the surroundings.

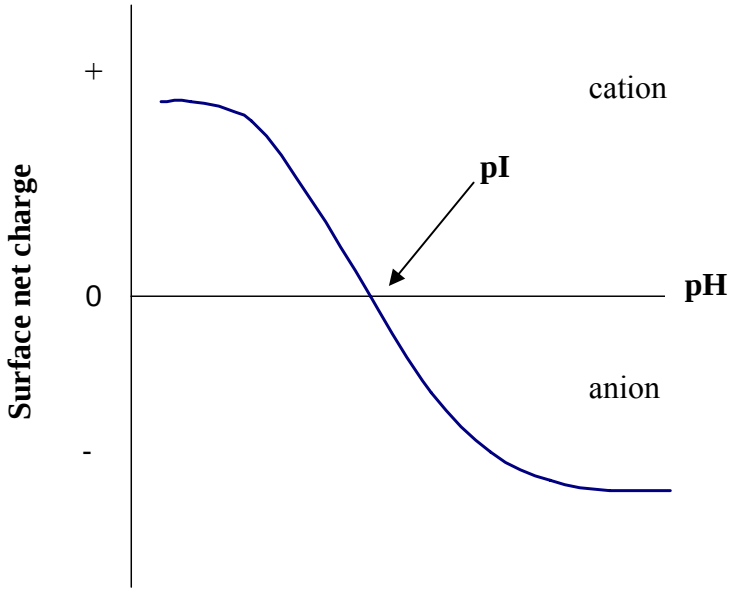

Figure 2.7 Theoretical protein titration curve, showing how net surface charge varies with pH.

As one of the most important steps of chromatography as well as being the focus of our study, adsorption including equilibrium, kinetics and different techniques will be further discussed in more detail in the forthcoming chapters.

2.2.6 Modelling chromatography

The first theoretical models of chromatography are dated back to the late 1930s and early 1940s. The pioneering works [Wicke and Kolloid, 1940; Wilson, 1940; De Vault, 1943; Martin and Synge, 1941; Martin and James, 1952; Craig, 1944] began with approaches aiming to develop and improve understanding of chromatography.

Linear kinetic rate constant model was first used by Wilson, 1940; Weiss, 1943; and De Vault, 1943 extended this model to nonlinear chromatography. Any hydrodynamic dispersion or mass transfer effects are neglected in this model. Earlier, Bohart and Adams (1920) derived equations for the film and pore diffusion model, but it does not seem that they attempted any calculations based on this model. Wicke and Kolloid (1939, 1940) derived the same model equation and discussed its application to gas chromatography on activated charcoal. The model has no analytical solutions. It was only around 1987 that the calculation of the band profiles of single compounds and binary mixtures began to become accessible [Guiochon *et al*., 1988].

Models for predicting the performance of chromatographic adsorption have been initially developed for nonporous adsorbent particles so that the intraparticle diffusion mass transfer mechanisms need not be considered in the kinetics of adsorption. Thus the mathematical complexity in solving the model equations are partly eliminated (Liapis et al., 1989; Mao et al., 1991). Other adsorption models for porous particles are based mostly on rate theories which considered only one rate limiting step; i.e. either rate of interaction or rate of diffusion (pore or film) as controlling the overall adsorption mechanism (Chase, 1984; Arnold *et al.*, 1985; Liapis *et al.*, 1989; Mao *et al.*, 1991; Finette *et al.*, 1998). Arve and Liapis (1988), on the other hand, have developed a sophisticated model for biospecific affinity chromatography considering three rate controlling mechanisms simultaneously, two for film and pore diffusion mass transfer mechanisms and one for the interaction between adsorbate and adsorbent. Hortsmann and Chase (1998) used this model to describe the adsorption kinetics of a series of paraquat-protein conjugates to an immunosorbent consisting of monoclonal anti-paraquat antibodies covalently immobilised to Sepharose 4B.

In general, two main models were proposed for the adsorption of proteins; namely the simple ‘kinetic rate constant’ model which is based on a single lumped kinetic

parameter, and the more rigorous 'pore-diffusion' model which considers the individual transport processes occurring prior to the adsorption reaction, that is taking into account diffusion across the liquid film surrounding individual particles and also the diffusion within the ion-exchanger particle itself. The literature pertaining to the use of these models in describing the ion-exchange adsorption will be reviewed in detail in the following chapters.

3 Theoretical

3.1 Adsorption equilibrium

3.1.1 Single-component systems

Chromatography and adsorption work by the differential adsorption of species to an adsorbent surface, or ligands, from a complex chemical mixture. The adsorption of a chemical species can be represented by the equilibrium reaction

$$A + S \underset{}{\overset{K_{eq}}{\longleftrightarrow}} AS \tag{3.1}$$

where A is the dissolved chemical species, S is an adsorption site, AS is the chemical bound to the site, and K_{eq} is the equilibrium constant governing the association reaction. The equilibrium constant for this adsorption is

$$K_{eq} = \frac{[AS]}{[A][S]} \tag{3.2}$$

Three assumptions are inherent in this representation of the adsorption reaction. Firstly, it is completely reversible, and the chemical's interaction with the adsorption site causes no alteration in its solution properties or solution state. Secondly, chemicals bind to sites in a one-to-one fashion, and they bind only to sites. In other words, the binding is "specific," and there is no "non-specific" binding, or interaction between molecules and the surface. Thirdly, there is only one mode of binding to the site; all binding is equal and is described by a single value for K_{eq}. Despite these limiting assumptions, this "site model" of adsorption still serves as a very accurate description of adsorption in liquid chromatography.

The most efficient operation uses all the adsorption sites available. In this case, the concentration of the empty adsorption sites available cannot be ignored. The

concentration of unoccupied sites is not readily measurable, but the total number of sites is

$$S_{\mathbf{tot}} \longleftrightarrow [AS] + [S] \qquad \mathbf{(3.3)}$$

where S_{tot} is the total site concentration. Combining the general expression for K_{eq}, Eq. (3.2) with Eq. (3.3) for S_{tot} gives

$$[AS] = \frac{K_{eq} S_{tot}[A]}{1 + K_{eq}[A]} \qquad \mathbf{(3.4)}$$

the well-known ***Langmuir* isotherm.** It is to be noted that in the following discussions [*A*], [AS], S_{tot} and ($1/K_{eq}$) will be referred to as C^* (the soluble protein concentration at equilibrium), q^* (the adsorbed protein concentration at equilibrium), q_m (the maximum protein binding capacity of the ion exchanger) and K_d (the dissociation or desorption constant for the protein-adsorption interaction and is equal to the reciprocal of the association constant $K_{adsorption}$), respectively. Since the Langmuir isotherm has often been used to correlate equilibrium adsorption data for proteins (Belter *et al.*, 1988; Leaver, 1984; Chase, 1984), and as the experimental data in this thesis complied with this type of isotherm, it was adopted throughout this work. This hyperbolic isotherm, which is a concave-downward isotherm, has a linear slope at low concentration and tends to a limiting plateau as the adsorbent becomes saturated (Harrison *et al.*, 2003). It can be expressed as

$$q^* = \frac{q_m C^*}{C^* + K_d} \qquad \mathbf{(3.5)}$$

Rearranging equation (3.5) gives the following linear forms

$$\frac{C^*}{q^*} = \frac{K_d}{q_m} + \frac{C^*}{q_m} \qquad \mathbf{(3.6)}$$

or,

$$\frac{q^*}{C^*} = \frac{q_m}{K_d} - \frac{q^*}{K_d} \qquad \textbf{(3.7)}$$

from which K_d and q_m can be calculated by least squares linear regression analysis (Skidmore *et al.*, 1990). It has to be noted that higher dissociation constant, K_d, implies lower association constant and therefore weaker binding to the adsorbent.

3.1.2 Two-component system

3.1.2.1 Non-competitive Langmuir model

This assumes that the adsorption sites for the two proteins are mutually independent, that is the adsorption of one type of protein to the ion-exchanger in no way affects the adsorption of the other species and there is therefore no competition between the proteins for the adsorption sites (Skidmore and Chase, 1990). Hence, the adsorption characteristics of the protein in the two-component system will be the same as that in single-component systems, i.e.

$$q_1^* = \frac{q_{m1} C_1^*}{C_1^* + K_{d1}} \quad \text{and} \quad q_2^* = \frac{q_{m2} C_2^*}{C_2^* + K_{d2}} \qquad \textbf{(3.8)}$$

where the subscripts 1 and 2 indicate adsorbate species 1 and 2.

3.1.2.2 Totally competitive Langmuir model

This assumes that there is total competition between proteins for adsorption to the ion-exchanger. The model involves a fractional occupancy of the adsorption capacity for each protein species and uses Langmuir parameters derived from single-component experiments (Skidmore and Chase, 1990). The governing equations at equilibrium are

$$q_1^* = \frac{q_{m1} C_1^*}{C_1^* + K_{d1} + \dfrac{K_{d1}}{K_{d2}} C_2^*} \qquad \textbf{(3.9)}$$

$$q_2^* = \frac{q_{m2} C_2^*}{C_2^* + K_{d2} + \dfrac{K_{d2}}{K_{d1}} C_1^*} \qquad \textbf{(3.10)}$$

The above two equations are solved simultaneously with the mass balance equations:

$$VC_{o1} = VC_1^* + vq_1^* \quad \textbf{(3.11)}$$

$$VC_{o2} = VC_2^* + vq_2^* \quad \textbf{(3.12)}$$

where v is the settled volume of ion exchanger, V the volume of liquid external to the ion exchanger, and C_{o1} and C_{o2} are the initial concentrations of the two proteins. A Matlab program was written by the author to solve Eq. 3.9, 3.10, 3.11, and 3.12 for values of C_1^*, C_2^*, q_1^*, and q_2^* for a particular set of initial conditions V, v, C_{o1} and C_{o2} using the values of K_{d1}, K_{d2}, q_{m1}, and q_{m2} determined in single-component adsorption isotherm measurements. The value of C_{o2} was taken as twice that of C_{o1} as is normally found in whey.

3.2 Adsorption kinetics

3.2.1 Traditional system

This technique is used to characterise the kinetics of adsorption through studying the time-course of protein uptake onto the adsorbent. Evidently, such kinetics cannot be inferred from equilibrium batch measurements made to determine the isotherm. The analysis of these kinetics begins with a mass balance on the solute in the liquid

$$V\, r_t = -V\, \frac{dC}{dt} = v\, \frac{dq}{dt} \quad \textbf{(3.13)}$$

where where r_t is the rate of adsorption per volume of solution external to the adsorbent, C the solute (soluble protein) concentration, q the adsorbed solute concentration, t time, v the settled volume of ion-exchanger (mentioned earlier), and V the volume of solution external to the adsorbent (mentioned earlier). This volume is given by

$$V = V_s + V_w \quad \textbf{(3.14)}$$

where V_s is the volume of original solution before adding the adsorbent suspension, and V_w is the volume of fluid contained within the 1:1 (v/v) adsorbent suspension and this comprises 50% of the total adsorbent volume.

This rate is dictated according to the employed kinetic model and, in that respect, two main models were proposed.

3.2.1.1 Kinetic rate constant model

The model takes an empirical approach to the adsorption process and assumes that all the rate limiting processes can be represented by kinetic rate constants. In such an approach, the rate of mass transfer of protein to the adsorbent is assumed to be described by

$$\frac{dq}{dt} = k_1 C(q_m - q) - k_{-1} q \qquad \textbf{(3.15)}$$

$$V\frac{dC}{dt} = -v\frac{dq}{dt} \qquad \textbf{(3.16)}$$

where k_1 and k_{-1} are the adsorption and desorption rate constants respectively.
For batch uptake adsorption, the protein concentration in solution at time t could be obtained by solving equations (3.15) and (3.16) numerically as will be discussed in the following experimental chapter. The alternative analytical solution of Eq. (3.15) would be

$$C = Co - \frac{v}{V}\frac{(b+a)(1-\exp\{-\frac{2av}{V}k_1 * t\})}{\left(\frac{b+a}{b-a}\right) - \exp\{-\frac{2av}{V}k_1 * t\}} \qquad \textbf{(3.17)}$$

where

$$a^2 = b^2 - \left(\frac{Co * V}{v}\right)qm \qquad \textbf{(3.18)}$$

$$b = \frac{1}{2}\left(\frac{CoV}{v} + qm + \frac{KdV}{v}\right) \qquad \textbf{(3.19)}$$

and C_o is the initial liquid phase protein concentration (Skidmore *et al.*, 1990).

3.2.1.2 Pore diffusion model

A more rigorous approach to modelling the adsorption process is to consider diffusion within the pores of the adsorbent. The following assumptions are used as the basis for the construction of the model:
(1) The adsorbent is made of a porous material, into which the solute must diffuse, in a manner described by an effective pore diffusivity, D, which is assumed to be independent

of solute concentration and adsorbent loading, and is based on the porosity of the particle to small molecules, rather than the actual extent to which molecules of a particular protein can penetrate the particle.

(2) The adsorbent particles are spherical, with uniform size and density, and the functional groups of the ion exchanger are distributed evenly throughout the interior of the particle (Skidmore *et al.*, 1990).

(3) The liquid film mass transfer resistance can be neglected because the adsorption is so fast and hence film diffusion is not a rate determining step.

For diffusion of protein in the liquid within the ion exchanger particle, the point concentration of protein, c, is given by

$$\varepsilon \frac{\partial c}{\partial t} = \varepsilon D\left(\frac{\partial^2 c}{\partial r^2} + \frac{2\partial c}{r\partial r}\right) - (1-\varepsilon)\frac{\partial q}{\partial t} \qquad \textbf{(3.20)}$$

where q is the point concentration of adsorbed protein and r the radial coordinate within the ion-exchanger particle (Ruthven, 1984). The particle porosity could be determined from knowledge of the solid content of the adsorbent. Sepharose resins are formulated from 6% (w/v) agarose and hence the particle porosity is taken as 0.94 (Skidmore *et al.*, 1990).

Assuming local equilibrium and differentiating the Langmuir equation (Eq. 3.5) with respect to t yields

$$\frac{\partial q}{\partial t} = \frac{\partial c}{\partial t}\left(\frac{q_m K_d}{(c + K_d)^2}\right) \qquad \textbf{(3.21)}$$

Substituting Eq. 3.21 into Eq. 3.20 gives

$$\left(\varepsilon + \frac{(1-\varepsilon)q_m K_d}{(c + K_d)^2}\right)\frac{\partial c}{\partial t} = \varepsilon D\left(\frac{\partial^2 c}{\partial r^2} + \frac{2\partial c}{r\partial r}\right) \qquad \textbf{(3.22)}$$

with the initial condition $t = 0,\ c = 0$

and the boundary conditions $r = 0$, $\dfrac{\partial c}{\partial r} = 0$; and

$r = R$ $c = c_R$, where c_R is the concentration in equilibrium with q^* obtained from the Langmuir equation.

3.2.2 Confocal microscopy system

3.2.2.1 Modification of the simple kinetic model

When applying the traditional simple kinetic model equations (Eq. 3.17, 3.18 and 3.19) to the uptake profiles obtained from the confocal system, it was assumed that the equilibrium integral fluorescence within the shell, F^*, is proportional to q^*. Thus, C_o, K_d, and q_m in Eq. 3.17, 3.18 and 3.19 were each multiplied by $\frac{F^*}{q^*}$ to obtain their respective counterparts of $C_o^{'}, K_d^{'}$ and F_{max} (AU). Throughout this thesis, the primed symbols pertain to the characteristics of adsorption obtained from measurements of fluorescence obtained by the confocal system in contrast to the unprimed symbols which refer to determination of the characteristics of adsorption by the traditional method of monitoring changes in the concentration of protein in the bulk liquid phase. Accordingly, $k_1(ml \cdot mg^{-1}\,\mathrm{min}^{-1})$ in Eq. (3.17) must be multiplied by $\frac{q^*}{F^*}$ to obtain the appropriate substitute $k_1'(AU^{-1}\,\mathrm{min}^{-1})$. The modified equations would thus be as follows:

$$C = C_o^{'} - \frac{v}{V}\frac{(b^{'} + a^{'})(1 - \exp\{-\frac{2a^{'}v}{V}k_1^{'} * t\})}{\left(\frac{b^{'} + a^{'}}{b^{'} - a^{'}}\right) - \exp\{-\frac{2a^{'}v}{V}k_1^{'} * t\}} \qquad \textbf{(3.23)}$$

where

$$a^{'2} = b^{'2} - \left(\frac{C_o^{'} * V}{v}\right)F_{max} \qquad \textbf{(3.24)}$$

$$b^{'} = \frac{1}{2}\left(\frac{C_o^{'}V}{v} + F_{max} + \frac{K_d^{'}V}{v}\right) \qquad \textbf{(3.25)}$$

3.3 Packed-bed adsorption

3.3.1 Simple kinetic model

For single-component systems, the equation of continuity in the mobile phase is given by

$$D_x \frac{\partial^2 C}{\partial x^2} - v_L \frac{\partial C}{\partial x} - \frac{\partial q}{\partial t} = \frac{\partial C}{\partial t} \qquad \textbf{(3.26)}$$

and the rate equation (Eq. 3.15) is recast to the form

$$\frac{\partial q}{\partial t} = k_1[C(q_m - q) - K_d q] \qquad \textbf{(3.27)}$$

where D_x is the axial dispersion coefficient, and x is the distance along the column (Cowan *et al.*, 1989).

The initial conditions are $t = 0,\ x = 0 \quad C(0,0) = C_f \quad q(0,0) = 0$

$t = 0,\ x \neq 0 \quad C(0,0) = 0 \quad q(x,0) = 0$

while the boundary conditions are $x = 0 \quad C(0,t) = C_f \quad q(0,t) = 0$ and

$x = l \quad C(l,0) = 0$ or $\frac{\partial C}{\partial x} = 0 \quad \frac{\partial q}{\partial x} = 0$

Considering the column dimensions and the flow rate employed, it was reasonable to neglect the axial dispersion term. Eq. (3.26) and (3.27) were then solved simultaneously to give the adsorption breakthrough curve. The numerical solution is discussed in the following experimental chapter.

For two-component systems with competition between species, the governing equations are as follows:

$$- v_L \frac{\partial C_1}{\partial x} - \frac{\partial q_1}{\partial t} = \frac{\partial C_1}{\partial t} \qquad \textbf{(3.28)}$$

$$\frac{\partial q_1}{\partial t} = k_{11}\left[C_1 q_{m1}\left(1 - \frac{q_1}{q_{m1}} - \frac{q_2}{q_{m2}}\right) - K_{d1} q_1 \right] \qquad \textbf{(3.29)}$$

$$- v_L \frac{\partial C_2}{\partial x} - \frac{\partial q_2}{\partial t} = \frac{\partial C_2}{\partial t} \tag{3.30}$$

$$\frac{\partial q_2}{\partial t} = k_{12}\left[C_2 q_{m2}\left(1 - \frac{q_1}{q_{m1}} - \frac{q_2}{q_{m2}} \right) - K_{d2} q_2 \right] \tag{3.31}$$

where the initial conditions are

$t = 0,\ x = 0 \quad C_1(0,0) = C_{f1} \quad q_1(0,0) = 0 \quad C_2(0,0) = C_{f2} \quad q_2(0,0) = 0$

$t = 0,\ x \neq 0 \quad C_1(x,0) = 0 \quad q_1(x,0) = 0 \quad C_2(x,0) = 0 \quad q_2(x,0) = 0$

and the boundary conditions are

$x = 0 \quad C_1(0,t) = C_{f1} \quad q_1(0,t) = 0$

$\quad C_2(0,t) = C_{f2} \quad q_2(0,t) = 0$

$x = l \quad C_1(l,0) = 0 \quad$ or $\quad \frac{\partial C_1}{\partial x} = 0 \quad \frac{\partial q_1}{\partial x} = 0$

$\frac{\partial C_2}{\partial x} = 0 \quad \frac{\partial q_2}{\partial x} = 0$

The above four equations were solved numerically to give the adsorption breakthrough curves as will be discussed in the following experimental chapter.

4 Experimental

4.1 Materials

Pure β-lactoglobulin from bovine milk, approximately 90% pure (by gel electrophoresis), chromatographically purified and lyophilized (MW 18 kDa), and pure α-lactalbumin from bovine milk, ≥ 90% pure (by gel electrophoresis), calcium depleted (MW 14 kDa) were purchased from Sigma-Aldrich (Gillingham, UK). Whey concentrate, MyPro whey protein WPC80 (80 wt% total protein) was purchased online from www.protein.co.uk. It has a protein composition (w/w) of 60% BLG, 20% ALA, 8% bovine serum albumin, 10% immunoglobulin, 1% lactoferrin and 1% others (manufacturer's data).

SP Sepharose FF (loose and columns), Superdex 200 columns and PD-10 Sephadex G-25 medium columns were obtained from GE Healthcare (Amersham, UK). Ultra-filtration membranes Vivaflow 50 for sample concentration were purchased from Sartorius Ltd. (Epsom, UK). AlexaFluor 647 and AlexaFluor 488 dyes were obtained from Invitrogen (Leiden, Netherlands).

Reagents used for buffer preparation (anhydrous sodium acetate and Tris-HCl, Fluka (Gillingham, UK); glacial acetic-acid, 99%; ethanol 99.8%, Riedel-de Haen (Seelze, Germany); sodium hydroxide, Fisher Scientific (Loughborough, UK); sodium chloride, Riedel-de Haen; phosphate buffered saline PBS powder of pH 7.4, Sigma-Aldrich (Gillingham, UK)) were all of analytical grade.
For all experiments, distilled deionised water was used.

4.2 Methods

4.2.1 Preparation of reagents

4.2.1.1 Ion-exchanger

SP Sepharose FF was supplied as a slurry in 20% ethanol solution containing 0.2M sodium acetate. The ion-exchanger was equilibrated with the appropriate buffer solutions by packing it in a PD-10 column and passing several bed volumes of buffer

through the bed. The adsorbent was then suspended in buffer and the suspension poured into a measuring cylinder. After allowing to settle, the volume of buffer in the measuring cylinder was adjusted to equal the volume of settled ion-exchanger. Samples of ion-exchanger were then obtained by suspending the ion-exchanger in the measuring cylinder and aliquoting known volumes of this (1:1 v/v) suspension, using a P-5000 automatic Gilson pipette.

4.2.1.2 Equilibrium buffer

8.2 g (0.1M) of anhydrous sodium acetate were weighed in a 1-litre volumetric flask. The amount was mixed and dissolved in 800-ml of distilled deionized water and the pH was brought down to the required value, using acid measuring, by adding the appropriate amount of glacial acetic acid. The volume was then made up to 1-litre, while readjusting the pH when needed.

The working pH values were chosen to be values below the isoelectric point of the protein, where the protein is positively-charged (i.e. a cation), as well as to lie within the effective pH range for the acetate buffer, stated to be 3.6-5.6 (Mohan, 2003).

4.2.1.3 Protein

Different concentrations of protein samples were prepared by dissolving the protein in equilibrating buffer. Since no information is available on the long-term storage of these proteins, the samples were freshly prepared. At the employed pH values, the protein solutions were clear with no evidence of turbidity or protein denaturation. In addition, the protein concentrations were analysed using size exclusion chromatography on Superdex 200 column and were found to be stable (no loss in concentration with time of exposure was detected).

4.2.2 Batch techniques

These were confined to single-component studies.

4.2.2.1 Procedure

To each of a series of falcon tubes containing 14-ml of protein solutions buffered at pH 3.7 and freshly-prepared at different concentrations was added 1-ml of a 50/50

(settled volume/solution volume) suspension of the cation exchanger. The tubes were left to shake overnight, at 20 ^{o}C ± 2 ^{o}C, on a rotating wheel, and then centrifuged for 20 minutes at 3000g. The experiments were performed in triplicate and the experimental error was within 5-10%.

4.2.2.2 Analysis-UV spectrophotometry

The supernatant was analysed on a UV spectrophotometer at 280 nm in 100-QG far-UV-light quartz cuvettes (Fisher Scientific (Loughborough, UK)). The optical density data were converted to their corresponding protein concentrations by reference to a standard calibration curve prepared with the respective protein. With the equilibrium protein concentration (C^*) so determined, the corresponding quantity of protein adsorbed onto the exchanger (q^*) was calculated by mass balance (Eq. 4.1).

$$q^* = q_i + \left(\frac{F_D}{W}\right)\left(C_i - C^*\right) \qquad \textbf{(4.1)}$$

where C^* and C_i are the equilibrium and initial concentrations in solution, respectively; likewise q^* and q_i are the equilibrium and initial concentrations on the adsorbent, F_D the mass of feed, and W the mass of adsorbent.

4.2.3 Packed-bed studies

These include single-, and two-component as well as whey concentrate systems.

4.2.3.1 Procedure

The frontal analysis packed-bed column experiments were performed on an 'AKTA Explorer 100' chromatography system (GE Healthcare). One-ml (0.7 cm internal diameter × 2.5 cm bed height) and 5-ml (1.6 cm internal diameter × 2.5 cm bed height) HiTrap SP Sepharose FF prepacked columns, purchased from the same company, were used. Buffers (for equilibration, elution and washing) and samples were loaded onto the column in a downflow manner using the system's piston and peristaltic pumps, respectively. All buffers and samples were filtered through 0.45 μm membranes, and degassed under vacuum, in order to mitigate bubble entrainment problems. The following

buffer systems were employed: 0.1M sodium-acetate buffer was used for column equilibration, 1M NaCl in 0.1M sodium acetate for elution in single-component systems and 0.1M Tris-HCl for elution in two-component and whey concentrate systems, 1M NaOH for periodical column cleaning, and 20% ethanol in 0.2M sodium acetate for long-term storage of the adsorbent.

For packed-bed column experiments, the bulk fluid protein concentration (column effluent concentration), C, is recorded as a function of time, t, to give what is known as the 'breakthrough curve', the area above which, in case of symmetrical curves only, is equal to $C_f \times t_{1/2}$, where C_f is the feed bulk concentration (inlet adsorbate concentration), and $t_{1/2}$ is the time corresponding to half the maximum concentration ($0.5 \times C_f$). This area is proportional to the total amount of protein adsorbed onto the ion exchanger. Using this proportionality together with the Langmuir isotherm equation, the capacity of the adsorbent in equilibrium with the inlet adsorbate concentration (q) is determined using the following relation

$$q = \frac{q_m C}{C + K_d} = \left(\frac{C_f \times t_{1/2} \times F}{V_L} \right) \qquad \textbf{(4.2)}$$

where V_L is the volume of the column, F is the flow rate. The general formula for calculating the amount of protein adsorbed onto the ion-exchanger, q, at any time in cases where the breakthrough curve is unsymmetrical, is given by

$$q = \int_0^\infty (C_f - C) \times \frac{F}{V_L} \; dt \qquad \textbf{(4.3)}$$

A q-time curve similar to the concentration-time breakthrough curve can be constructed. The packed-bed experiments were performed in duplicate and the experimental error was within 10-15%.

It has to be noted that the dead volume was taken as the retention volume existing between the point of injection and the point where the first drop of effluent comes off the column when pure buffer (not containing the protein) is passed through the system. The

retention time corresponding to this volume was excluded from the time of the breakthrough curve.

4.2.3.2 Analysis

4.2.3.2.1 Size-exclusion chromatography (SEC)

Size-exclusion experiments were carried out on a Fast Protein Liquid Chromatography (FPLC) system using a Superdex 200 column GL, purchased from GE Healthcare, of 1-cm internal diameter, and a height of 30 cm.

The size-exclusion technique separates BLG and ALA on the basis of the difference in their molecular weights at pH 3.7, BLG being a dimer of total size 36 kDa (Sawyer and Kontopidis, 2000) and ALA a monomer of 14 kDa. A 0.2-ml protein sample was injected onto the column using a 1-ml syringe, while 0.1M sodium acetate buffer of pH 3.7 at flow rate of 0.5 ml/min was passed onto the column in order to elute the protein. As expected, BLG was eluted first with a peak retention volume of 17.5 ml, whereas ALA was eluted at 19.5 ml. It was not possible to obtain two completely separate peaks for each of BLG and ALA, and therefore the peak areas could not be converted to their corresponding concentrations using the standard calibration curve of the pure proteins.

Calibration method

Alternatively, a linear calibration curve plotting the absolute peak area pertaining to each protein versus the respective protein concentration in the binary mixture (Figure 4.1) was constructed by preparing several protein mixtures with different proportions of ALA and BLG ranging from 0% (pure ALA) to 100% (pure BLG). For each of these protein samples, the total concentration as well as the composition was known, and thus the concentration of each protein in the mixture was determined. Additionally, the FPLC system calculated the absolute peak areas for each protein by integrating area below the peak. Investigating different total protein concentrations, it was found that the slope of the calibration line did not vary, i.e. the absolute peak area was only a function of the composition of the protein mixture.

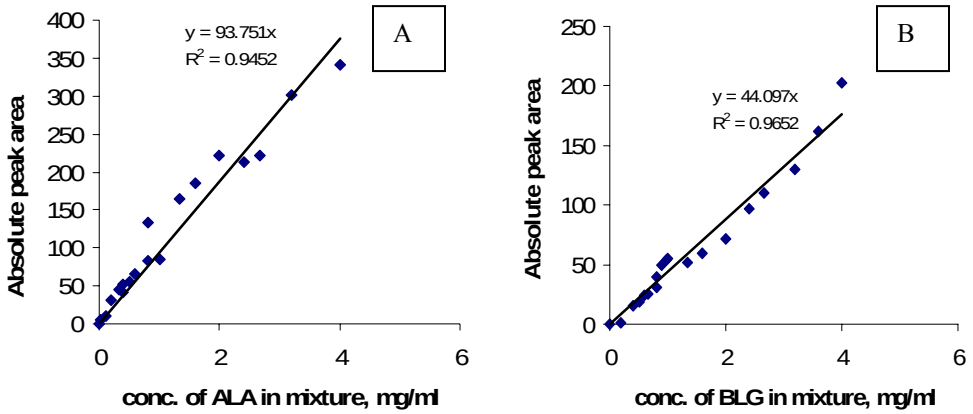

Figure 4.1 Calibration lines for ALA (A) and BLG (B) on the size-exclusion protein analysis system.

The fractions of the column effluent were analysed for individual protein content by converting the peak areas for each of the two proteins, obtained by the FPLC system, into their corresponding protein concentrations using the calibration curves described above.

Calculating concentrations for merged peaks

In some cases, it was noticed that the two peaks pertaining to the two proteins were merged into one single peak (i.e. the chromatogram did not demonstrate two distinct peaks), thus making it impossible to obtain the two areas, and thereby the concentrations, associated with each. This problem was solved in the following way. At each data point, the total peak area, A_{tot}, is the sum of those of the two components.

$$A_{tot} = A_A + A_B \qquad \textbf{(4.4)}$$

where

A_{tot} = total absolute peak areas of the two proteins, i.e. area of the merged peaks

A_A = absolute peak area of ALA

A_B = absolute peak area of BLG

In terms of concentration C:

$$A_{tot} = S_A \times C_A + S_B \times C_B \qquad \textbf{(4.5)}$$

where S_A and S_B are the slopes of the calibration curves in Figure 4.1.

In this binary mixture at any time, the concentration can be expressed in terms of mass fraction, x, times total effluent concentration, $C_{tot,}$ which is the sum of (C_A + C_B). C_{tot} was calculated from the following identity:

$$C_{tot}/C_f = Abs_{tot}/Abs_f \quad \textbf{(4.6)}$$

where C_f is the total feed concentration, Abs_{tot} is the effluent absorbance corresponding to the total effluent concentration, and Abs_f is the total feed absorbance. For the study at hand, C_f was equal to 4.5 mg/ml and Abs_f was approximately equal to 1300 mAu.

In terms of mass fraction, x, Eq. (4.5) becomes:

$$A_{tot} = S_A \times C_{tot} \times x_A + S_B \times C_{tot} \times x_B \quad \textbf{(4.7)}$$

which ultimately leads to the next expression

$$C_A = x_A \times C_{tot} = \frac{A_{tot} - S_B C_{tot}}{S_A - S_B} \quad \textbf{(4.8)}$$

where all terms on the right hand side are known.

4.2.3.2.2 Sodium dodecyl sulphate-polyacrylamide gel electrophoresis (SDS-PAGE)

The protein samples (collected fractions) were prepared according to the manufacturer's protocol (Invitrogen) under reducing conditions using dithiol-threitol (DTT) as a reducing agent. Samples were then heated at 70^{o}C for 10 min prior to electrophoresis. A 7 μL volume of each sample was loaded per well. Electrophoresis was afterwards run at a potential difference of 200 volts for 35 min, using NuPAGE Novex 4-12% Bis-Tris gel and NuPAGE MES running buffer, purchased from Invitrogen. The protein was fixed for 20 min using 40% methanol and 7% acetic acid solution before it

was stained overnight with Coomassie Brilliant Blue R250 (reddish with a dye strength indicator of 250) having the molecular formula $C_{47}H_{50}N_3O_7S_2^+$, a molecular mass of 833.048, and a composition of 0.2% Coomassie blue, 7.5% acetic acid and 50% ethanol. The protein was then destained in the same fixing solution. The protein bands were quantified using ImageJ software by plotting the intensity of these gel bands and integrating the area under the plot.

4.2.3.3 Modelling and simulation

In order to predict the breakthrough curves for single-component packed-bed adsorption, the simple kinetic rate constant model (see Chapter 3) was solved using a built-in Partial Differential Equation Matlab programme (pdepe solver), the details of which are given in the Appendix. The programme solves initial-boundary value problems for systems of partial differential equations in one space variable and time. Some modifications were made to the programme to take account of the initial and boundary conditions of the problem at hand as well as the display of output results required (for e.g. C/C_f instead of C). The programme solves for C/C_f (given as u_1 in the programme script) and q (u_2) against time, and its input parameters are;

- dimensions of packed bed, internal diameter and apparent height (d,x);
- volumetric flow rate (F);
- time-length (t);
- initial feed bulk fluid concentration (C_f);
- Langmuir adsorption isotherm dissociation constant of the protein/ion exchanger interaction (K_d);
- Langmuir adsorption isotherm maximum capacity of the ion-exchanger (q_m);
- overall forward rate constant (k_1).

Of these parameters, the first four were measured physical characteristics of the experimental system, the next two, K_d and q_m, were determined from batch experiments, k_1 was calculated from the batch uptake profile, discussed earlier.

The programme was tested on lysozyme adsorption data obtained from previous literature (Skidmore *et al.*, 1990) and it proved to be fairly satisfactory, as it gave the same shape of

breakthrough curves predicted in the literature, when using the same values of input parameters.

Since the Matlab built-in programme solves only systems of two equations, another Matlab programme was written by Dr. Bart Hallmark in the Chemical Engineering and Biotechnology Department, University of Cambridge (see Appendix) to solve simultaneously the system of four equations describing the modelling of two-component systems (see Chapter 3).

4.2.4 Confocal laser scanning microscopy (CLSM) techniques

4.2.4.1 Instrumentation

Confocal microscopy measurements were performed using a Leica TCS SP5 laser scanning microscope (Leica, Milton Keynes, UK) equipped with a multi-line argon ion laser and red and green helium neon (543 and 633) lasers as excitation sources. Up to three detection channels could be acquired simultaneously. Image acquisition and analysis were performed using the built-in LAS AF (Leica Application Suite, Advanced Fluorescence, Beta Version) software.

4.2.4.2 Finite bath experiments

Experiments were conducted on pure BLG with an initial concentration of 3 mg/ml and settled exchanger volume to solution volume (v/V) ratio of 1:14, and pure ALA under various conditions of initial concentration and v/V ratio. Before conducting the finite bath experiments, three preceding steps were required. These will be described in turn.

1. *Labelling the protein with a fluorescent dye.*

   The required protein concentration was prepared by dissolving the protein in 0.1 M PBS buffer at pH 7.4. The protein was then labelled with a fluorescent dye according to the standard protocol provided by the manufacturer. It should be noted that the dye coupling reaction took place at a pH range of 7.5 to 8.5 by adding sodium bicarbonate to the original protein solution. BLG was labelled with AlexaFluor 647 fluorescent dye (absorption and emission maxima of 650 and 668 nm, respectively), while ALA was labelled with AlexaFluor 488 fluorescent dye

(absorption and emission maxima of 494 and 519 nm, respectively). The two proteins were labelled with two different dyes that have non-overlapping absorption and emission spectra in order to facilitate their identification in the two-component experiments.

2. *Excess dye removal and buffer exchange*

   The conjugated protein was then passed through a PD-10 Sephadex G-25 size-exclusion chromatography column to separate labelled protein from excess unconjugated dye, as well as to exchange the buffer in which the protein was dissolved from 0.1 PBS to 0.1 M acetate buffer of pH 3.7.

3. *Protein concentration*

   Since the protein was diluted in the previous step, it was necessary to bring it back to its original concentration using Vivaflow membranes and centrifugation at 4500 rpm and 4^{o}C for 25 min. The degree of labelling (DOL) (moles of dye/moles of protein) was then measured according to the manufacturer's instructions and was found to be 1.03 for BLG and 0.37 for ALA.

The finite bath experiments were then carried out as follows. In order to minimise the consumption of fluorophore per experiment as well as to avoid light attenuation due to reabsorption or inner filtering (Harinarayan *et al.*, 2006; Ljunglöf, 2002; and Ljunglöf and Thommes, 1998), the labelled protein was mixed with unlabeled protein. To ascertain the appropriate amount of dye-labelled protein needed to be present in order to give a satisfactory degree of fluorescence, different ratios of labelled to unlabeled proteins were prepared and imaged under the microscope. A ratio of labelled to unlabeled proteins of 1:34 was chosen as the working ratio. A volume of 0.1 ml of conjugated protein was mixed with 3.4 ml of unlabeled protein and was placed in a reaction vessel placed on an orbital shaker. The adsorption experiment was started by adding 0.5 ml of adsorbent slurry (settled adsorbent diluted 1:1 with 0.1 M acetate buffer of pH 3.7) to the stirred protein solution. Aliquots of 100 μl volume were withdrawn from the vessel at fixed times. It should be noted that adsorption was allowed to proceed

overnight in order to allow adsorption to approach equilibrium and samples were taken thereafter for analysis. These samples will henceforth be referred to as the equilibrium samples. The particles were re-suspended in 0.5 ml excess buffer and centrifuged at 6000 rpm for 5 min. The centrifugation/re-suspension cycle was repeated six times to remove non-bound proteins. The washed re-suspended beads were then imaged under the confocal microscope.

4.2.4.3 Confocal microscopy experiments

Individual adsorbent particles were analysed using horizontal scanning by acquisition of two-dimensional confocal images perpendicular to the optical axis. Only the central slice near the maximum diameter of each bead image was used for further image analysis and all images presented in this thesis represent these central slices. A 40*0.6 immersion (oil) objective lens was used for all measurements. The pinhole aperture was set to 50 μm. The He/Ne 633 laser provided excitation of AlexaFluor 647 at 633 nm and the emitted fluorescent light was detected between 660 and 680 nm, whereas the argon laser (set at 20% power) provided excitation for AlexaFluor 488 at 488 nm and the emitted fluorescent light was detected between 490 and 515 nm. The images were then taken as an overlay of the scans obtained in the two separate channels. The image size for all images was 512*512 pixels and the pixel size was 1.45 μm. Control experiments were carried out by adsorbing underivatized protein to SP Sepharose FF and imaging samples of the beads after washing. Insignificant fluorescence was detected.

The fluorescence intensity profiles of the labelled protein bound to the adsorbent across central horizontal cross sections of the beads were compiled for each time interval using imageJ software. The adsorbent particle diameter was found to vary between 60-120 μm. The depth of penetration of the fluorescently-labelled protein was monitored in beads of comparable sizes, in order to minimise any heterogeneity effects resulting from disparity in bead size. The resulting fluorescence profiles showed that three slightly different behaviours occurred, pertaining to each of the three particle-size ranges investigated.

4.2.4.4 Data analysis of confocal microscopy results

The fluorescence profiles were integrated by calculating the area under the fluorescence intensity-time curve, F_{ring}, using either ImageJ or Matlab Curve Fitting Toolbox. The results obtained from both methods were comparable.

The relative solid-phase capacity (Q_{rel}) was obtained in arbitrary units per m^3 of adsorbent using Eq. (4.9)

$$Q_{rel} = \frac{F_{ring}}{V_b} \cdot \frac{\frac{4}{3}\pi\left(r_o^3 - r_i^3\right)}{\frac{4}{3}\pi\left(r_o^3\right)} = \frac{F_{ring}}{V_b}\left[1 - \left(\frac{r_i}{r_o}\right)^3\right] = \frac{F_s}{V_b} \qquad \textbf{(4.9)}$$

where r_i is the inner radius of the fluorescent ring in μm, r_o is the outer radius of the fluorescent ring in μm, V_b the bead volume, and F_s is the integral fluorescence within the shell.

In order to construct the batch uptake curve, the relative capacities were related to the relative capacity at equilibrium (Q_{rel}^{∞}) and the degree of saturation versus time (R_F) was calculated according to Eq. (4.10) (Ljunglöf and Thommes, 1998).

$$R_F = \frac{Q_{rel}}{Q_{rel}^{\infty}} = \frac{F_s}{F^*} \qquad \textbf{(4.10)}$$

where F^* is the equilibrium integral fluorescence within the shell.

4.2.5 Batch uptake techniques

A schematic diagram of the experimental set-up of a continuous adsorption system with recycling is illustrated in Figure 4.2. A protein sample of known concentration together with the suspended ion-exchanger were agitated in a beaker (1) using an orbital shaker (2) and maintained at 20°C by means of a temperature regulator (3). The solution was then pumped by a peristaltic pump (5) to a UV flow-spectrophotometer (6). In order to prevent ion-exchanger beads being pumped through the UV spectrophotometer (280 nm wavelength range), the solution was filtered on uptake. This filtration was provided by means of a standard 1.6 cm-diameter chromatography column adapter fitted with a 20-μm net (4). The analogue output signal

from the UV spectrophotometer was connected to an analogue-to-digital converter (7) and on to a personal computer, PC (8), to be recorded using 'Labview' software. The solution pumped out of the UV spectrophotometer was recycled back to the beaker, so as to keep the sample volume constant throughout the duration of the experiment. Initially, the UV spectrophotometer was zeroed by passing pure buffer through the system. Afterwards, the buffer was replaced by the protein sample and the voltage reading corresponding to the employed protein concentration was recorded in order to calibrate the measurement of liquid-phase protein concentration. Using this concentration-to-voltage ratio, the voltage readings were later converted to their corresponding concentration values. On starting the experiment (zero-time), a sample of the ion-exchange adsorbent was pipetted into the protein solution already present in the beaker and the voltage reading was recorded and plotted versus time. Typically between 1-5 ml of ion-exchanger were used with a recycle flow rate of 1-1.5 ml/min, and the initial volume of protein solution varied between 30-40 ml.

A concentration-time plot was constructed from the voltage-time curve using the concentration-to-voltage ratio mentioned earlier. The amount of protein adsorbed, q, was calculated by mass balance and plotted as a normalised value, R_q, against time expressed in minutes. The experiments were performed in triplicate and the error was within 3-5%.

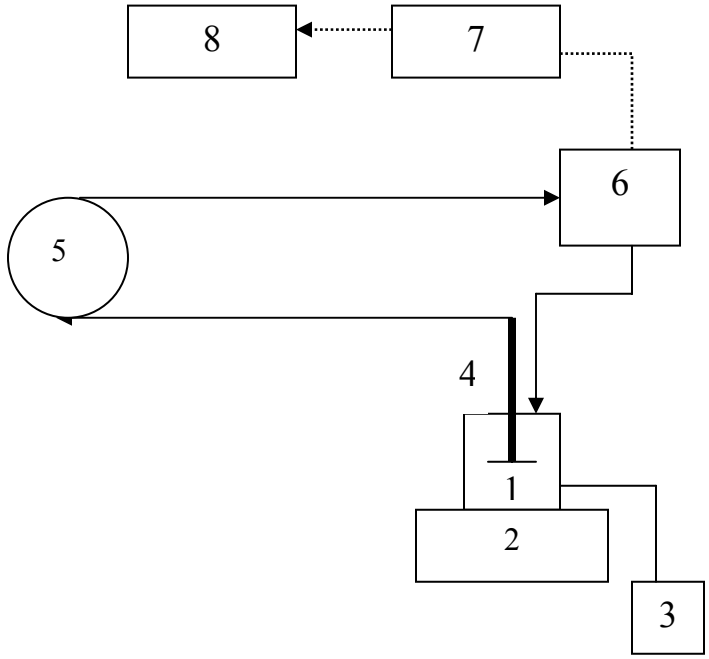

Figure 4.2 Schematic diagram of the continuous-flow system.

1. beaker 2. orbital shaker 3. temperature regulator
4. chromatography column adapter 5. peristaltic pump (P-1)
6. UV flow spectrophotometer 7. Analogue-to-digital converter (ATD)
8. personal computer (PC)

4.2.5.1 Estimating the forward rate constant (k_1)

The k_1 value that gave the best fit to the experimental data was determined by solving the simple kinetic model (see Chapter 3). The model was solved using an Ordinary Differential Equation built-in Matlab programme (ode45 solver). The programme outputs are plots of either C or q versus time. The programme input parameters were as follows,

- volume of liquid external to the ion-exchanger particles (V);
- volume of settled ion exchanger (v);
- initial bulk fluid protein concentration (C_o);
- time-length (t);
- Langmuir adsorption isotherm dissociation constant of the protein/ion exchanger interaction (K_d);

- Langmuir adsorption isotherm maximum capacity of the ion-exchanger (q_m);
- overall forward rate constant (k_1).

Of these seven parameters, the first four were measured physical characteristics of the experimental system, the next two, K_d and q_m, were determined from the batch isotherm experiments, thus k_1 was the only unknown parameter. The k_1 value that gave the best fit to the experimental data was determined using statistical regression. The profiles of C versus t calculated numerically from the programme were in good agreement with those obtained from the analytical solution (Eq. 3.17) with accuracy within 3%.

4.2.5.2 Estimating the diffusivity (*D*)

The pore diffusion model was solved using a Partial Differential Equation built-in Matlab programme (pdepe solver). The programme outputs are plots of c versus time. The programme input parameters were:

- volume of liquid external to the ion-exchanger particles (V);
- volume of settled ion exchanger (v);
- initial point protein concentration (c_o) which is equal to zero;
- time-length (t);
- Langmuir adsorption isotherm dissociation constant of the protein/ion exchanger interaction (K_d);
- Langmuir adsorption isotherm maximum capacity of the ion-exchanger (q_m);
- protein point concentration at $r = R$ (c_R) that is in equilibrium with q^*, and this is obtained using Langmuir equation;
- particle porosity (ε) and this is taken as being 0.94 (Skidmore *et al.*, 1990); and
- effective diffusivity (D).

The c-t curve at $r = R$-ΔR was converted to its corresponding C-t curve using the mass balance equation in conjunction with Langmuir equation

$$\frac{q_m c}{K_d + c} \times \frac{v}{V} = C_o - C \qquad \textbf{(4.11)}$$

The value of D that gave the best fit to the experimental data was determined using statistical regression. This value was then compared to the molecular diffusivity of the protein in free aqueous solution, D_{AB}, estimated using the semi-empirical equation (Polson, 1950)

$$D_{AB} = 9.4 \times 10^{-15} \frac{T}{\mu (M_A)^{\frac{1}{3}}} \qquad \textbf{(4.12)}$$

where M_A is the relative molecular mass of the protein, μ the viscosity of the protein solution and T the absolute temperature. The viscosity of the protein solution was taken to be that of water.

5 Equilibrium adsorption isotherms for the pure whey proteins

5.1 Introduction

The equilibrium adsorption isotherms of ALA and BLG have been studied by a number of workers onto various types of adsorbents and they were all found to follow a Langmuirian-type behaviour. Galisteo and Norde (1995) studied the adsorption isotherms of ALA on poly (styrene-sulphonate) (PSS) lattices of different surface charge densities as a function of pH and ionic strength. Different concentrations of KCl were used without any buffers and the pH was adjusted using KOH or HCl. The adsorption characteristics of two ALA conformers, namely apo-ALA (Ca-depleted ALA) and Ca-ALA (ALA bound to a Ca^{2+} ion), were investigated. Unusually high protein adsorption was detected on the employed adsorbent relative to most other colloidal adsorbents, but the maximum binding capacity for both conformers was the same. Cabilio *et al.* (2000) investigated the adsorption behaviour of ALA at a Pt/electrolyte interface in an acidic, neutral and alkaline media over a temperature range of 273 to 353 K using the cyclic voltammetry technique. It was shown that the surface charge density determined by protein adsorption is directly proportional to the amount of adsorbed protein. The Langmuir isotherm showed that the protein expressed the highest affinity for adsorption at pH 2 and the lowest at pH 11. Conrado *et al.* (2005) studied the Langmuir adsorption isotherm for ALA onto the hydrophobic adsorbent Streamline Phenyl at pH 7.5 using 50 mM Tris buffer with 35 mM EDTA. The maximum binding capacity was found to be 19.28 mg protein/g of resin, and the dissociation constant was 0.61 mg protein/g of resin.

As for BLG, McCreath *et al.* (1997) estimated the Langmuir adsorption parameters of the protein onto SP-PVA-FEP (a polyvinyl alcohol (PVA) coated particulate perfluoropolymer (FEP) support functionalised with anion-exchanger groups (DEAE and Q)) at pH 8.0 using 20 mM sodium phosphate buffer. The maximum adsorption capacity and dissociation constant were found to be 14.9 mg/ml and 0.054 mg/ml, respectively onto DEAE-PVA-FEP, and 17.2 mg/ml and 0.089 mg/ml, respectively onto Q-PVA-FEP.

For multi-component systems, a theoretical discussion of an approach to modelling multicomponent protein adsorption was published by Velayudhan and Horvath (1988), although they did not present any associated experimental data. Experimental results from a non-protein system were published in an earlier paper (Jacobson *et al.*, 1987) from the same laboratory. This paper presented two methods for determining competitive adsorption isotherms from the results of frontal analysis chromatography and included a theoretical discussion of the derivation and use of the parameters of the Langmuir isotherm. Skidmore and Chase (1990) investigated multicomponent adsorption of a model system consisting of bovine serum albumin and lysozyme to the cation-exchanger S Sepharose FF. Two equilibrium models, one based on competitive adsorption to the ion-exchanger and the other based on non-competitive adsorption, were compared to experimental results. Some discrepancies were found suggesting the necessity of taking additional factors into account. Garke *et al.* (1999) studied the adsorption behaviour of lysozyme and gamma-globulin on the strong cation-exchanger Streamline SP by determining the equilibrium isotherms with batch experiments. Adsorption isotherms of the binary mixture of both proteins were modelled using the Langmuir parameters derived from single-component systems. Comparison of experimental results with the competitive Langmuir model displayed significant deviations for the adsorption of lysozyme in the mixture. An extended Langmuir model, accounting for the distinct accessibility of the sorbent's surface for the competing proteins, revealed much better consistency with experimental data. Cano *et al.* (2005) reported a novel approach to determining competitive protein adsorption isotherms in which the competitor concentration is held constant across the entire isotherm. Using labelling techniques, the effect of competing species on equilibrium behaviour and the apparent heterogeneity of anion-exchange adsorbents in the presence of competitors can be quantitatively studied by fitting the data to two popular single-component binding models, the Temkin and the Langmuir-Freundlich (L-F) isotherms. The same workers also investigated the effectiveness of three multi-component binding models, the extended Langmuir–Freundlich, Langmuir and Jovanovic–Freundlich models, in describing the binary competitive equilibrium adsorption of two cytochrome b_5 mutants (Cano *et al.*, 2007). James (1994) studied the binary adsorption equilibrium of the two minor whey

proteins, lactoferrin and lactoperoxidase, at different pH values. Multi-component isotherm results showed clear evidence of competitive adsorption between the two proteins. Results from batch studies were examined using the Extended Langmuir model and the thermodynamically consistent Ideal Adsorbed Solution (IAS) theory derived for the Langmuir isotherm equation. Discrepancies were observed between experimental data and the model results determined using single-component equilibrium parameters.

For a whey mixture, Carrere *et al.* (1996) obtained the equilibrium parameters onto the strong anion exchanger Spherosil QMA from batch experiments at pH 8.0 using 0.02 M Tris HCL buffer. The maximum binding capacity for the total proteins in whey was 129.3 kg/m^3 and the dissociation constant was 0.72 kg/m^3.

5.2 Single-component systems

Adsorption isotherms for BLG at pH values of 3.7, 4.0, 4.5 and 5.0 and for ALA at pH values of 3.7, 3.8 and 3.9 were measured experimentally. Figure 5.1A shows an example of these isotherms for each of the two proteins at pH 3.7. This pH was chosen to be the working pH for our study for reasons that will be explained later. Each of the discrete points in Figure 5.1A represents an experimental result relating the amount of protein adsorbed (q^*) to the corresponding equilibrium concentration of protein in the liquid phase (C^*). The data points were found to comply with the Langmuir adsorption isotherm (Eq. 3.5).

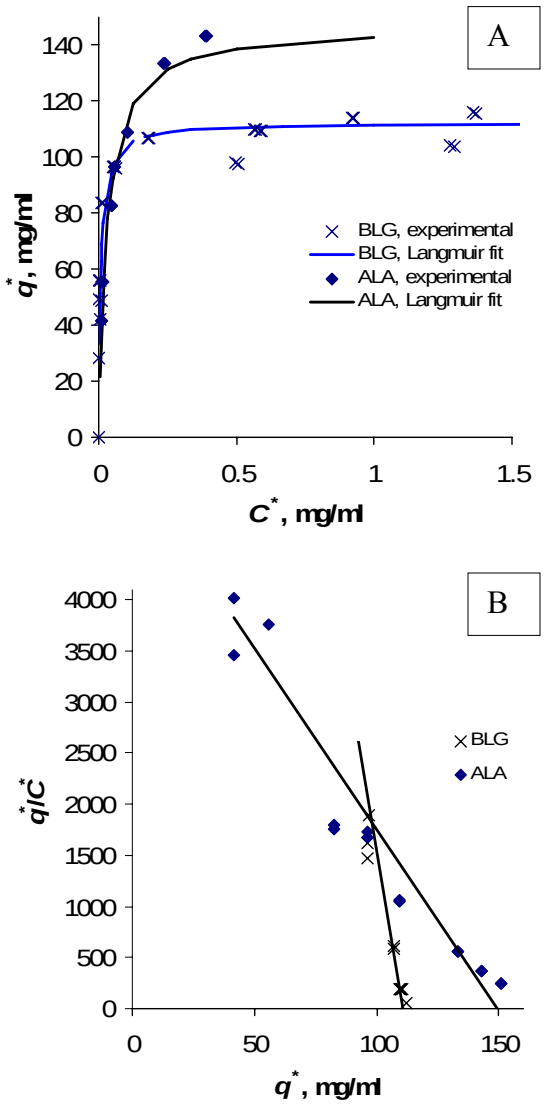

Figure 5.1 Langmuir isotherms (A) and their linear plots (B) for the binding of BLG and ALA to SP Sepharose FF in 0.1M acetate buffer at pH 3.7 and 20^{o}C.

The agreement with a Langmuir isotherm is evident from the linearity of the plots in Figure 5.1B where the data have been linearized using Eq. (3.7). This linear form was adopted here because it provides a better distribution of data points as compared to the other common forms.

The two parameters that define the isotherm, q_m and K_d, are obtained from the ordinate intercept, q_m/K_d, and the slope, $-1/K_d$, of the line. Values so determined for these parameters, recorded in Table 5.1, were utilised to construct the solid lines in Figure 5.1A representing the calculated shapes of the Langmuir isotherms. As can be seen from Table

5.1, both K_d and q_m pertaining to ALA were found to have higher numerical values than those of BLG, implying differences in the characteristics of adsorption of the two proteins on this adsorbent. At pH 3.7, K_d for ALA was almost four times larger than that for BLG, while its q_m was 30% higher. Thus, ALA is the weaker-bound protein (higher K_d) and is evidently accessible to greater proportion of binding sites within the adsorbent (larger q_m) probably because of its smaller size. The relevant isotherm parameters for the other pH values were determined likewise and the values obtained are compiled in Table 5.1.

Table 5.1 Values of the equilibrium isotherm parameters, calculated by linear regression, for BLG and ALA at different pH values.

	pH	q_m, mg/ml	K_d, mg/ml
BLG	3.7	113 ±3	0.008 ±5*10^{-4}
	4.0	133 ±2	0.053 ±0.004
	4.5	130 ±3	0.13 ±0.01
	5.0	79 ±2	0.719 ±0.03
ALA	3.7	147.0 ±8.5	0.029 ±0.0003
	3.8	119.9 ±3.5	0.071 ±0.0007
	3.9	95.9 ±2.3	0.088 ±0.0008

Variation of the desorption constant, K_d, with pH in Table 5.1 is understandable in light of the fact that it is a conditional constant and for adsorption of a macromolecule such as a protein, it is given by $K_d = K_{int*} K_{coul}$ where K_{int} is the intrinsic constant accounting for adsorption when the macromolecule carries no net surface electric charge and K_{coul} is that for coulombic adsorption and the latter varies with changes in pH and ionic strength (Morel, 1983; Tanford, 1961). The graphical pK_d versus pH relation (where pK_d= -log K_d) shown in Figure 5.2A was obtained at a constant ionic strength of 0.1M, thus the linear increase of pK_d with a drop of pH implies an exponential decrease of K_d as the pH falls. As the pH is increased, however, the line appears to be heading for a pH value close to the well-established pI value of 5.2-5.3 for BLG (Wong *et al.*, 1996; Cayot and Lorient, 1997) and 4.2-4.5 for ALA, Gerberding and Byers, 1998.

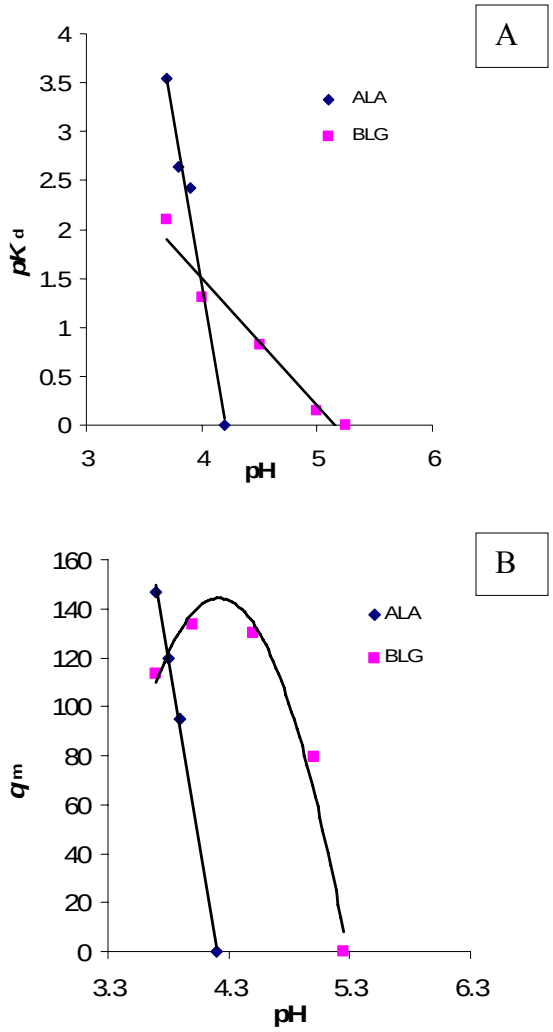

Figure 5.2 Dissociation constant (A), K_d, and maximum binding capacity (B), q_m, for ALA and BLG adsorption to SP Sepharose FF as a function of pH.

This behaviour appears to be the basis of a promising general method for pinpointing the exact value of the pI of a protein. All that is needed is an analogous line on the other side of pI (conducted with an anion-exchanger) at the same ionic strength. Theoretically, these two lines should meet at one point on the pH-axis. Otherwise, if the two lines did not meet at one point, the appropriate value of pI will be the point half way between the intersections of the two lines with the pH-axis. Thus the rise of the line in Figure 5.2A as the pH is lowered from the pI reflects stronger binding (lower K_d) evidently due to the build up of net charge in that direction. Clearly in case of ALA, pK_d drops sharply as the pH gets closer to the isoelectric point and the solubility of the protein

decreases. It is to be noted that in case of ALA and for pH values less than 3.7, it was not possible to obtain a satisfactory Langmuir isotherm and the results were erratic probably due to either competition between free protons and the protein cations for the adsorption sites, or due to protein denaturation at acidic pH. This could also well be the reason for the decline of q_m pertaining to BLG below the pH of maximum adsorption in Figure 5.2B.

In conclusion, a q_m versus pH relation for ALA in conjunction with that for BLG in Figure 5.2B is instrumental in selecting the working pH that maximises the adsorption of both proteins. Furthermore, q_m versus pH and pK_d versus pH relations for both proteins are helpful in selecting the best pH for elution if needed.

In view of the above and taking into consideration the solubility of ALA, pH 3.7 was chosen as the working pH for the remainder of our single, two-component and whey studies.

5.3 Two-component system

It was not possible to obtain the complete experimental equilibrium profiles of ALA and BLG in the two-component system. The individual concentrations of the two proteins in some instances could not be quantified using size-exclusion analysis since the relevant peaks could not be identified as they merged into one peak; and since the total concentration was not known and could not be measured, it was not possible to use the relevant method outlined in Section 4.2.3.2.1.

The equilibrium profiles of ALA and BLG were theoretically predicted using Langmuir model for the two-component systems as depicted in Figure 5.3.

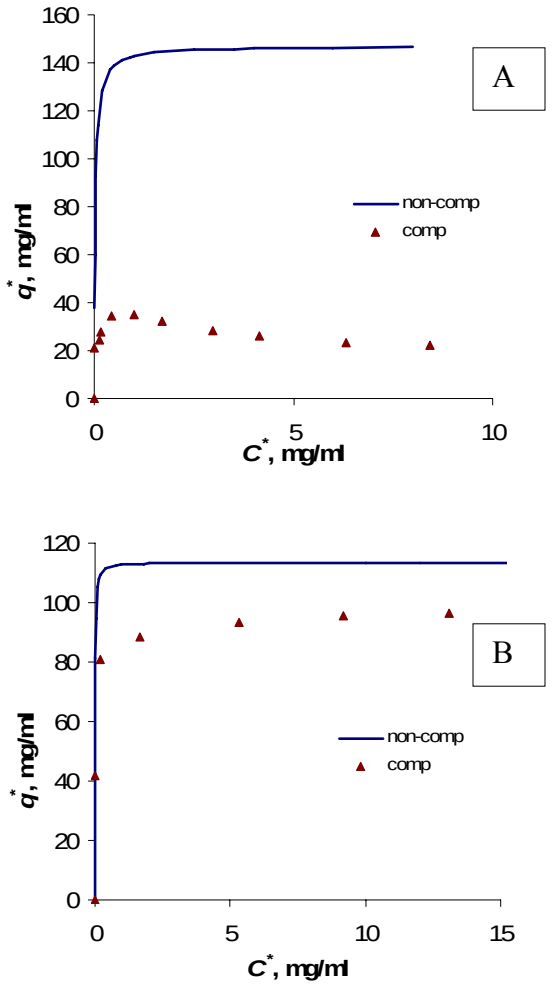

Figure 5.3 Equilibrium profiles for ALA (A) and BLG (B) in two-component systems as predicted using the non-competitive and the totally-competitive Langmuir models.

The solid lines pertain to the profiles predicted using the non-competitive model (Section 3.1.2.1), while the discrete points pertain to those predicted using the totally-competitive model (Section 3.1.2.2). The single-component Langmuir isotherm parameters, determined in the previous section, were used to obtain these profiles. As can be seen in Figure 5.3, the non-competitive model profiles are equivalent to those of single-component systems. Unlike BLG, the totally competitive profiles for ALA do not follow a Langmuirian-type behaviour. The predicted equilibrium parameters, q_m and K_d, for the two proteins were calculated by linearizing the equilibrium profiles (as was shown in the single-component studies). The relevant values are listed in Table 5.2. Clearly, it

was not possible to determine the equilibrium parameters for ALA using the totally-competitive model since the relevant ALA profile did not exhibit a Langmuirian-type behaviour.

Table 5.2 Equilibrium parameters for ALA and BLG in two-component systems as predicted by the non-competitive and the totally-competitive Langmuir models.

	non-competitive		Totally-competitive	
	q_m, mg/ml	K_d, mg/ml	q_m, mg/ml	K_d, mg/ml
ALA	147.0	0.029	ND*	ND*
BLG	113.6	0.008	91.7	0.007

* Not determined

As can be seen in the table, the totally-competitive model predicts lower q_m value for BLG as compared to the non-competitive model. In addition, the value of K_d for ALA predicted by the totally-competitive model is slightly lower than that predicted by the non-competitive model. This implies that the competitive adsorption in the two-component system should in theory entail a slightly stronger binding for BLG.

5.4 Conclusions

Single-component batch experiments were performed on the adsorption of pure ALA and BLG to the cation exchanger SP Sepharose FF. Equilibrium Langmuir isotherm parameters for ALA and BLG were determined at different pH values. q_m versus pH and pK_d versus pH relations for both proteins proved instrumental in delineating an optimum working pH of 3.7. Results at this pH showed that K_d for ALA was almost four times larger than that of BLG, while q_m for ALA was 30% higher. The lower K_d for BLG implies stronger binding.

The two-component isotherm profiles were predicted using both the non-competitive and the totally-competitive Langmuir models. As expected, for both proteins the isotherm parameters predicted by the non-competitive model were the same as those of the single-component systems. The BLG Langmuir isotherm predicted by the totally-competitive model yielded q_m and K_d values lower than those obtained in the single-

component system. The predicted isotherm for ALA, however, did not follow a Langmuirian-type isotherm.

6 Kinetic studies for the adsorption of pure whey proteins

6.1 Introduction

In the traditional method of studying the adsorption kinetics of proteins, the protein uptake profiles are usually obtained indirectly in traditional batch uptake experiments by measuring the change in protein concentration in the bulk liquid phase. The protein solid-phase concentration is then calculated from the reduction of its fluid-phase concentration using mass balance, i.e. assuming that each molecule which disappears from the solution is bound to the adsorbent. The confocal laser scanning microscopy (CLSM) method which has been used rather recently for direct measurements of protein uptake during batch experiments in a finite bath, appears to offer an attractive alternative. By coupling of a fluorescent dye to the protein molecules, the penetration of the protein within single adsorbent beads at different times during batch uptake could be visualised. Intensity profiles of the protein distribution within a single adsorbent bead could be obtained by horizontal scanning. Integrating these intensity profiles yields the overall fluorescence within a bead, which when plotted at different incubation times produces the protein batch uptake profiles. In this section, the literature pertaining to the traditional method will be reviewed first followed by that pertaining to the CLSM method.

For single-component systems, Skidmore *et al.* (1990) determined the kinetic characteristics of the adsorption of bovine serum albumin (BSA) and lysozyme to the strong cation exchanger S Sepharose FF and compared the rates of protein adsorption to two different models, namely the simple kinetic model and the film and pore diffusion model. While the experimental batch uptake profile for lysozyme was consistent with both models, that of BSA was consistent only with the pore diffusion model. Following the same line of work, Aboudzadeh *et al.* (2006) studied the adsorption of human serum albumin (HSA) and ovalbumin on the weak anion exchanger DEAE Sepharose FF. The adsorption of ovalbumin was predicted well using both models whereas that of human serum albumin could only be predicted using the film and pore diffusion model. Chen *et al.* (2002) studied the adsorption kinetics of BSA and gamma-globulin to an anion-

exchanger DEAE Spherodex M using batch adsorption experiments. Various models; namely pore diffusion, surface diffusion, homogeneous diffusion and parallel diffusion were analysed and tested for their feasibility to predict the experimental adsorption profiles. The surface and homogeneous diffusion models failed to predict the BSA adsorption profile, since the adsorption isotherm of BSA is rectangular which entails that surface diffusion is not rate limiting. Both models, however, were able to predict the adsorption profile of gamma-globulin. On the other hand, the adsorption kinetics of both proteins were well predicted by both the parallel and the pore diffusion models. The same author (Chen *et al.*, 2003) studied the effect of the initial protein concentration and adsorption density on the pore diffusivity. It was found that the rate of pore diffusion decreased exponentially with increasing protein adsorption density. Moreover, the pore diffusivity decreased with increasing the initial protein concentration because of the increase of the adsorption density or the steric hindrance effect for the proteins.

For multi-component systems, Lewus and Carta (1999b) investigated the kinetics of two-component protein adsorption on the cation exchanger S HyperD-M for mixtures of cytochrome c and lysozyme. S HyperD-M comprises porous silica particles whose pores are filled with a charged poly (acrylamide) gel. The observed adsorption kinetics were found to be consistent with diffusional transport through a tight fitting charged gel mesh. Thus, single and two-component mass transfer rates were described in terms of a homogeneous diffusion model, where the driving force for diffusion was given by the adsorbed protein concentration gradient. Accordingly, the ensuing intraparticle concentration profiles were predicted to be smooth (i.e. have homogeneous fluorescence intensity distribution). Based on microscopic visualisation studies with capillary supported gels, the existence of such smooth profiles consistent with the homogeneous diffusion model was later confirmed experimentally for both single and multicomponent systems (Lewus and Carta, 1999a; Lewus and Carta, 2001; Russel *et al.*, 2003; Russel and Carta, 2005). A theoretical study of two-component protein adsorption in spherical ion exchange particles was reported by Gallant (2004) based on the numerical solution of a pore diffusion model. Garke *et al.* (1999) investigated the influence of protein size on the adsorption kinetics of lysozyme and gamma-globulin on the strong cation-exchanger Streamline SP. The kinetics were modelled using the film and pore diffusion model,

taking into account diffusion across the liquid film and within the adsorption pores. It was shown that the effective pore diffusion coefficients of both proteins depend on the total protein concentration and the concentration ratio of the competing proteins in the liquid phase. In the binary mixture, the diffusion rate of the faster diffusing protein, lysozyme, was slowed down by the lower diffusion rate of the larger protein, gamma-globulin. Coetzee and Petersen (2005) described a simplified resistance model for reversible multicomponent ion-exchange. The study investigated the use of a simple film-diffusion mechanism to describe mass-transfer kinetics. Furthermore, a simplified Fritz and Schleunder isotherm was used to overcome complex iterative techniques in order to obtain equilibrium conditions at the solid/liquid interface. The procedure was evaluated using a chelating resin in a ternary system and proved to be very effective with reversibility well explained. Martin *et al.* (2005) studied the two-component protein adsorption kinetics of a binary mixture of lysozyme and cytochrome c in the porous cation-exchanger SP Sepharose FF. The experimental batch uptake results showed that the two proteins were competitively adsorbed and that an overshoot of adsorbed cytochrome *c* occurred during simultaneous adsorption. Model predictions based on the assumption that the adsorption isotherms are rectangular and that lysozyme completely displaces cytochrome *c* were in qualitative and quantitative agreement with the experimental kinetics suggesting that the overshoot phenomena observed with multicomponent systems in these resins can be explained with a diffusion model without the need to account for flux coupling or electrophoretic contributions to transport.

Confocal laser scanning microscopy is an important modern technique for the study of protein adsorption within chromatographic beads. Originally introduced by Ljunglöf and Hjorth (1996), it has become popular as it allows direct observation of protein adsorption patterns within optically transparent beads (Stone and Carta, 2007). Ljunglöf and Hjorth (1996) studied the adsorption of protein A to IgG Sepharose 6 Fast Flow. Hubbuch *et al.* (2003) carried out an experimental study on the interplay of sorbent structure and fluid phase conditions in the single- and two-component adsorption and transport of BSA and IgG 2a on SP Sepharose FF and SP Sepharose XL. Harinarayan *et al.* (2006) performed capacity measurements on two different commercial ion-exchange resins with three different monoclonal antibodies at various pH and conductivity values.

Linden *et al.* (2002) investigated the effect of pH and ionic strength on the uptake profiles of BSA and monoclonal antibody. Boushaba *et al.* (2007) used dual fluorescence CLSM to visualise the binding of a fluorescently labelled polyclonal ovine anti-fluorescein $F(ab')_2$ antibody to immobilised fluorescein. Ljunglöf and Thommes (1998) studied protein uptake for lysozyme and human IgG to two different porous adsorbents during batch experiments in a finite bath. Results from direct confocal microscopy measurement corresponded well to the data obtained from indirect fluid phase measurements. However, other authors reported that the techniques used in CLSM, particularly the need to use dye-labelled protein to achieve protein visualisation, can alter the adsorption properties of the protein (Russel and Carta, 2005; and Ljunglöf *et al.*, 2006) leading to artefacts. In addition, it was shown that competition between dye-labelled and native protein molecules for the adsorption sites results in apparent adsorption patterns that exhibit either overshoots when the native protein is more favourably adsorbed, or smooth profiles when adsorption of the labelled protein is favoured (Teske *et al.*, 2005; Gallant, 2004; Martin *et al.*, 2005; and Teske *et al.*, 2006). For the two-component systems, Linden *et al.* (1999) were the first to use CLSM to visualise the two-component diffusion of two labelled proteins within a porous stationary phase. They studied the finite bath uptake of bovine serum albumin and human immunoglobulin G to two different ion-exchange adsorbents and to an affinity adsorbent.

6.2 Traditional method

The discussion below deals first with single-component adsorption where only one protein is present, and will be followed by the two-component system involving a mixture of the two proteins.

6.2.1 Single-component studies

In this section and the following one, the adsorption kinetics of each of ALA and BLG onto SP Sepharose FF were mainly studied at pH 3.7, settled exchanger volume to solution volume (v/V) ratio of 1:14, and initial concentrations of ALA and BLG (C_o) of 1.5 and 3 mg/ml, respectively; these are approximately the concentrations of these two proteins that are normally found in whey. However to further elucidate the nature of the

adsorption process, the effects of the initial concentration as well as the v/V ratio were investigated in a separate Section (Section 6.2.3). It is to be stressed that these experiments 'approach' rather than 'reach' equilibrium, as they were performed only for a time duration that did not exceed 4 hours. Therefore the values of the time taken to reach equilibrium (where the curve flattens out) as well as the actual equilibrium position (equilibrium concentration) will not necessarily equal their corresponding values achieved in equilibrium batch experiments. They are expected though to eventually reach these values when given equivalent period of time (overnight or 18 hours).

The experimental and theoretical time courses for ALA and BLG uptake are depicted in Figures 6.1A and 6.1B, respectively. The theoretical profiles were predicted by the simple kinetic model (Section 3.2.1.1) and the estimated values of k_1 that gave the best fit to the experimental results were found to be $30*10^{-3}$ $mlmg^{-1}min^{-1}$ and $35*10^{-3}$ $mlmg^{-1}min^{-1}$ respectively for ALA and BLG. As judged from these values, the adsorption of BLG is expected to be faster than that of ALA.

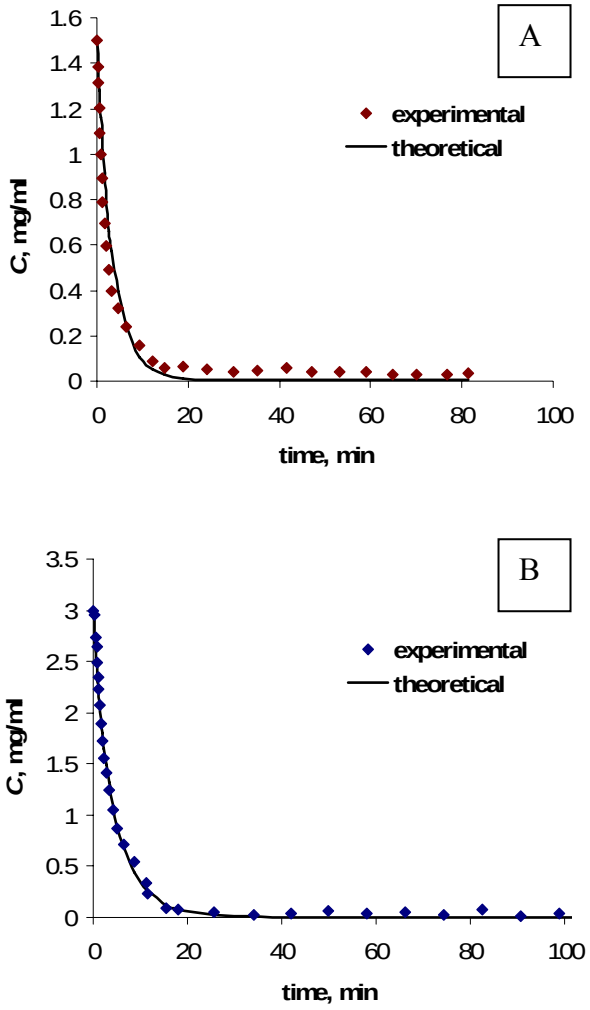

Figure 6.1 Experimental and predicted time courses of ALA (A) and BLG (B) uptake onto SP Sepharose FF at *v*/*V* of 1:14, and initial concentrations of 1.5 mg/ml and 3 mg/ml, respectively. The theoretical time courses were predicted using the simple kinetic model and fitted to the experimental results with an accuracy of 3-5%.

The corresponding time courses for the amount of protein adsorbed (q) for ALA and BLG are shown in Figures 6.2A and 6.2B, respectively. As shown in the Figures, the adsorption profile pertaining to BLG flattens out at a maximum value of q (q^* = 40 mg/ml) equal to twice that of ALA (q^* = 20 mg/ml).

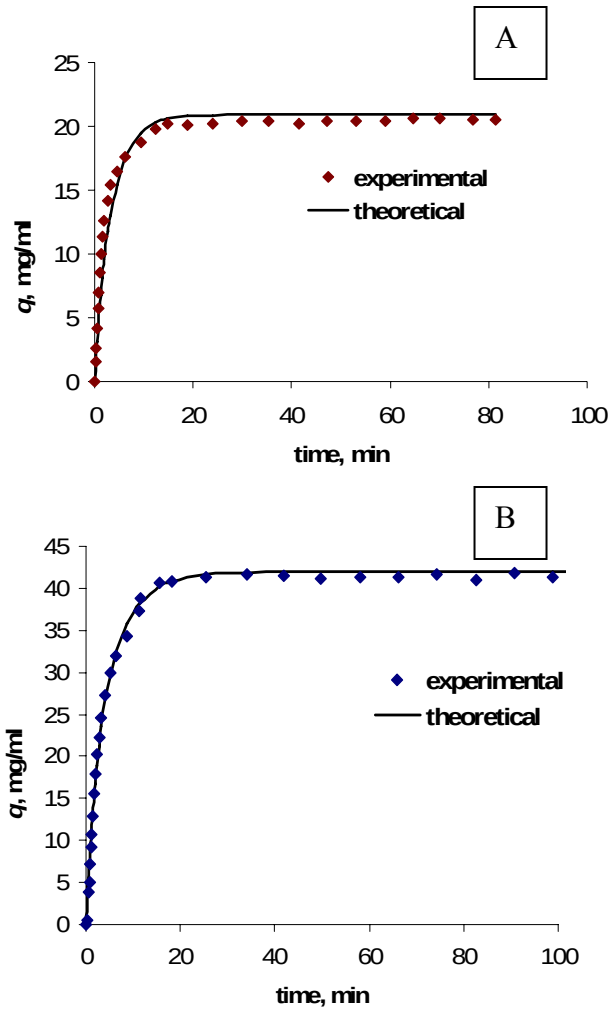

Figure 6.2 Experimental and predicted amount of ALA (A) and BLG (B) adsorbed onto SP Sepharose FF as a function of time at *v*/*V* of 1:14, and initial concentrations of 1.5 mg/ml and 3 mg/ml, respectively. The theoretical profiles were predicted by the simple kinetic model and fitted to the experimental results with an accuracy of 3-5%.

Alternatively, ALA and BLG adsorption profiles were predicted by the pore diffusion model as shown in Figures 6.3A and 6.3B, respectively.

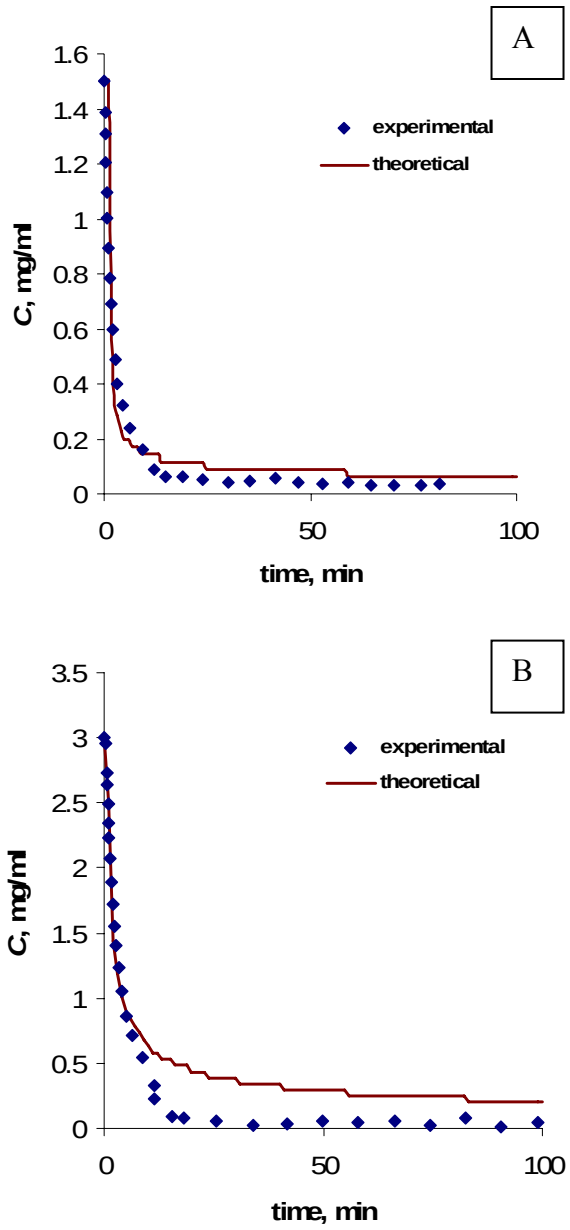

Figure 6.3 Experimental and predicted time courses of ALA (A) and BLG (B) uptake onto SP Sepharose FF at *v*/*V* of 1:14, and initial concentrations of 1.5 mg/ml and 3 mg/ml, respectively. The theoretical time courses were predicted by the pore diffusion model.

For BLG, the theoretical prediction did not agree well with the experimental results as the model only predicted the initial stages of adsorption with accuracy within 5%. The theoretical profiles for ALA were in fair agreement with the experimental results with accuracy within 5-10%. This indicates that the kinetics of BLG is better described

by the simple kinetic model, whereas that of ALA can be described by both the simple kinetic model and the pore diffusion model. The estimated diffusivities for ALA and BLG were $0.01*10^{-10}$ m^2/s and $0.002*10^{-10}$ m^2/s (their molecular diffusivities in free solution were $1.15*10^{-10}$ m^2/s and $0.08*10^{-10}$ m^2/s, respectively). The diffusivity of ALA is larger than that of BLG which implies that the adsorption of ALA appears to be five times faster than that of BLG. This is contradictory to the results obtained earlier using the simple kinetic model, where the value of k_1 for BLG was larger than that of ALA. This discrepancy would be expected in light of the fact that the pore diffusion model failed to predict the BLG adsorption profile. In view of the above, the simple kinetic model will be adopted for the remainder of this study.

6.2.2 Two-component studies

The time courses for the total and individual uptakes of ALA and BLG in a binary mixture onto SP Sepharose FF, at pH 3.7 and *v*/*V* of 1:14 and initial concentrations of 1.5 and 3 mg/ml, respectively are shown in Figure 6.4.

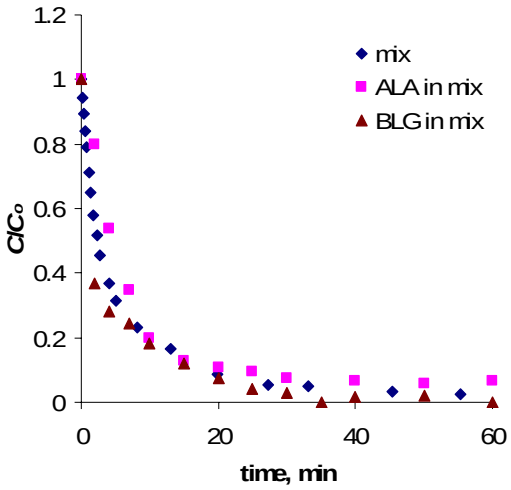

Figure 6.4 Experimental time courses for the total uptake of both ALA and BLG in a binary mixture, together with their individual uptakes onto SP Sepharose FF at pH 3.7, *v*/*V* of 1:14, and initial concentrations of 1.5 and 3 mg/ml, respectively.

To obtain the individual batch uptake adsorption profiles for each of ALA and BLG, 1-ml fractions were withdrawn from the initial sample volume during the course of

the experiment, centrifuged at 3000g for 5 min, and then analysed on the size-exclusion chromatography system to determine the concentrations of the collected fractions. The plot of these concentrations relative to the initial concentration, C/C_o, with time represents the individual batch uptake adsorption profiles for ALA and BLG (Figures 6.5A and 6.5B). Each of these profiles is compared to its respective counterpart pertaining to the pure protein (single-component system), obtained earlier, as presented in Figures 6.5A and 6.5B, respectively. The theoretical adsorption profiles of ALA and BLG in mixture were predicted by the simple kinetic model and the k_1 values so obtained were $15*10^{-3}$ $mlmg^{-1}min^{-1}$ and $25*10^{-3}$ $mlmg^{-1}min^{-1}$ for ALA and BLG, respectively. Evidently, the values of k_1 in the two-component system decreased by about 50% and 30% compared to their values in single-component systems ($30*10^{-3}$ $mlmg^{-1}min^{-1}$ and $35*10^{-3}$ $mlmg^{-1}min^{-1}$) for ALA and BLG, respectively.

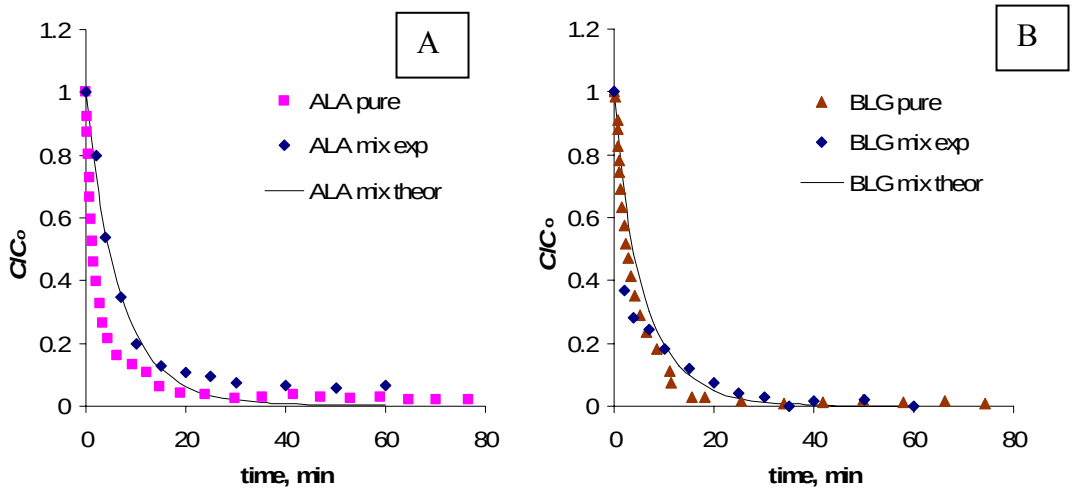

Figure 6.5 Experimental and predicted time courses for 1.5 mg/ml ALA (A) and 3 mg/ml BLG (B) uptake, when applied in a binary mixture of both ALA and BLG onto SP Sepharose FF at pH 3.7 and *v/V* of 1:14. The corresponding experimental time courses for ALA and BLG in single-component systems are also shown.

In order to predict the adsorption profile for the total concentration of ALA and BLG in mixture, q_m and K_d values for the mixture were estimated. The q_m value for the mixture of ALA and BLG was determined as the arithmetic mean of the two individual q_m values of the two pure proteins. K_d for the mixture, on the other hand, was calculated as the geometric mean of the individual K_d values (because K_d is an intensity parameter rather than a capacity one). The simple kinetic model was solved using the values of q_m

and K_d for the mixture. The value of k_1 was taken to be the one that gave the best fit to the experimental data (Figure 6.6), and was found to be $33*10^{-3}$ $mlmg^{-1}min^{-1}$, which is approximately the weighted-average of the two k_1 values of pure ALA ($30*10^{-3}$ $mlmg^{-1}min^{1}$) and BLG ($35*10^{-3}$ $mlmg^{-1}min^{-1}$) obtained earlier. As can be seen from the figure, the model only predicted the early part of the experimental batch uptake profile with accuracy within 5%, but failed to predict the later stages where adsorption approaches equilibrium. This discrepancy between the predicted and experimental results could point to presence of a strong competitive adsorption between the two proteins that was not considered in this treatment. Therefore, the difference that appeared between the single-component and the two-component batch uptake profiles pertaining to each protein would thus be expected (Figures 6.5A and 6.5B).

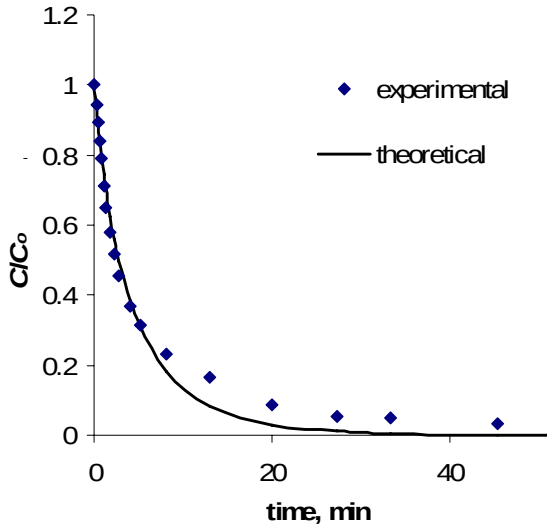

Figure 6.6 Predicted and experimental batch uptake profiles for a mixture of ALA and BLG onto SP Sepharose FF at *v*/*V* of 1:14, pH 3.7 and initial concentrations of 1.5 and 3 mg/ml, respectively.

6.2.3 Effect of initial concentration and *v*/*V* ratio

Traditional batch uptake experiments were performed at different initial concentrations of ALA and BLG and *v*/*V* ratio of 1:14. The concentrations were chosen to be in a range close to the normal concentrations of the two proteins in whey. The corresponding adsorption profiles were constructed and the values of q^* so obtained were

plotted against the corresponding values of the initial concentration (Figure 6.7). As can be seen from the q^*-C_o plot in Figure 6.7, q^* increases linearly with increasing C_o for both ALA and BLG in the employed range of concentrations. The rate of increase, i.e. the slope of the line, is constant for both proteins and has a value of 13.5.

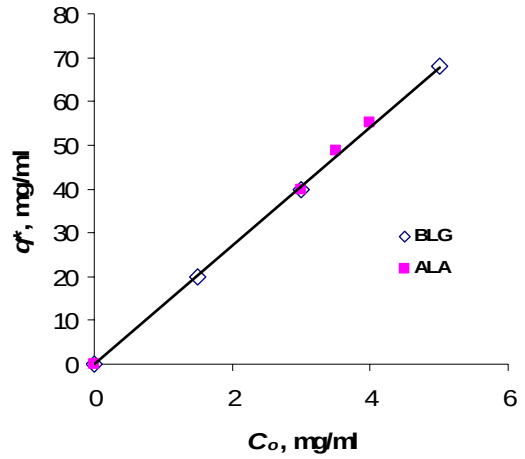

Figure 6.7 Effect of the initial concentration of ALA and BLG on the equilibrium adsorption capacity q^* at v/V of 1:14.

It should be noted that at higher values of v/V ratio and wider range of initial concentrations, the q^*-C_o relation for BLG is not linear as shown in Figure 6.8. It could, however, be approximated to a linear relation at low concentrations.

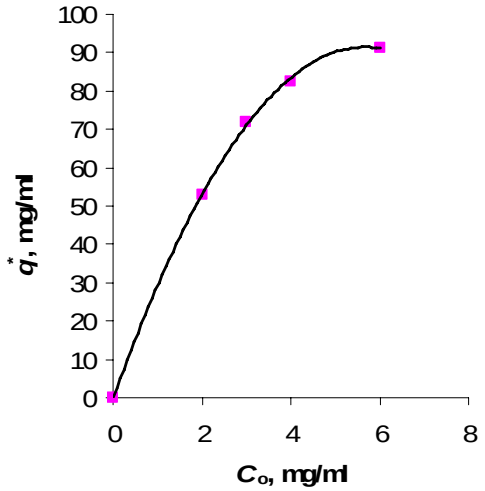

Figure 6.8 Effect of the initial concentration of BLG on the equilibrium adsorption capacity q^* at v/V of 1:27.

The effect of initial concentration on the rate of BLG uptake is shown in Figure 6.9. The rate of uptake increases with increasing initial concentration. The same behaviour holds true for ALA as will be shown later in Figure 6.15B.

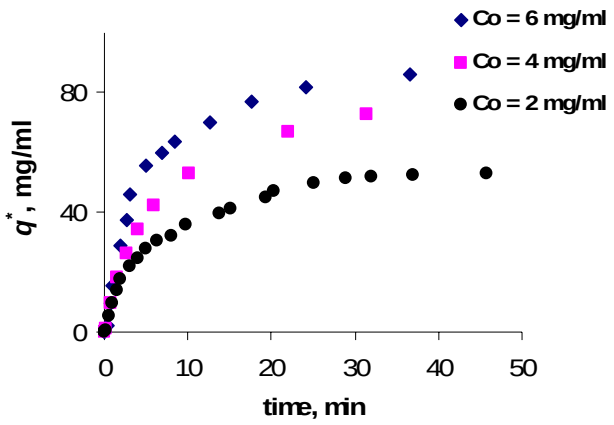

Figure 6.9 Effect of initial concentration on time course of BLG uptake onto SP Sepharose FF at *v*/*V* of 1: 27 and pH 3.7.

Table 6.1 shows the values of q^* for ALA and BLG at different values of initial concentration and *v*/*V* ratio. For each protein, two sets of *v*/*V* ratios each corresponding to one initial concentration are presented.

Table 6.1 Effect of *v*/*V* on the values of q^*.

		v/*V*	Q^* (mg/ml)
ALA	C_o = 1.5	1:14	20.0
		1:42	60.0
	C_o = 5.0	1:14	89.0
		1:17	109.0
BLG	C_o = 3.0	1:14	40.0
		1:27	71.7
	C_o = 4.0	1:14	55.1
		1:27	82.5

For a constant initial concentration of ALA, it is clear that q^* increases proportionally with dilution (i.e. decreasing v/V ratio). The same does not hold true for BLG particularly at an initial concentration of 4 mg/ml. This indicates that the q^*-v/V relation for BLG particularly at higher concentrations is probably not linear, a behaviour similar to that was encountered earlier with the q^*-C_o relation of the same protein (Figure 6.8).

The effect of the v/V ratio on the rate of uptake for ALA and BLG is similar to that of the initial concentration.

6.3 Confocal microscopy method

The results herein are reported on the location and amounts of adsorbing proteins within adsorbent beads of diameters 80-90 μm that represent the average of the bead size distribution normally present in SP Sepharose FF. Larger-size (90-120 μm) and smaller-size (60-80 μm) beads were also inspected but the significance of the modest differences observed are discussed in a separate forthcoming subsection (Section 6.3.3).

Furthermore, the main set of experiments were conducted at a settled exchanger volume to solution volume, v/V, ratio of 1:14 using initial protein concentrations of 3 mg/ml and 1.5 mg/ml for BLG and ALA, respectively. Other values for these two variables (v/V ratio and initial protein concentration) were used only in the section entitled 'additional exploratory experiments on the adsorption of ALA' (Section 6.3.1.1).

6.3.1 Single-component studies

Figure 6.10 shows two sets of time courses of confocal scans of beads of SP Sepharose FF incubated with either 3 mg/ml of fluorescently-labelled BLG (Figure 6.10A) or 1.5 mg/ml of fluorescently-labelled ALA (Figure 6.10B). The proteins were adsorbed at pH 3.7 and a v/V ratio of 1:14. The scans of samples withdrawn at different times, demonstrate the time course of penetration of the dyed-protein through the adsorbent particle.

A)

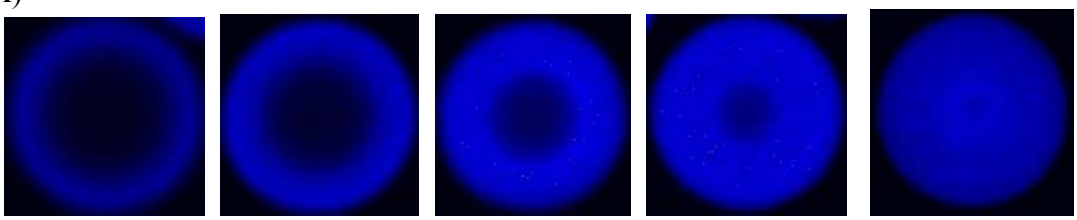

t = 1 min t = 2 min t = 15 min t = 60 min t = 18 h

B)

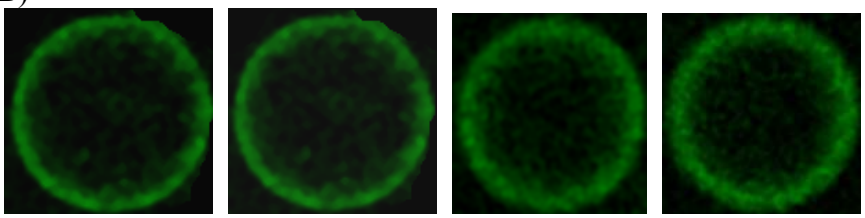

t = 5 min t = 20 min t = 2 h t = 18 h

Figure 6.10 Time series of confocal microscopy scans describing the binding of 3 mg/ml pure BLG (A) and 1.5 mg/ml pure ALA (B) at *v*/*V* of 1:14 to SP Sepharose FF beads at pH 3.7 and medium particle size of the adsorbent.

For BLG, the confocal images revealed that the protein was adsorbed in a shell-wise fashion where it was first bound initially solely to the outer parts of the bead and then gradually filled the whole volume of the bead from the outermost region towards the centre of the bead. ALA, on the other hand, was observed to adsorb initially to the outer surfaces of the adsorbent beads in a shell-wise fashion. The thickness of the shell ($\Delta r = r_o - r_i$) increased gradually with time, with its inner edge progressing a little way towards the centre of the particle. Unlike BLG, ALA did not fill the entire volume of the beads under these experimental conditions. The images show the penetration of protein into the bead, for BLG in the form of a steady incursion reminiscent of the shrinking core model in catalysis (Levenspiel, 1972), while for ALA it shows a shell which does not penetrate further. These cannot be compared with the simple kinetic model as this does not predict the distribution of protein within the bead. Inspection indicates that $(\Delta r)^4 = k\ t$ for both proteins which is not given by standard models. The proportionality constant (k) for BLG was much higher than that of ALA which is consistent with the faster adsorption for BLG.

The corresponding fluorescence intensity profiles across the particle radius are shown in Figure 6.11. Each plot in this figure embodies a set of intensity-distance curves at different times. The general trends displayed in these plots were in accord with the qualitative information discernable from the scans in Figure 6.10.

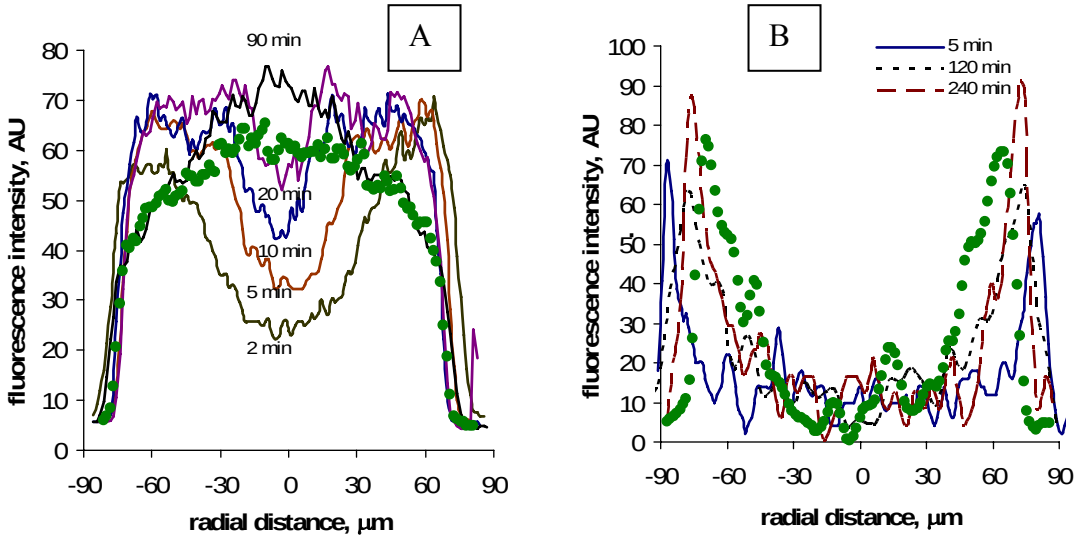

Figure 6.11 Fluorescence intensity profiles for the images in Figure 6.10 pertaining to BLG (A) and ALA (B). Green circles represent the fluorescence profiles after 18 hours.

In Figure 6.11 plot (A) pertaining to BLG, a sharp adsorption front was observed at 2 min. It then became shallower with time until it eventually flattened out (i.e. the particle was completely and homogeneously filled with BLG). The curve then exhibited an overshoot at 90 min. Overshoots are defined as adsorbed phase concentrations that are higher at certain radial positions within the particle compared with positions nearer the particle surface (Ljunglöf *et al.*, 2006). The overshoot phenomenon was also encountered by Hubbuch *et al.* (2003) when studying the adsorption of IgG 2a to SP Sepharose FF at pH 4.5. The dynamics of protein adsorption and transport were described by the latter authors as a 'wave' of molecules building up towards the inner section of the bead and leading to an overshoot in the centre of the particle. The overshoot observed in case of BLG supports the earlier finding that the transport mechanism of this protein is not a pore-diffusional one as $\partial c / \partial r \neq 0$ at the particle centre.

From the fluorescence intensity profile of BLG, it can be deduced that some of the BLG-AlexaFluor 467 originally bound at the outer rim of the support is subsequently transported to the inner part of the sorbent. This is evident from the decrease of the intensity observed at the outer shell and the development of a 'wave-like' profile at the inner section of the support before resulting in an overshoot in the centre of the support.

The overshoot was found to be temporary, especially since it was followed by the establishment of an apparent equilibrium situation, where a homogeneous sorption profile over the whole particle radius was observed.

Different explanations have been given to the overshoot phenomenon. Grimes and Liapis (2002) constructed a model to show how the interplay of diffusive and electrophoretic transport mechanisms affect functioning of the electrical double layer present inside pores of charged adsorbent particles and hence could contribute to the 'overshoot' behaviour. Dziennik *et al.* (2003) discussed an electrokinetic contribution to the transport in ion-exchange particle and found that the 'overshoot' effect could be correlated to high adsorbent surface charge densities. Liapis *et al.* (2001); and Zhang *et al.* (2004) included an additional contribution to the transport equations from a double-layer-induced electrophoretic transport mechanism. Recently, other workers (Martin *et al.*, 2005; Carta *et al.*, 2005; and Teske *et al.* (2005, 2006)) have proposed that the overshoot is caused by the displacement of weaker-binding fluorescently-labelled protein by its stronger-binding unlabelled native counterpart.

In Figure 6.11 plot (B) pertaining to ALA, the sharp adsorption front present at the beginning of adsorption (5 min) did not get much shallower with time. The reason for this could possibly be the low concentration of ALA in solution (only half the concentration used in the experiments with BLG), since if all or most of ALA had been taken up by the adsorbent in the early stages of the experiment, none or very little would be left in solution to penetrate further within the bead (depletion effect). This hypothesis will be tested in a forthcoming subsection.

Integrating the intensity profiles of Figure 6.11 yielded F_{ring} (AU), which was then converted to the fluorescence intensity within the shell, F_s, and then normalised to give R_F. For each protein, the R_F-t plot in Figure 6.12 is compared to the R_q-t curve obtained from traditional batch uptake experiments (solid discrete circles in the figure). For BLG (Figure 6.12A), the R_F-t plot was in good agreement with its R_q-t counterpart. It is to be noted that the theoretical prediction of the shape of the R_q-t curve using the simple kinetic model with the best-fit estimate of k_1 of $35*10^{-3}$ $mlmg^{-1}min^{-1}$ (solid line) was also in good accord with the experimental results. For ALA (Figure 6.12B), there was no agreement between the R_q-t and the R_F-t profiles. The theoretical prediction of the R_q-t curve from

the simple kinetic rate model yielded a curve that was in good agreement with the experimental R_q-t results (Figure 6.12B, solid line). The best-fit value of k_1 for this curve was found to be $30*10^{-3}$ ml $mg^{-1}min^{-1}$.

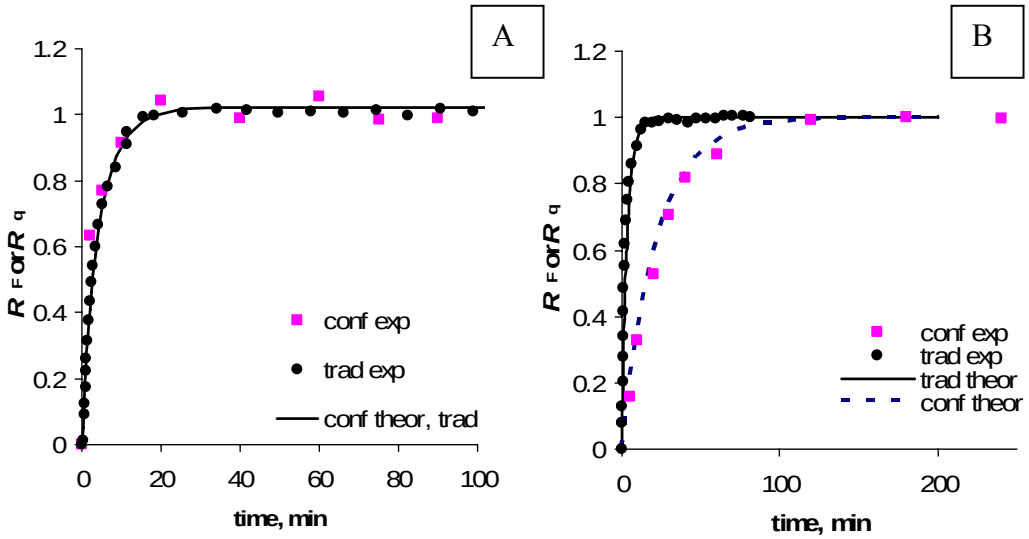

Figure 6.12 Fractional approach to equilibrium during finite bath adsorption of 3 mg/ml BLG (A) and 1.5 mg/ml ALA (B) to medium particle-size SP Sepharose FF at pH 3.7 and *v*/*V* of 1:14.

In order to corroborate the confocal microscopy findings quantitatively, an attempt was made to derive a rate constant for the kinetic uptake profiles for BLG and ALA obtained from the microscopic measurements of adsorbed protein profiles using the simple kinetic model described earlier. The model reasonably predicted the protein uptake profile throughout the entire duration of the protein adsorption experiment (Figure 6.12). The best-fit values of k_1' were found to be $36*10^{-3}$ ml $mg^{-1}min^{-1}$ and $4*10^{-3}$ ml $mg^{-1}min^{-1}$ for BLG and ALA, respectively. The value of k_1' for BLG was approximately equal to that obtained using the traditional method (k_1), while k_1' for ALA was considerably lower which is consistent with the qualitative disagreement observed in Figure 6.12B.

The discrepancy between the R_q-t and the R_F-t profiles in the case of ALA could be due to a competitive adsorption taking place between the native unlabelled proteins and their fluorescently-labelled counterparts. In this case, the unlabelled protein (presumed to be bound less strongly to the adsorbent) could have been adsorbed more

quickly onto the bead at the start of the experiment and was later displaced by the more strongly-bound labelled variant. The implication is that unlabelled proteins were adsorbed to the bead at the beginning of the experiment, but could not be detected by the microscope. This could also explain the low rate of ALA penetration as well as the apparent inability of ALA to penetrate deep within the bead. If so, the opposite effect could explain the overshoot observed earlier with BLG, where the labelled protein could possibly have been adsorbed first and then later displaced by its unlabelled counterpart. The above suggestions imply that the conjugation of the protein with a fluorophore can affect its adsorption characteristics as has already been pointed out earlier by a number of workers (Teske *et al.*, 2005; Russel and Carta, 2005; and Ljunglöf *et al.*, 2006). There is a possibility that the risk of alteration of the mass transfer properties may be higher when working with low-molecular weight proteins (compared to large molecules like antibodies). Ljunglöf *et al.* (2007) showed that labelling of an antibody fragment slightly affects its mass transfer properties as judged from the relevant values of the retention factors of labelled and unlabelled proteins obtained using gradient elution.

According to this argument, the lack of agreement in case of ALA could well be an indication that the presumed effect of the presence of the fluorophore covalently attached to the protein on the adsorption characteristics is more pronounced for this protein than it was for BLG.

6.3.1.1 Additional exploratory experiments on the adsorption of ALA

Further experiments were conducted in order to elucidate the nature of the binding of ALA to the adsorbent as well as to understand the reason behind the different behaviour, relative to BLG, that ALA exhibited with regard to the characteristics of penetration within the adsorbent beads. Adsorption of fluorescently-labelled ALA both at a lower v/V ratio of 1:42 maintaining a concentration of 1.5 mg/ml, and at a higher concentration of 3 mg/ml maintaining a v/V ratio of 1:14 was investigated. Lowering v/V ratio by one third without changing the concentration triples the number of ALA molecules in solution and thus avoids the suspected depletion alluded to earlier. The confocal scans for these two situations are given in Figure 6.13.

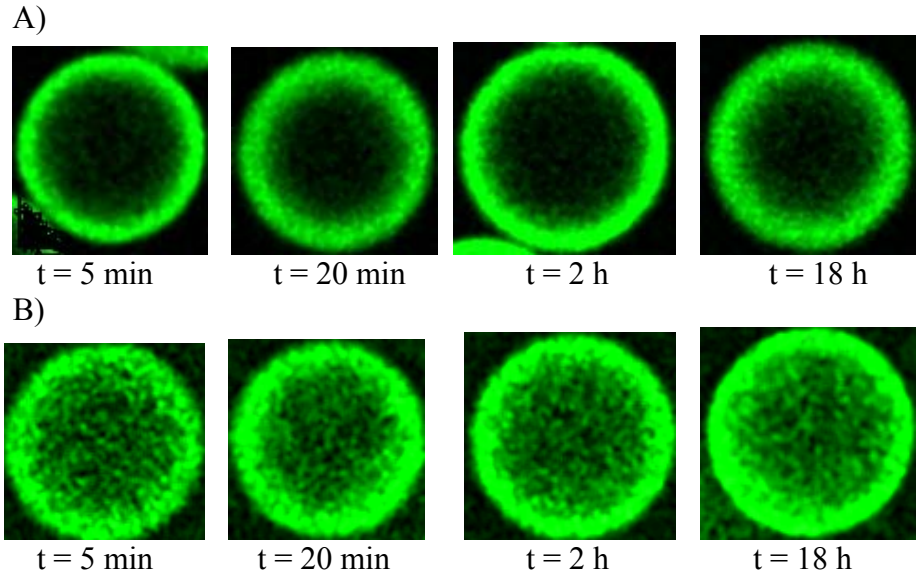

Figure 6.13 Time series of confocal microscopy scans describing the binding of pure ALA to SP Sepharose FF beads at pH 3.7 using A) 1.5 mg/ml and *v*/*V* of 1:42, and B) 3 mg/ml and *v*/*V* of 1:14 at a medium particle size of the adsorbent.

Regarding the effect of reducing *v*/*V* (Figure 6.13A), ALA appears to be adsorbed to the outer regions of the particles in a shell-wise fashion as was previously observed with *v*/*V* of 1:14, but still did not penetrate to the centre of the beads.

As to the effect of doubling the initial ALA concentration in solution (Figure 6.13B), ALA seems to be first adsorbed to the outer rim of the adsorbent bead in a shell-wise fashion, while some ALA molecules randomly penetrated to the innermost regions of the bead in an uneven manner resulting in distinct "areas" where ALA appeared to be adsorbed, and other areas apparently devoid of ALA molecules. With time, the thickness of the fluorescent shell increased slightly and more ALA molecules were observed to penetrate deeper into the beads again in the same uneven, "granular" manner as described immediately above.

The relevant fluorescence intensity profiles (Figure 6.14) support the confocal imaging results. The profile pertaining to ALA at *v*/*V* ratio of 1:42 (Figure 6.14A) shows almost the same intensity maxima as those detected at a *v*/*V* ratio of 1:14. In addition, the thicknesses of the fluorescent shells were slightly increased relative to those obtained with the reference value of the *v*/*V* ratio. A sharp front was observed at the beginning and

remained the same throughout the entire period of the experiment. This shows that with decreasing *v*/*V*, more ALA was bound to the outermost region of the adsorbent bead but it did not penetrate any further into the centre.

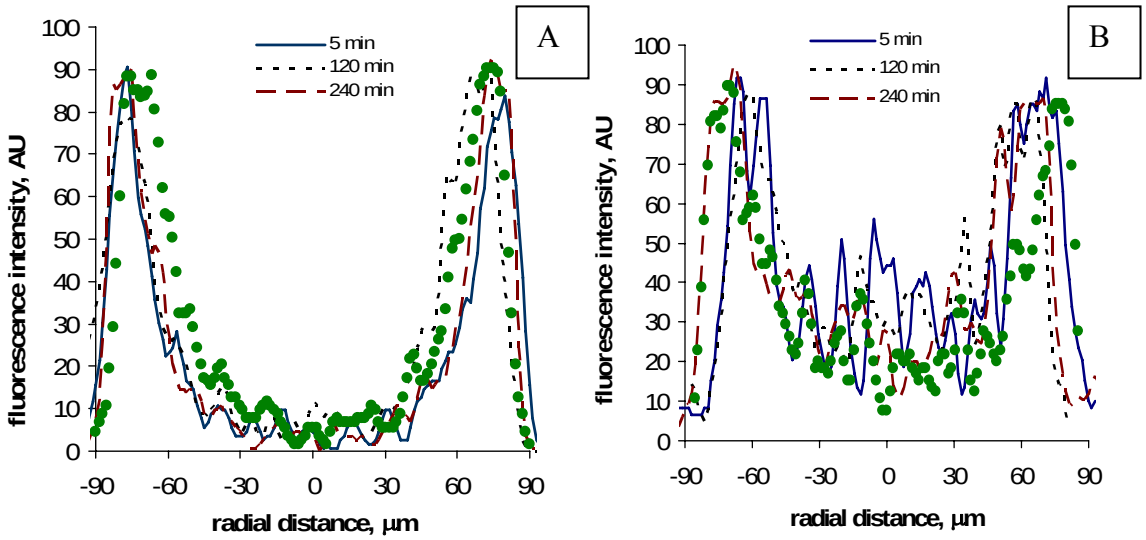

Figure 6.14 Fluorescence intensity profiles for 1.5 mg/ml ALA and *v*/*V* of 1:42 (A) and 3 mg/ml BLG and *v*/*V* of 1:14 (B) at medium particle size of the adsorbent. Green circles represent the fluorescence profiles after 18 hours.

The fluorescence intensity profile pertaining to 3 mg/ml ALA (Figure 6.14B) shows substantially higher fluorescence intensity at the adsorption front but almost the same values of the intensity maxima as was shown by the profile of ALA obtained from experiments conducted at 1.5 mg/ml (Figure 6.11B). A comparison of the *F*-*t* curves (for simplicity F_s-*t* curves will be henceforth referred to as *F*-*t* curves) (CLSM method) and the *q*-*t* curves (traditional method) obtained for the different ALA uptake conditions is shown in Figures 6.15A and 6.15B, respectively. One feature that is common to all these curves is related to the rate of uptake.

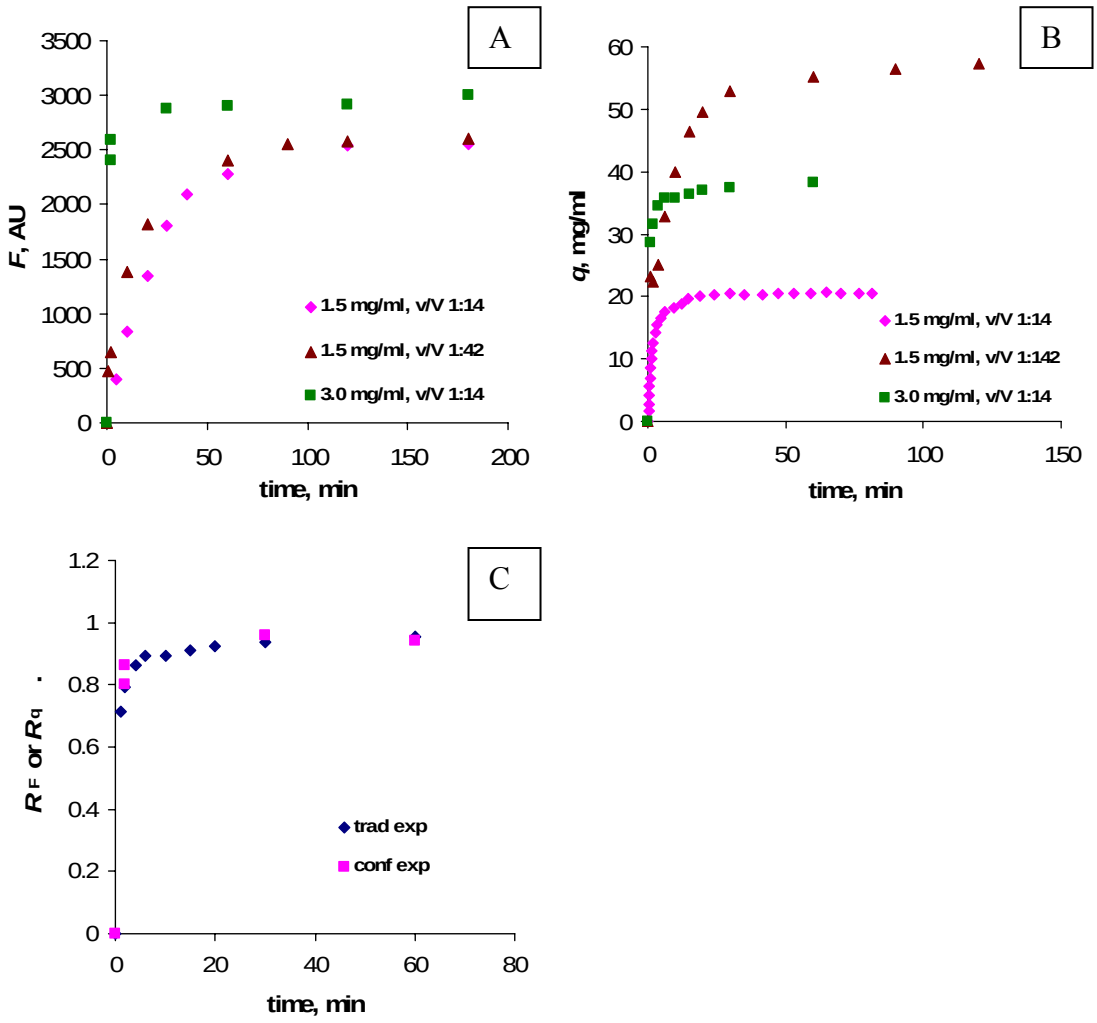

Figure 6.15 Comparison between *F*-*t* curves (A) and *q*-*t* curves (B) for the different ALA adsorption experiments involving the medium particle size (80-90 μm). The normalised curves at 3 mg/ml and *v*/*V* of 1:14 are also compared (C).

Judging from the inclination of the curves in Figures 6.15A and 6.15B, it is deduced that the confocal and traditional methods yielded the same trend for the rate of uptake: doubling the concentration > reducing *v*/*V* > reference condition. The increase in the rate of uptake upon reducing *v*/*V* corroborates the previous suspicion that the number of protein molecules in the original solution was limited and significant depletion might have occurred as a result of adsorption. The confocal (Figure 6.15A) and traditional (Figure 6.15B) results differ in one respect namely the value of their maxima. The traditional maxima varied linearly with the initial ALA concentration since the q^* value

doubled as the initial ALA concentration doubled and tripled as the initial number of ALA molecules tripled. This was not the case for the confocal maxima (F^*) and the implied lack of proportionality between F^* and q^*precluded obtaining the confocal rate constants for these situations. It is of interest, however, to note that when the two curves (*F-t* and *q-t*) pertaining to the doubled concentration were normalised, they agreed well (Figure 6.15C). The indication is that the discrepancy which was encountered in Figure 6.12B for ALA at the reference condition disappeared. This suggests that the effect of dye-conjugation on the protein adsorption characteristics is related to the protein concentration. Unfortunately, it is necessary to use the reference concentrations for the separation process aspects of this work as these represent the protein concentrations normally found in whey.

6.3.2 Two-component studies

Figure 6.16 depicts the time series of confocal images for a mixture of 1.5 mg/ml ALA and 3 mg/ml BLG when adsorbed to SP Sepharose FF at *v*/*V* of 1:14. As can be seen from the figure, the innermost volume of the beads is mostly filled with BLG (blue) while the outermost is mostly occupied by ALA (green). BLG filled the entire bead in only 5 min. The ALA fluorescent shell (green) became thicker with time as more ALA penetrated toward the centre of the bead. In addition, the blue colour corresponding to the adsorbed BLG became less intense with time as more ALA penetrated toward the innermost regions. This behaviour shows that BLG was apparently adsorbed much faster than ALA at the beginning of each experiment. Afterwards, however, there is clear evidence that ALA was able to displace some of the adsorbed BLG.

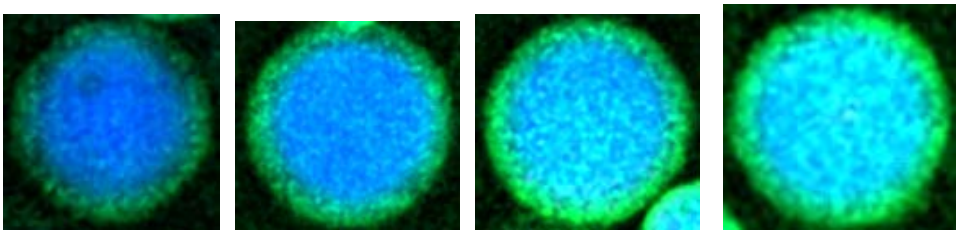

Figure 6.16 Time series of confocal microscopy scans describing the binding of a mixture of 3 mg/ml pure BLG and 1.5 mg/ml pure ALA to SP Sepharose FF beads at pH 3.7 and medium particle size of the adsorbent.

The ALA and BLG fluorescence intensity profiles support this argument (Figure 6.17). The BLG profile in the mixture followed a behaviour similar to that encountered in single-component adsorption. An increase of the locally adsorbed BLG occurred towards the centre, followed by an overshoot in the adsorbed protein concentration towards the centre of the bead and a subsequent decline to a homogeneous equilibrium value. ALA, on the other hand, adsorbed mainly to the outer part of the adsorbent with some molecules penetrating in an uneven manner to the centre of the bead. As more ALA adsorbed to the outermost regions of the particle, the intensity of ALA within the outer shells increased while that of BLG decreased. This indicates that ALA was able to displace previously adsorbed BLG despite the apparently lower affinity of ALA to the adsorbent (as evidenced by its higher K_d value). The value of F for BLG after 18 hours dropped by 20% relative to its maximum value (F^*) (cf. Figure 6.18) which indicates that 20% of BLG that had been adsorbed was subsequently driven off the beads, presumably as a result of successful competition of ALA for the adsorption sites.

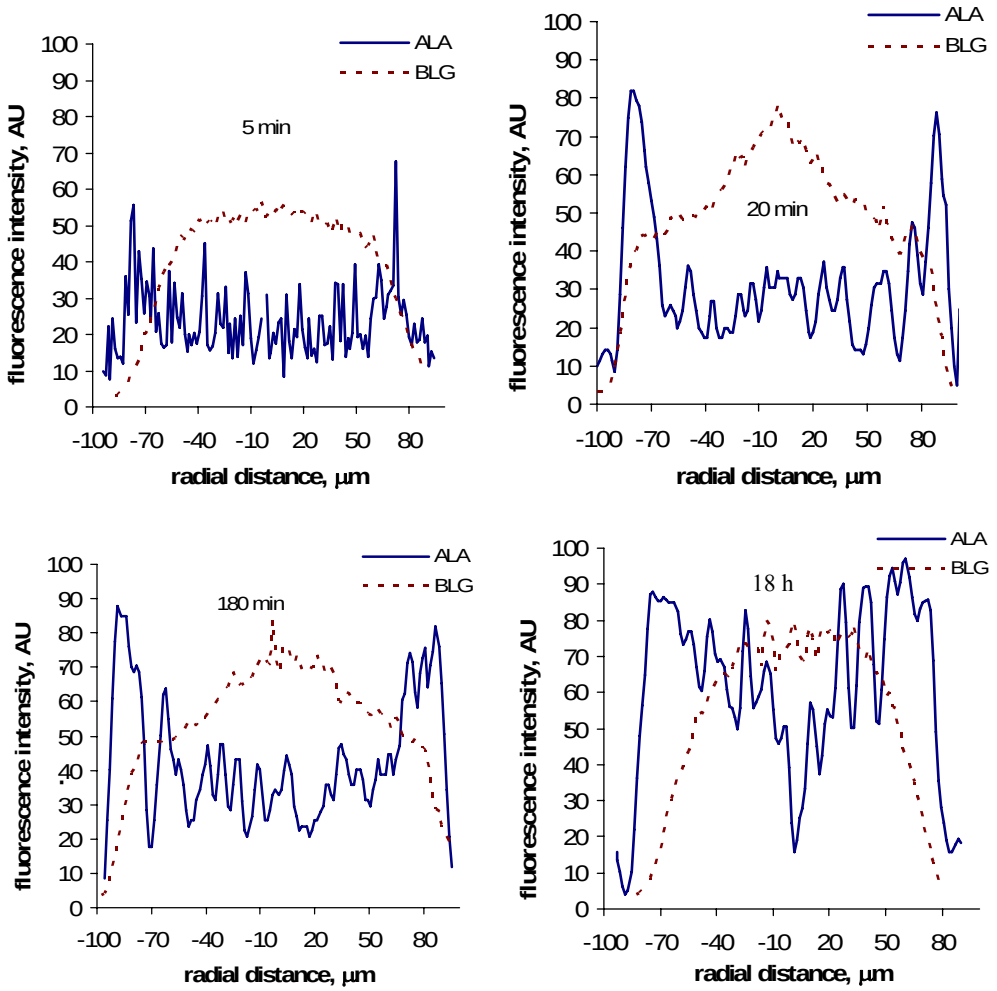

Figure 6.17 Fluorescence intensity profiles for the images in Figure 6.16 at the medium particle-size of the adsorbent.

Similar behaviour was reported by Hubbuch *et al.* (2003) when studying the adsorption of a mixture of IgG 2a and BSA to SP Sepharose XL at pH 4.5. The adsorption front detected for IgG 2a was described by a concentration gradient of bound/accumulated molecules moving towards the centre of the adsorbent followed by an overshoot of bound/accumulated protein at the centre of the bead. The displacement of IgG 2a by BSA in spite of the lower affinity of the latter to the adsorbent was attributed to the different transport mechanisms governing the adsorption of the respective protein molecules; BSA being characterised by a pore-diffusional transport whereas IgG 2a characterised by an electrokinetically-based secondary transport that is non-diffusive.

In the situation at hand, the following explanation is proposed to account for the fact that BLG appeared to be adsorbed much faster than ALA and that the lower-affinity

protein (ALA) was able to displace the higher-affinity one. It is reasonable to assume that the motion of BLG within the porous adsorbent bead is dictated by electrical forces (non-diffusive) while that of ALA is more governed by its concentration gradient (diffusive). Thus the faster-moving BLG gets adsorbed first (cation-exchange of BLG for Na^+) leaving ALA lagging behind. The displacement could be envisaged as another cation-exchange adsorption occurring later when the lingering ALA manages to catch up with the adsorbed BLG. Yet, it would not be possible to assume that the adsorbed BLG so displaced was adsorbed directly on the adsorbent surface since neither the relative K_d values of the two proteins (ALA is larger by a factor of 4), nor their relative concentrations (ALA is lower by a factor of 2) is conducive to such replacement. It is therefore more likely that the belated exchange takes place in the diffuse-layer part of the adsorbed BLG. In complexation parlance, the expelled BLG is conceived to have been an outer-sphere complex separated from the surface by at least one molecular layer of the solvent. The redistribution of ions in this layer that occur when invaded by ALA must lead to the expulsion of BLG in order to maintain electro-neutrality. It seems that the widespread notion that the more-strongly adsorbed (lower K_d) protein would be expected to displace the weaker one needs to be reconsidered. It is only when the mass transfer resistances are not rate-limiting (or the mass transfer rate limitation is the same for both proteins) that we can expect this notion to hold under similar experimental conditions for the two proteins.

The *F-t* curves for ALA and BLG during two-component adsorption to SP Sepharose FF are presented in Figure 6.18. The figure also shows a comparison of the two-component results with their single-component counterparts. Values of the rate constant, k_1', were calculated using the simple kinetic model as was explained previously in the single-component studies. The best-fit values of k_1' for BLG and ALA in the two-component system were estimated to be $23*10^{-3}$ $mlmg^{-1}min^{-1}$ and $2.1*10^{-3}$ $mlmg^{-1}min^{-1}$, respectively (Figure 6.19 and Table 6.2). The table also contains the values of their single-component counterparts as well as the corresponding best-fit values of k_1 obtained from traditional batch uptake experiments. In both confocal and traditional experiments, the value of the rate constant for BLG in mixture decreased to about two-thirds of the value obtained when pure BLG was investigated, whereas the rate constant of ALA in the

mixture dropped to about one half of its value when pure. Evidently, the proportionality between the confocal and traditional results for ALA was realized only when the same experimental conditions of *v*/*V* and initial concentration were maintained whether in the single- or two-component systems which did not hold true when the experimental conditions were varied as shown earlier.

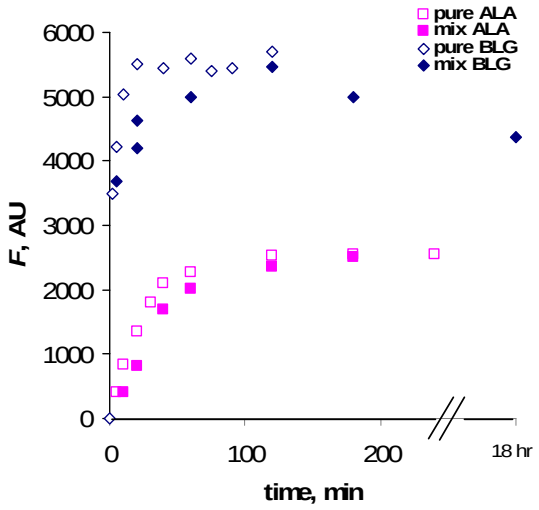

Figure 6.18 *F*-t curves for ALA and BLG during finite bath adsorption when a mixture of 1.5 mg/ml of ALA and 3 mg/ml of BLG at *v*/*V* of 1:14 is adsorbed to SP Sepharose FF of medium particle size. The single-component profiles for both proteins are also shown.

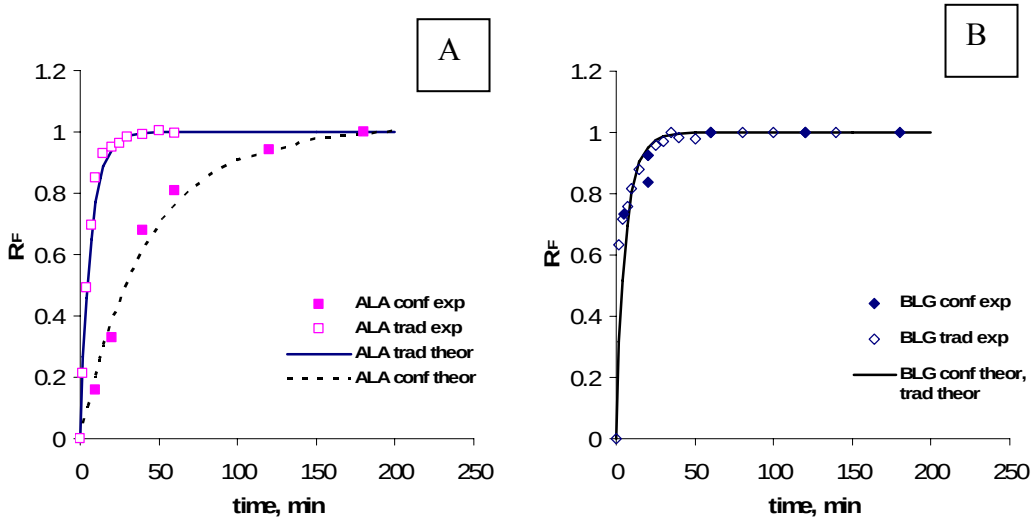

Figure 6.19 Confocal versus traditional batch uptake for ALA (A) and BLG (B) when a mixture of 1.5 mg/ml of ALA and 3 mg/ml of BLG at *v*/*V* of 1:14 is adsorbed to SP Sepharose FF of medium particle size.

Table 6.2 Confocal and traditional rate constants for BLG and ALA adsorption both individually and in mixture, along with their corresponding F^* and q^* values.

		F^* (AU)	$k_1'.10^3$ [a] ($mlmg^{-1}\ min^{-1}$)	q^* ($mgml^{-1}$)	$k_1.10^3$ ($mlmg^{-1}\ min^{-1}$)
BLG	**pure**	5500	36	40	35
	mix	5463	23	40	25
ALA	**pure**	2555	4.0	20	30
	mix	2500	2.1	20	15

a these values were determined using the simple kinetic model as there is a proportionality between F^* and q^*.

In comparing the confocal results in mixture with their corresponding traditional batch uptake results under the same conditions, the following features can be concluded: for BLG, the confocal and traditional results were in good agreement; however for ALA the discrepancy between the confocal and traditional profiles repeated what was encountered in the relevant profiles obtained with pure ALA (Figure 6.12B). It is evident that the apparent values of both k_1' and k_1 in the two-component system decreased by about 50% and 30% compared to their values in pure systems for ALA and BLG, respectively. This result is in good agreement with the decrease in k_1' values obtained from the CLSM experiments for both proteins.

For both single- and two-component systems, the rate constant values for BLG were larger than ALA. This explains the fact that BLG in the two-component system preceded ALA in penetrating the adsorbent particle.

6.3.3 Effect of particle size

The effect of particle size on the batch uptake adsorption of ALA and BLG was studied using CLSM. In view of the resulting fluorescence profiles, three different behaviours, pertaining to three particle-size ranges, were observed. As the adsorbent

particle diameter was found to vary between 60-120 μm, the investigated particle-size ranges were 60-80 μm, 80-90 μm, and 90-120 μm. The medium-size range has been investigated earlier (Sections 6.3.1 and 6.3.2), and therefore this section will deal only with the study of the smallest and largest particle–size ranges. In some instances, however, the medium-size range will be referred to for the sake of comparison.

6.3.3.1 Single-component systems

For BLG, these experiments were conducted at a *v*/*V* ratio of 1:14 and an initial concentration of 3 mg/ml. The confocal time scans of beads of SP Sepharose FF incubated with fluorescently-labelled BLG are shown in Figure 6.20. As was the case with the medium-particle size (Figure 6.10), BLG gradually filled the beads in a shell-wise fashion until the whole beads were completely filled. For the smallest particle-size range of 60-80 μm, BLG filled the entire bead in about 20 min, whereas for the largest particle-size range of 90-120 μm, full penetration of the bead did not occur within two hours.

A) particle-size range of 60-80 μm

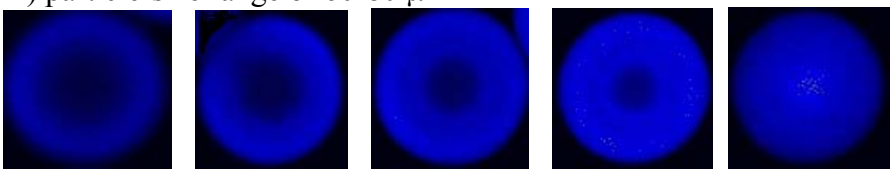

t = 1 min t = 2 min t = 5 min t = 15 min t = 20 min

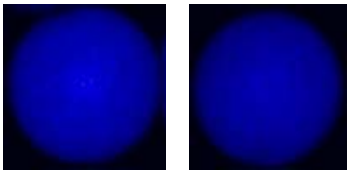

t = 120 min t = 18 h

B) particle-size range of 90-120 μm

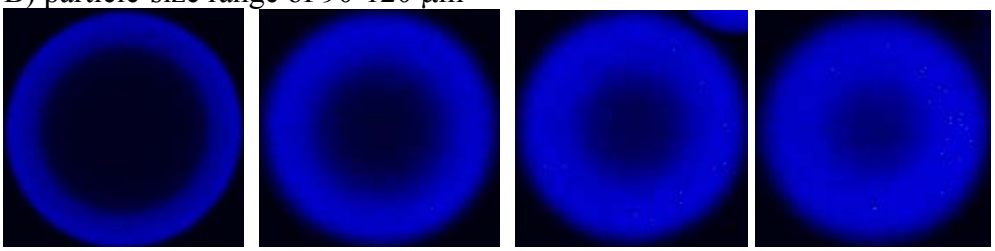

t = 2 min t = 10 min t = 40 min t = 120 min

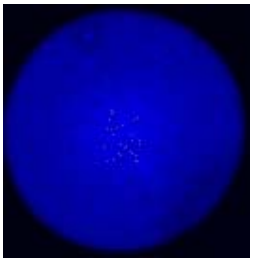

t = 18 h

Figure 6.20 Time series of confocal microscopy scans describing the binding of 3 mg/ml pure BLG to SP Sepharose FF beads at pH 3.7 for the smallest and largest particle-size ranges of the adsorbent.

The general trends displayed in the corresponding fluorescence intensity profiles (Figure 6.21) were in accord with the qualitative information discernable from the scans in Figure 6.20. The curves in Figure 6.21 exhibited overshoots at the two employed particle-size ranges as was previously encountered with the medium-size range. The time of overshoot increased with increasing the particle size. The overshoot occurred at 90 min for the smallest particle size (plot A), and the particle was entirely filled shortly before

that time. For the 90-120 μm particles in plot (B), the overshoot was only observed after 18 hours.

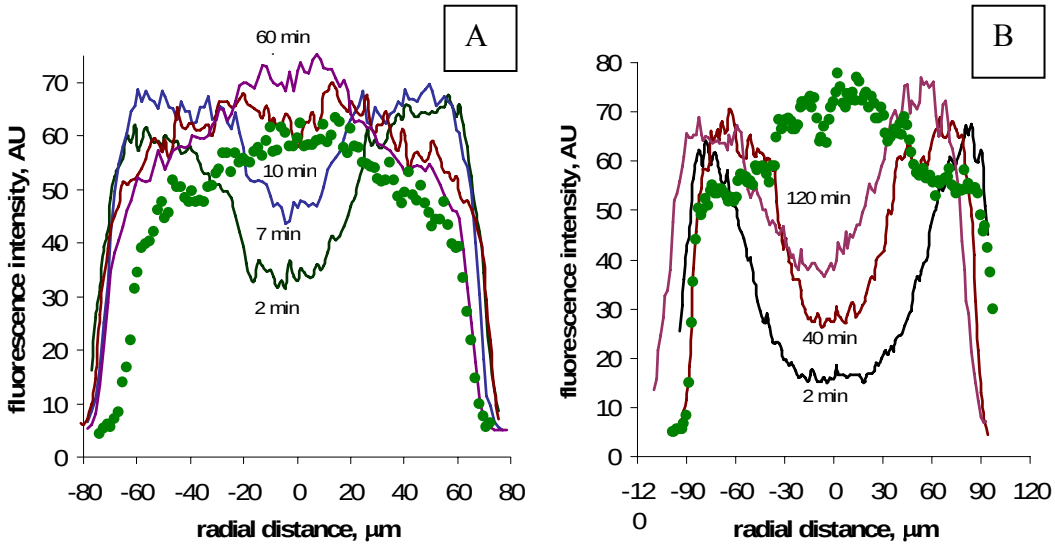

Figure 6.21 Fluorescence intensity profiles for the images in Figure 6.20. Plots A and B represent the profiles for 60-80 μm, and 90-120 μm particles, respectively. Green circles represent the profiles after 18 hours.

The ALA adsorption experiments were performed at the reference conditions of 1.5 mg/ml initial concentration and *v*/*V* ratio 1:14, at a lower *v*/*V* ratio of 1:42 maintaining the same initial concentration, and at a higher concentration of 3 mg/ml maintaining the same *v*/*V* ratio. The relevant time series of the confocal scans are depicted in Figure 6.22. The general penetration behaviour of ALA within the smallest and largest particle-size ranges was the same as that encountered previously with the medium-size range. Unlike BLG, ALA did not fill the entire volume of the beads.

a) particle-size range of 60-80 μm

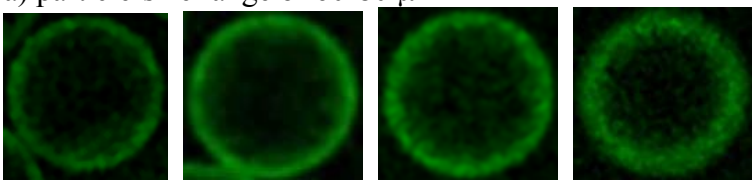

t = 5 min t = 20 min t = 120 min t = 18 h

A) particle-size range of 90-120 μm

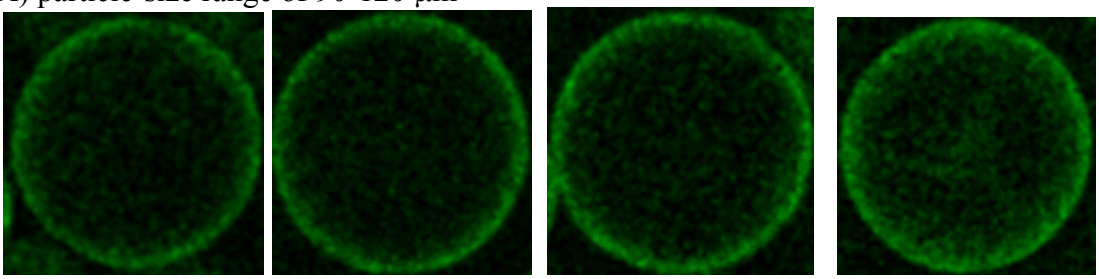

t = 5 min t = 20 min t = 2 h t = 18 h

b) particle-size range of 60-80 μm

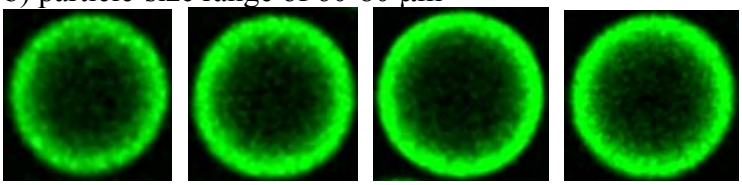

t = 5 min t = 20 min t = 2 h t = 18 h

B) particle-size range of 90-120 μm

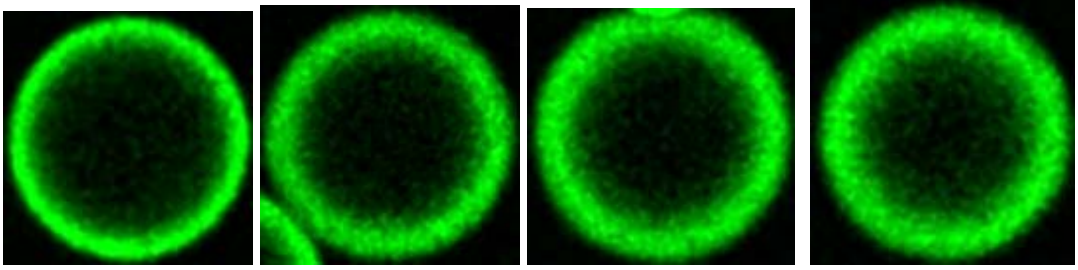

t = 5 min t = 20 min t = 2 h t = 18 h

c) particle-size range of 60-80 μm

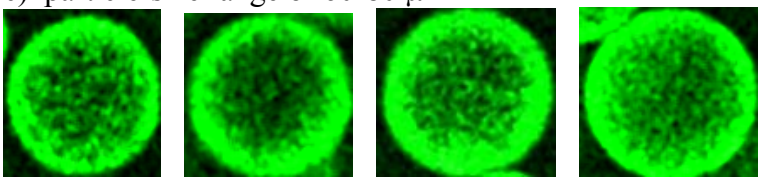

t = 5 min t = 20 min t = 120 min t = 18 h

C) particle-size range of 90-120 μm

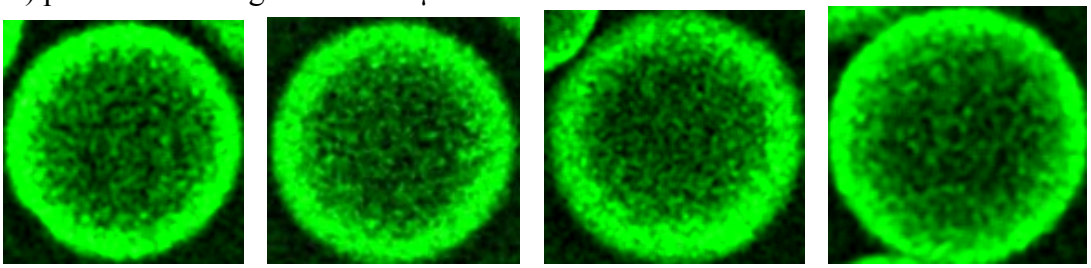

t = 5 min t = 20 min t = 120 min t = 18 h

Figure 6.22 Time series of confocal microscopy scans describing the binding of pure ALA to SP Sepharose FF beads at pH 3.7, for the smallest and largest particle-size ranges of the adsorbent. Scan series (a and A) pertain to 1.5 mg/ml ALA at *v*/*V* of 1:14; scan series (b and B) pertain to 1.5 mg/ml ALA at *v*/*V* of 1:42; and scan series (c and C) pertain to 3 mg/ml ALA at *v*/*V* of 1:14.

The thickness of the fluorescent shells increased when the *v*/*V* ratio was decreased three times. The same was true when the concentration was doubled. Nevertheless, ALA did not fill the entire beads in both cases even for the smallest particle size. As expected, the largest particles exhibited the smallest absolute thickness for the fluorescent shell, whereas the smallest particles had the largest shell thickness. The corresponding fluorescence profiles in Figure 6.23 support this finding since the length of the adsorption front was longer for larger particles (for example, from -90 to +90 μm in Figure 6.23A, right). On the other hand, the height of the adsorption front was slightly higher for smaller particles (for example, from 0 to +20 μm in Figure 6.23A, left).

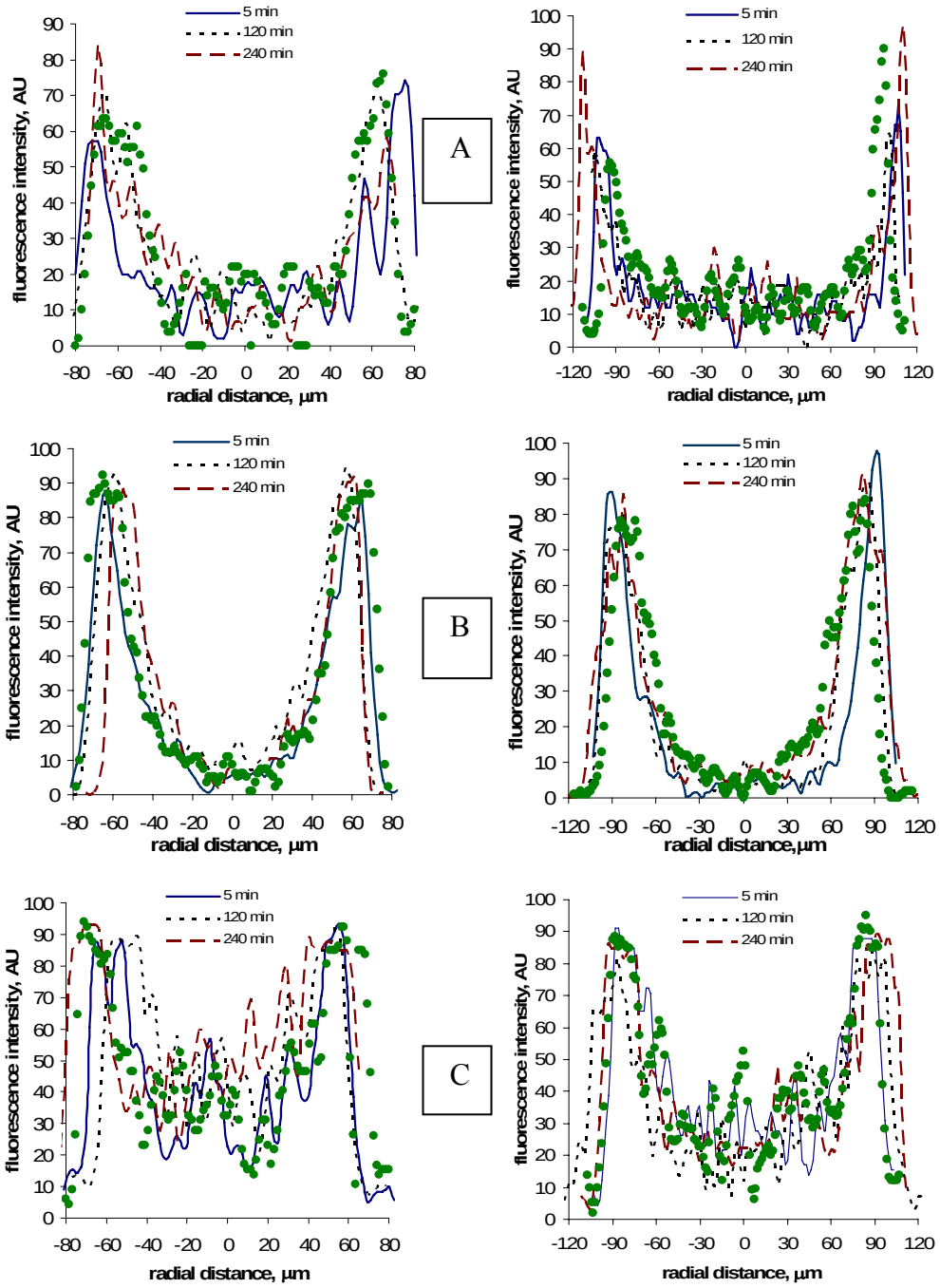

Figure 6.23 Fluorescence intensity profiles for ALA at 1.5 mg/ml and *v*/*V* ratio 1:14 (A), 1.5 mg/ml and *v*/*V* ratio 1:42 (B), and 3 mg/ml and *v*/*V* ratio 1:14 (C). The plots on the left and the right columns pertain to the 60-80 μm, and 90-120 μm particles, respectively. Green circles represent the profiles after 18 hours.

The *F-t* curves for the BLG and ALA adsorption experiments at the reference conditions (whey conditions) for the three employed particle-size ranges are shown in Figure 6.24.

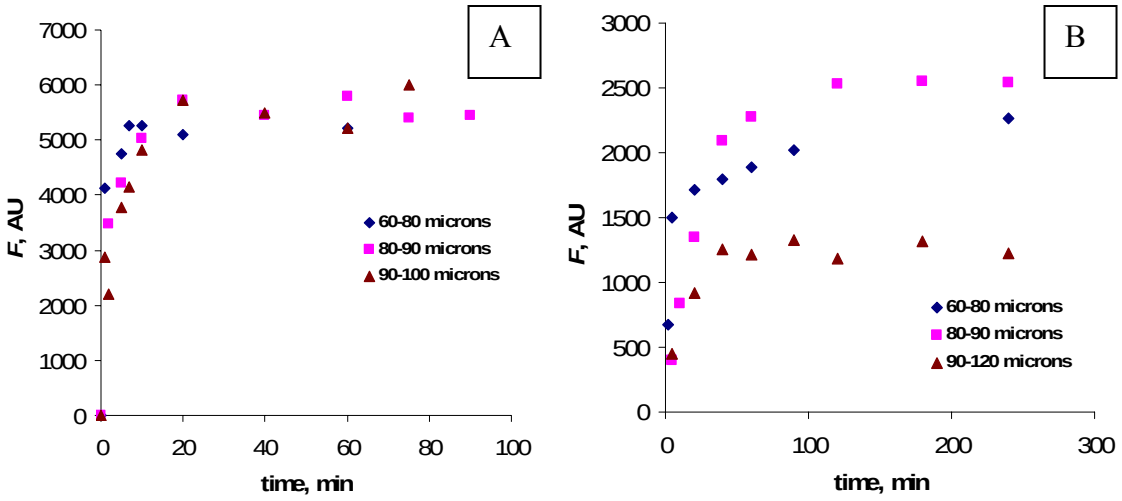

Figure 6.24 *F-t* curves for BLG (A) and ALA (B) at the reference conditions for the various particle-size ranges.

For BLG (Figure 6.24A), the three batch uptake profiles pertaining to the three particle-size ranges reached a maximum (F^*) at approximately the same value of 5500 AU. This implies that the same amount of protein (per bead) was adsorbed within the three ranges of particle size. Judging from the inclination of the curves, it can be seen that the rate of uptake slightly decreases with increasing the particle size. It has to be noted here that the value of k_1' for the smallest particle-size range is $55*10^{-3}$ $mlmg^{-1}min^{-1}$. The importance of this will be evident in Chapter 9. For ALA (Figure 6.24B), the value of F^* has the lowest value at the largest particle size and has the highest value at the medium size. This indicates that the largest amount of protein is adsorbed in the medium-size particles. Furthermore, the highest initial rate of uptake is within the smallest particle size. The adsorption within the medium and largest particle sizes has approximately the same initial rate of uptake. The same behaviour persisted for ALA at the other experimental conditions (Figure 6.25).

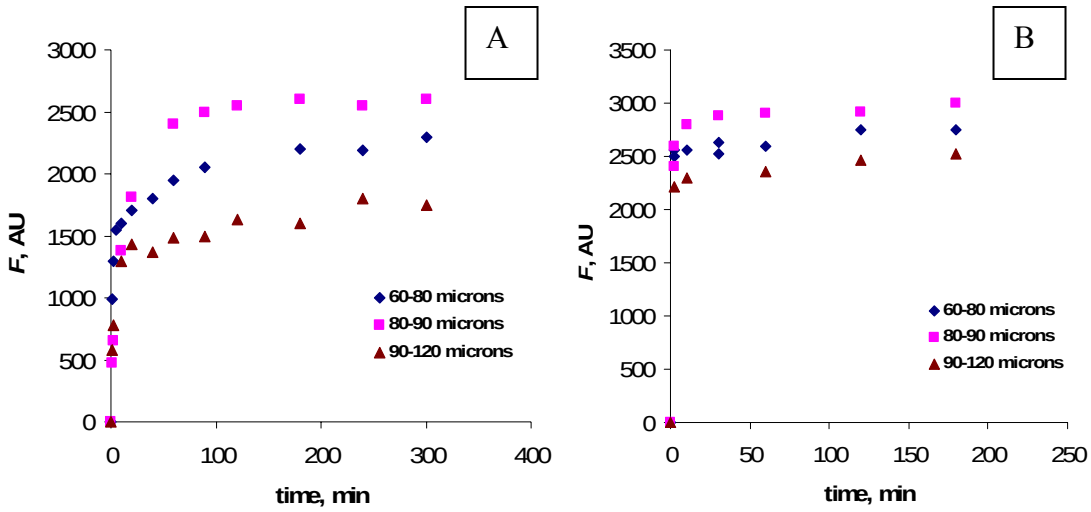

Figure 6.25 *F-t* curves for the different ALA adsorption experiments at the various particle-size ranges; 1.5 mg/ml ALA and *v/V* 1:42 (A), and 3 mg/ml ALA and *v/V* 1:14 (B).

6.3.3.2 Two-component system

Figure 6.26 depicts the time series of confocal images for a mixture of 1.5 mg/ml ALA and 3 mg/ml BLG when adsorbed to SP Sepharose FF at *v/V* of 1:14.

A) particle-size range of 60-80 μm

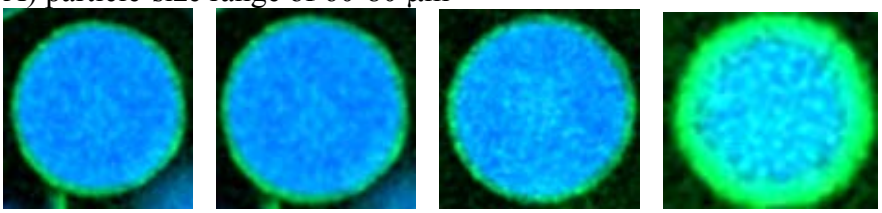

t = 5 min t = 10 min t = 40 min t = 18 h

B) particle-size range of 90-120 μm

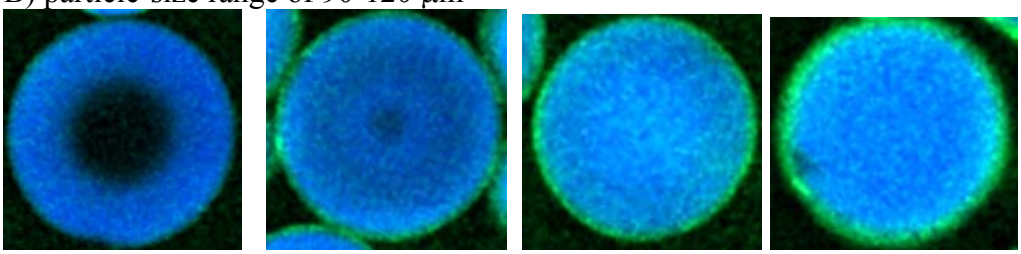

t = 2 min t = 5 min t = 60 min t = 18 h

Figure 6.26 Time series of confocal microscopy scans describing the binding of a mixture of 3 mg/ml pure BLG and 1.5 mg/ml pure ALA to SP Sepharose FF beads at pH 3.7 and different particle-size ranges of the adsorbent.

BLG gradually filled the beads in a shell-wise fashion as can be clearly seen in the largest particle-size images. The smallest size was completely filled in 5 min, as was previously encountered with the medium size. The thickness of the ALA fluorescent shell decreased with increasing the particle-size of the bead, and less ALA penetrated to the innermost regions as observed from the intensity of the blue colour observed with the largest size relative to that observed with the smallest size. The same behaviour is also clear in the corresponding fluorescence intensity profiles (Figure 6.27).

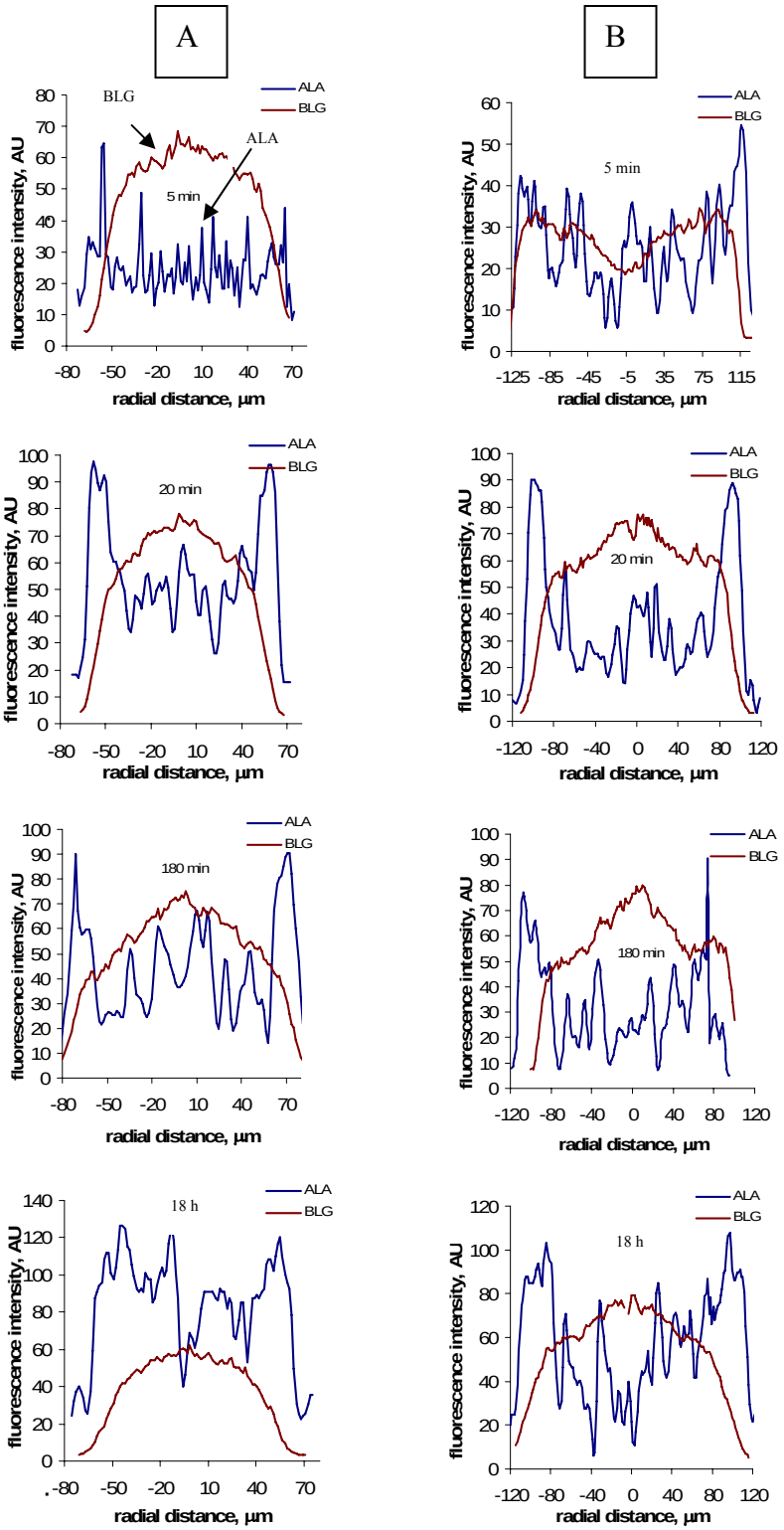

Figure 6.27 Fluorescence intensity profiles for the images in Figure 6.26 at the smallest (A), and largest particle–size ranges (B).

The *F-t* curves for BLG and ALA in the two-component system at the reference conditions are shown in Figure 6.28. The BLG adsorption profiles for the three particle-size ranges exhibited the same maximum value of 5500 AU (equal to that in single-component system), and the rates of uptake were not significantly different for the three ranges of particle-size as was the case with the single-component system. The adsorption profiles for ALA showed the highest maximum value at the medium-size range, and the lowest at the largest-size range. The highest value for F^* is 2550 AU which is equal to the corresponding value in the single-component system. Unlike the single-component system, the differences between the F^* values pertaining to the three particle sizes are not very significant. The adsorption within the smallest particles had the highest initial rate of uptake, whilst the initial rates of uptake within the medium and largest particles were not significantly different, a behaviour similar to that encountered with the single-component system.

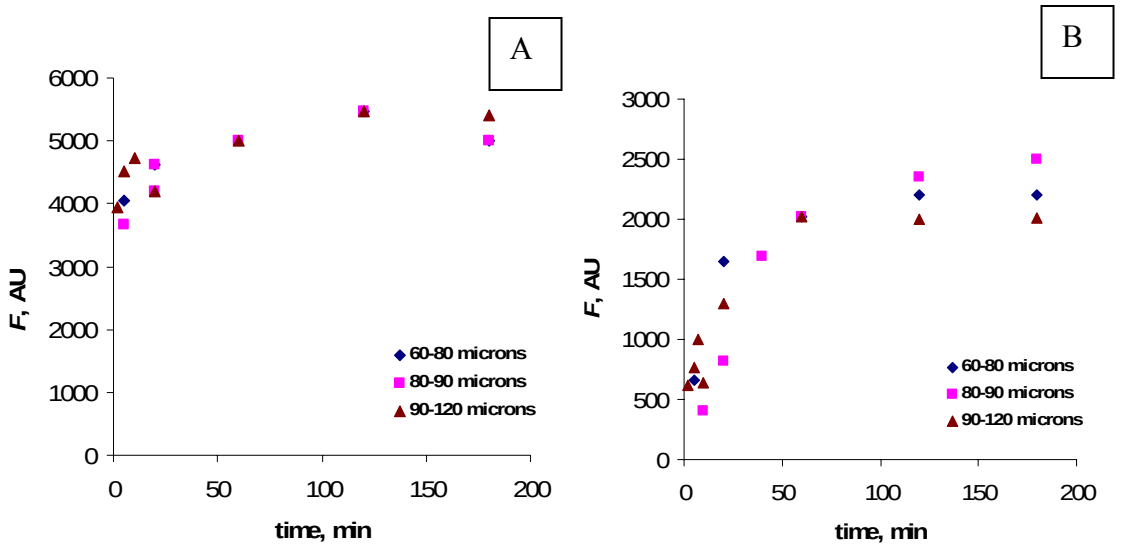

Figure 6.28 *F-t* curves for 3 mg/ml BLG (A) and 1.5 mg/ml ALA (B) in the two-component system at *v*/*V* of 1:14 and various particle-size ranges.

6.4 Conclusions

In the single-component traditional experiments, it was possible to describe the adsorption kinetics of both ALA and BLG at the employed operating conditions using the

simple kinetic model. It was not possible, however, to describe the adsorption kinetics of BLG using the pore diffusion model.

The value of the rate constant for BLG, as estimated using the simple kinetic model, was found to be 1.2 times higher than that of ALA, which indicates that BLG was adsorbed faster than ALA.

For the two-component system, the individual batch uptake profiles for ALA and BLG showed no evidence for competitive adsorption between the two proteins. The values of the rate constants for ALA and BLG in the two-component system respectively dropped by about one-half and one-third of its corresponding values in the single-component systems. The value of k_1 for BLG was therefore 1.6 times higher than that of ALA and hence the adsorption of BLG was faster.

The CLSM technique was useful in visualising the adsorption onto SP Sepharose FF of ALA and BLG at the level of an individual bead and in determining the location of the adsorption sites for both proteins. For pure systems, the CLSM results showed differences in the behaviour of ALA and BLG with regard to their penetration into the adsorbent bead. BLG filled the bead more rapidly than ALA in a shell-wise fashion until the whole bead was filled. The binding of ALA to the adsorbent, however, took place in a shell-wise fashion only at the outermost region of the bead, with some ALA molecules penetrating in an uneven manner into the innermost region. This suggests that the two proteins have different transport mechanisms.

It was possible to compare both qualitatively and quantitatively the *F*-*t* and *q*-*t* curves for ALA and BLG in single- and two-component systems. The simple kinetic rate model traditionally used to determine the kinetic rate constant, k_1, for batch uptake experiments was modified in order to describe batch uptake kinetics based on CLSM data.

The confocal method was able to successfully reproduce the value of the BLG rate constant obtained traditionally for both single- and two-component systems. However, it failed to do so with ALA (k_1' was about 1/7 of k_1), probably because the mass transfer properties of the protein were altered as a result of its conjugation to the dye. It can thus be concluded that provided the labelling of the protein does not affect its transport properties, the CLSM technique supports the traditional method.

Furthermore, the CLSM technique had an additional merit over the traditional method particularly when studying the adsorption of proteins in mixtures as it permitted direct visualisation of the displacement of BLG by ALA. The *F-t* curves obtained showed that the *F* values of BLG reached a maximum after which they declined. The traditional method, on the other hand, showed no evidence of competitive adsorption.

In view of the above, CLSM could be a useful technique in understanding the events underlying the separation of proteins and in gaining additional insight into the nature of the adsorption process in comparison to traditional methods that rely on monitoring changes in the concentration of adsorbates in the bulk liquid phase.

7 Packed-bed studies for the adsorption of pure whey proteins

7.1 Introduction

Several studies have been reported on the single-component ion-exchange adsorption of proteins. Skidmore and Chase (1990) studied the packed-bed adsorption of bovine serum albumin (BSA) and lysozyme to the strong cation exchanger S Sepharose FF. The experimental breakthrough profiles were compared to theoretical profiles obtained using the simple kinetic model and the pore and film diffusion model. Aboudzadeh *et al.* (2006) used the same two models to predict the breakthrough curves of human serum albumin (HSA) and ovalbumin (OVA) on the weak anion exchanger DEAE Sepharose FF. The adsorption of HSA was consistent with both models; however, neither model could correctly predict the latter part of the breakthrough profile of OVA. Avci *et al.* (2000) investigated theoretically and experimentally the adsorption of BSA to the weak anion exchanger DE52 in packed columns. The theoretical analysis was based on a dynamic pore-diffusion model that took into account the interfacial and intraparticle mass transfer as well as surface reaction phenomena. This model was also used by other workers to predict the performance of continuous expanded-bed adsorption of proteins such as lysozyme (Owen and Chase, 1999), and to anticipate breakthrough curves for the packed-bed adsorption of lysozyme, BSA and HSA; incorporating extra terms for axial particle size distribution (Bruce and Chase, 2002; Tong *et al.*, 2003; Chen *et al.*, 2003) and particle classification in expanded beds (Yun *et al.*, 2005). Packed-bed experiments were performed by McCreath *et al.* (1997) using the cation-exchanger SP-PVA-FEP to purify lysozyme from egg white, and the anion-exchanger Q-PVA-FEP to purify G6PDH from a clarified homogenate of bakers' yeast. Melter *et al.* (2008) characterized the retention behaviour of a monoclonal antibody on a weak cation exchanger, Fractogel EMD COO^-(s).

For two-component systems, results of studies of the adsorption of a mixture of albumin and β-lactamase to encapsulated ion exchangers were presented by Nigam *et al.*

(1988); where they reported that competition between the two adsorbing proteins occurred, with albumin displacing the more weakly bound β-lactamase from the ion-exchanger. Skidmore *et al.* (1990) investigated multicomponent adsorption of a model system consisting of bovine serum albumin and lysozyme to the cation-exchanger S Sepharose FF. Evidence of competitive adsorption was seen in the breakthrough profiles.

Less work has been performed on two-component, competitive adsorption of protein systems involving the two major whey proteins, α-lactalbumin (ALA) and β-lactoglobulin (BLG). Flashner *et al.* (1983) studied the high performance anion exchanger chromatographic separation of four proteins cytochrome c, α_1-acid glycoprotein, ovalbumin, and β-lactoglobulin on polyethyleneimine (PEI)-silica gel column using a 20-min linear gradient from 0.025 M to 0.50 M potassium phosphate at pH 6.80. Wahlgren *et al.* (1993) investigated the adsorption of a mixture of BLG, lactoferrin and lysozyme on hydrophilic silica surfaces. BLG (negatively-charged) adsorbed in small amounts while lactoferrin and lysozyme (both positively-charged) adsorbed in higher quantities. They deduced that the adsorption from binary mixtures of oppositely charged proteins was affected by protein-protein interactions. According to them, there was either a cooperative adsorption leading to higher amounts of adsorbed proteins or a competitive adsorption depending on the solution conditions, the protein and the surface. Outinen *et al.* (1996) evaluated the adsorption characteristics of α-lactalbumin and β-lactoglobulin on eleven strongly-basic anion-exchange adsorbents by performing frontal analysis with sweet whey (pH 6.5). Significant fractionation of the two proteins was obtained only with Diaion HPA, and optimum fractionation conditions (pH 6–7, β-lactoglobulin load of 16–20 mg per cm^3 of resin, degree of demineralization 0–50) were determined in batch adsorption experiments in which 75–80% recovery of α-lactalbumin was obtained. Kim and Kuga (2002) studied the separation of the two variants of BLG (A and B) using a cellulose-based anion exchanger bearing water-soluble polycations. In all of the above column-chromatography studies, the method of protein separation was based on selective elution following adsorption rather than selective adsorption. In addition to column-chromatography studies, a few relevant, competitive adsorption studies have been performed on ion-exchange membranes. Weinbrenner and Etzel (1994) studied the competitive adsorption of α-lactalbumin and

bovine serum albumin to a sulphopropyl ion-exchange membrane. Competitive adsorption caused displacement of bound BSA monomer by the more strongly bound BSA dimer, illustrating that even apparently single protein systems may display multicomponent competitive behaviour. In the two-protein experiment, ALA was competitively displaced by the more strongly bound BSA monomer and dimer, indicating that the binding strength was in the order: BSA dimer > BSA monomer > ALA. Goodall *et al.* (2008) constructed binary solution breakthrough curves to show that ALA and BSA were displaced from the strong and weak anion exchanger membranes by BLG. One limitation of this method was the low protein binding capacities observed.

The results reported in this chapter will be divided into two main sections pertaining to: A) single-component studies where only one pure protein, either ALA or BLG is adsorbed to the cation exchanger SP Sepharose FF in a packed-bed mode, and B) two-component or binary studies where both proteins are simultaneously adsorbed onto a packed-bed of the cation exchanger.

7.2 Single-component systems

The packed-bed profiles pertaining to the adsorption of either 3 mg/ml BLG or 1.5 mg/ml ALA onto a 1-ml column of SP Sepharose at pH 3.7 and linear velocity of 158 cm/h (flow rate of 1 ml/min) are shown in Figure 7.1. Initial feed concentrations of ALA and BLG were chosen as those normally found in real whey mixtures.

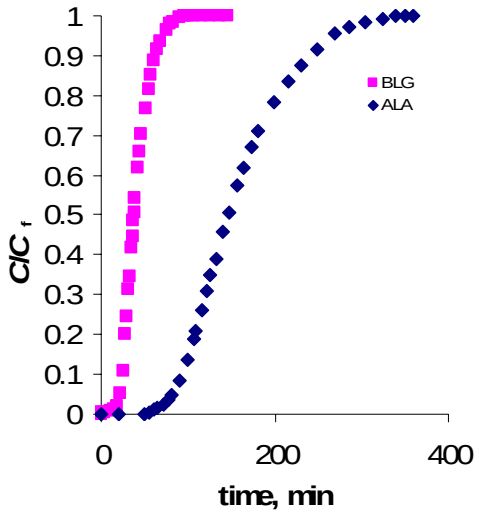

Figure 7.1 Single-component breakthrough curves for the adsorption of BLG and ALA onto a 1-ml packed-bed of SP Sepharose FF at pH 3.7, feed concentrations of 3 and 1.5 mg/ml respectively, linear velocity of 158 ml/min (flow rate of 1 ml/min), and temperature 20°C.

As can be seen in the figure, the breakthrough curves for both proteins eventually reached a C/C_f value of unity. The $t_{1/2}$ value for ALA (150 min) was found to be about four times longer than that for BLG (38 min). It can also be observed that the BLG breakthrough curve is steeper than that of ALA probably due to the higher concentration of BLG in the feed. Values of the slopes of the breakthrough curves together with the rest of the dynamic adsorption data are given in Table 7.1.

Table 7.1 Single and two-component dynamic adsorption data for ALA and BLG on a 1-ml column of SP Sepharose FF at pH 3.7.

	v_L (cm/h)	$t_{1/2}$ (min)	$t_{10\%brkthru}$ (min)	max C/C_f	$slope_{brkthru}$ (min^{-1})
BLG	**158***	**38**	**25**	**1.0**	**0.0252**
	158	**32**	**24**	**1.0**	**0.0490**
ALA	**158***	**150**	**95**	**1.0**	**0.0070**
	158	**120**	**50**	**1.0**	**0.0070**

*** single-component results**
Values of the slopes were taken as average values excluding the early and later stages of the breakthrough curves where values of C/C_f are constant with time.

The difference in the values of $t_{1/2}$ along with the already cited isotherm parameters for BLG and ALA (obtained from the batch experiments, Chapter 5) suggest

the possibility of separating the two proteins when adsorbed simultaneously. This will be further investigated in the following section.

7.3 Two-component system

A mixture of 1.5 mg/ml ALA and 3 mg/ml BLG at pH 3.7 was pumped through a 1-ml column of SP Sepharose FF at a linear velocity of 158 cm/h (flow rate of 1 ml/min). The concentration of total proteins in the column effluent fractions was measured on the AKTA Explorer 100 with respect to time and is the dotted curve shown in Figure 7.2. This curve displays a $t_{1/2}$ of 42 min, which is fairly close to that obtained earlier for pure BLG (38 min) under the same conditions.

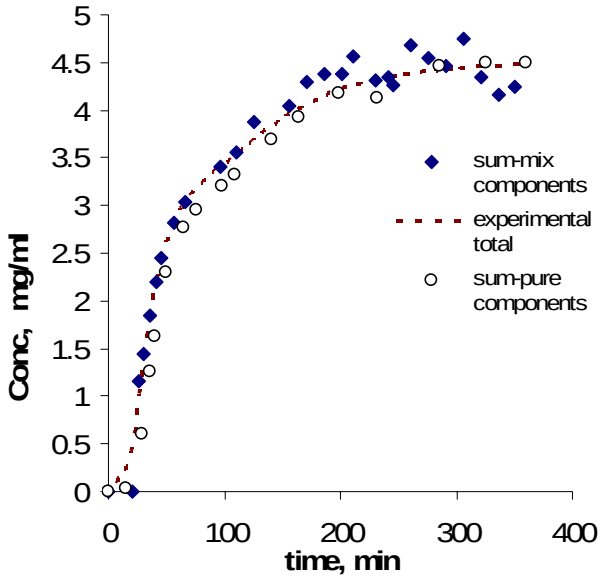

Figure 7.2 Packed-bed adsorption profiles for a mixture of ALA and BLG of feed concentrations 1.5 and 3 mg/ml, respectively onto SP Sepharose FF at pH 3.7 and linear velocity of 158 cm/h (---- experimental profile of total protein concentration, ◆ profile produced by summing up the individual protein concentrations in the analysed fractions, o **profile obtained by summing up the two profiles obtained in experiments with pure proteins).**

In order to get the corresponding profiles for the individual components, the column effluent fractions were analysed on a size-exclusion system and the results are shown in Figure 7.3 as discrete points. Also included in Figure 7.3 as solid curves are the two single-component adsorption profiles for the two individual pure proteins which were

obtained earlier. Agreement between the discrete points and the solid curve for the same protein is much better for BLG than for ALA, suggesting that the adsorption behaviour of BLG is the same in mixture as when alone under these experimental conditions. The relevant dynamic data for the individual breakthrough profiles of ALA and BLG are given in Table 7.1.

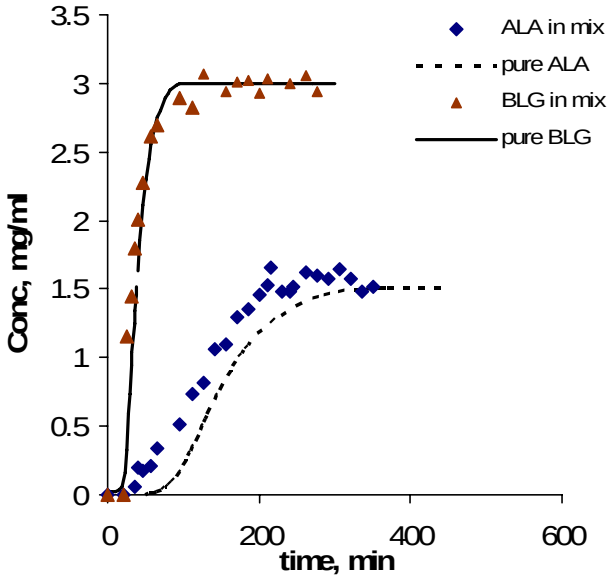

Figure 7.3 Single-component adsorption profiles of ALA and BLG both in the mixture and as pure proteins onto (1-ml) SP Sepharose FF beds at pH 3.7, linear velocity of 158 cm/h, and feed concentrations of 1.5 and 3 mg/ml, respectively.

As can be seen from Figure 7.3, the BLG profiles are steeper than the ALA ones. This could be due to the fact that the ALA concentration is lower than that of BLG, and although likely to be bound less strongly to the adsorbent (as it has higher K_d than BLG), the path of ALA through the column should be more tortuous owing to its accessibility to finer pores as it is a smaller protein. Adding up the two discrete profiles shown in Figure 7.3, pertaining to the breakthroughs of both proteins in the mixture, yields the discrete profile shown in Figure 7.2 as rhombic symbols, whereas summing up the profiles pertaining to each of the separate pure proteins (solid curves, Figure 7.3) produces the profile shown in Figure 7.2 as hollow circles. The fair degree of correspondence between the dotted curve and the rhombic points in Figure 7.2 lends credence to the applicability

of both the calibration and calculation methods adopted. In addition, the pure-proteins profile (circle) is obviously very similar to the profile of the protein mixture (rhombic symbols). It can thus be deduced that the behaviour of each of the two proteins in the mixture is very much similar to that when applied to the column as single components. In other words, there is no clear evidence for a degree of competition between the proteins for binding to the adsorption sites under these adsorption conditions.

In view of the foregoing results, it would not be possible to separate ALA from BLG during the adsorption stage using a 1-ml column, perhaps due to insufficient adsorption capacity under the employed chromatography conditions. Hence, a possible approach to the problem was to scale up the column volume to 5 ml. The adsorption profiles of both BLG and ALA thus obtained are shown in Figure 7.4.

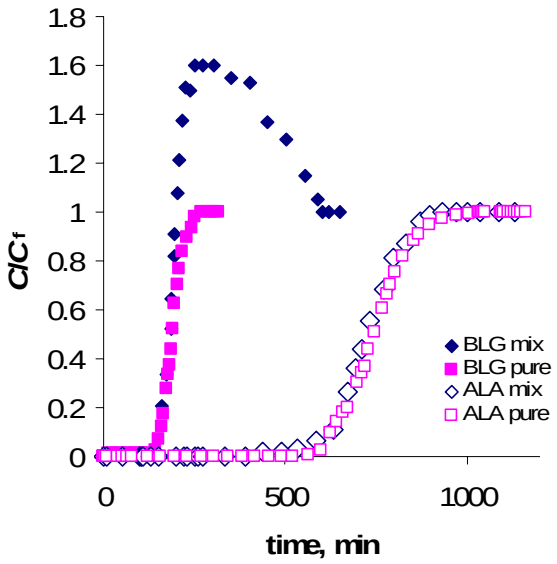

Figure 7.4 Two-component breakthrough profiles of ALA and BLG when a mixture of both proteins is applied onto a (5-ml) SP Sepharose FF bed at pH 3.7, linear velocity of 30 cm/h (flow rate of 1 ml/min), and feed concentrations of 1.5 and 3 mg/ml, respectively. The single-component profiles for pure ALA and pure BLG under the same conditions are also shown in the figure.

A distinctive breakthrough curve for each protein can be observed, with BLG breaking through first with a $t_{1/2}$ of 190 min followed by ALA with a $t_{1/2}$ of 725 min. It can also be observed that the breakthrough profiles of the two proteins have different

slopes as the BLG breakthrough curve is much steeper than that of ALA which is probably due to the higher concentration of BLG in the feed (Table 7.2).

Figure 7.4 also depicts the breakthrough profiles for ALA and BLG respectively in the binary mixture as compared with their corresponding single-component profiles (also shown in the figure). It is clear that the $t_{1/2}$ values for both proteins in the two-component mixture are not significantly different from their pure component counterparts. The behaviours of both proteins in the mixture are almost identical to their behaviours when pure, except for the significant overshooting of the BLG concentration which occurred in the two-component profile. Values of the relevant adsorption dynamic data are presented in Table 7.2.

Table 7.2 Single and two-component dynamic adsorption data for ALA and BLG on a 5-ml column of SP Sepharose FF at pH 3.7.

	v_L (cm/h)	$t_{1/2}$ (min)	$t_{10\%brkthru}$ (min)	max C/C_f	slope$_{brkthru}$ (min^{-1})
BLG	**30***	**190**	**160**	**1.0**	**0.0122**
	30	**190**	**165**	**1.6**	**0.0223**
	60	**93**	**80**	**1.6**	**0.0269**
	150	**38**	**28**	**1.6**	**0.0303**
ALA	**30***	**725**	**630**	**1.0**	**0.0035**
	30	**725**	**630**	**1.0**	**0.0035**
	60	**330**	**270**	**1.0**	**0.0048**
	150	**150**	**100**	**1.0**	**0.0067**

*** single-component results**
Values of the slopes were taken as average values excluding the early and later stages of the breakthrough curves where values of C/C_f are constant with time.

Of particular interest is the observation that the normalised concentration of BLG overshot its value in the feed by more than 50% before if fell back to the feed value of unity. This implies that ALA is able to displace and, thereby elute, a certain amount of adsorbed BLG. The overshoot phenomenon was previously encountered in a number of studies on different systems of multiple proteins under different operating conditions (Cowan *et al.*, 1989; Skidmore *et al.*, 1990; Hubbuch *et al.*, 2003; and Goodall *et al.*, 2008). From the equilibrium data (Table 5.1), it is clear that ALA has a higher K_d and hence is more weakly-bound to the adsorbent than BLG. However, ALA was able to displace BLG; a finding that is consistent with the CLSM results obtained earlier

(Chapter 6, Section 6.3.2). A similar behaviour was reported by Hubbuch *et al.* (2003) when studying the binary adsorption of IgG 2A and BSA to SP Sepharose XL at pH 4.5, where the strongly-bound IgG 2A was displaced by the weakly-bound BSA. This behaviour is different from that encountered by other workers studying other protein systems (Garke *et al.*, 1999; Cowan *et al.*, 1989; Skidmore *et al.*, 1990) where the strongly-bound protein (as judged from its K_d value) was found to displace the weaker-bound one.

To determine quantitatively the amount of BLG eluted by ALA, the experiment was performed again but this time was terminated just before the ALA breakthrough point (~500 min). The protein exiting the column was collected up to this point, and was analysed using a size-exclusion chromatography system. The concentration of BLG in this fraction was found to be equivalent to the inlet concentration (3 mg/ml) (Figure 7.5) which indicates that ALA had eluted all the BLG off the column. This result, in turn, suggests that the separation of the two proteins from each other could be successfully achieved under the existing conditions.

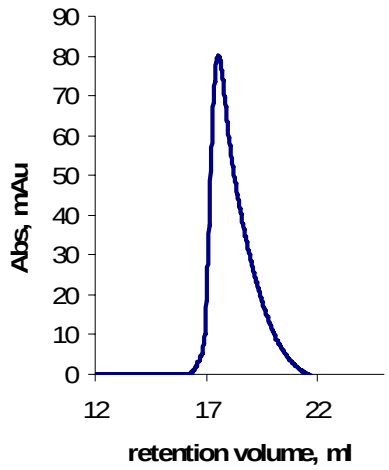

Figure 7.5 Analytical size exclusion chromatography on Superdex 200 for the SP Sepharose column effluent produced during the course of the BLG breakthrough shown in the previous figure. A 0.2-ml sample volume was applied to the size-exclusion column and eluted with 0.1M sodium acetate buffer of pH 3.7.

Now that conditions could be found under which all the BLG was eluted and only ALA remained adsorbed onto the column, an elution study was required to determine the

optimum conditions for obtaining the highest recovery of ALA. Preliminary elution experiments were first carried out on a 1-ml column; loading a 20-ml sample and using as eluents, solutions of 0.1M sodium acetate buffer containing 1M NaCl and adjusted to pH values of 3.7, 3.0 and 2.5. The eluted peaks were collected and analysed using size-exclusion chromatography to obtain the corresponding concentration of ALA (C_c) and, in turn, calculate the percentage recovery as follows:

$$\textbf{\%recovery}= \left(\frac{C_f V_f - C_c V_c}{C_f V_f} \right) \times 100 \qquad \textbf{(7.1)}$$

where

C_f = initial feed concentration of protein (mg/ml)

C_c = concentration of protein in the collected peak (mg/ml)

V_f = volume of feed sample loaded onto the column (ml)

V_c = volume of collected peak (ml)

The respective recovery values so obtained were 35, 39 and 53% for pH values of 3.7, 3.0 and 2.5. An additional trial was conducted at pH 3.0 in which the concentration of NaCl was doubled to 2M but this yielded a very low 8% recovery. The low recoveries of protein during elution with salt led to the notion of performing the elution process above the p*I* where the protein becomes negatively charged (the same as the exchanger) and can thus be eluted without the need for salt addition. Thus 0.1M buffer solution alone was used as an eluent at pH values of 5.6, 8.0 and 9.0 and the respective recoveries were 75%, 86% and 99%. However, since no buffering action was expected for the acetate solution at pH 8.0 or 9.0 (the effective range for the acetate buffer is 3.6-5.6, Mohan (2003), it was replaced by a 0.1M Tris-HCl buffer at pH 9.0 and the somewhat more modest 91% recovery obtained therewith was deemed to be satisfactory. The addition of 0.1 M NaCl to the eluent was expected to have a screening effect (shielding the adsorbent charge and thus lowering the electrostatic interactions between the protein and the adsorbent) that might improve elution, but it made no significant difference (87% recovery of ALA was obtained). The elution protocol involving 0.1M Tris-HCl buffer at

pH 9.0 was applied to the scaled-up process using the 5-ml column with a linear velocity of 30 ml/min and it yielded equivalent results. Figure 7.6 shows the ALA eluted peak on an FPLC using size exclusion. The use of Tris-HCl buffer for elution without salt addition is advantageous since the use of salt is undesirable because it is expensive to recover or use just once (Doultani *et al.*, 2004; Etzel, 1999). An additional merit in using Tris-buffer is its pH buffering range of 7.0-9.0 which would enable reducing the pH of the eluted ALA when necessary, from pH 9.0 to a neutral pH of 7.0.

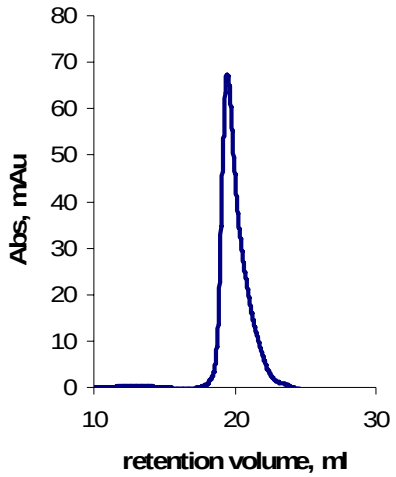

Figure 7.6 Size-exclusion analysis of ALA eluted fraction on Superdex 200, obtained when eluting with 0.1M Tris-HCl buffer at pH 9.0. A 0.2-ml sample volume was applied to the size-exclusion column and eluted with 0.1M sodium acetate buffer of pH 3.7.

To further optimise the process of separating ALA and BLG, the effect of linear velocity (flow rate) on the column adsorption characteristics was studied (Figure 7.7). Table 7.2 presents the adsorption dynamic data for ALA and BLG when a binary mixture of both proteins was applied to a 5-ml SP Sepharose FF bed at pH 3.7, with feed concentrations of ALA and BLG of 1.5 and 3 mg/ml, respectively, and linear velocities of 30, 60 and 150 cm/h (corresponding to flow rates of 1, 2 and 5 ml/min, respectively). The table also shows the dynamic data pertaining to pure single-component ALA and BLG at a linear velocity of 30 cm/h on the 5-ml column.

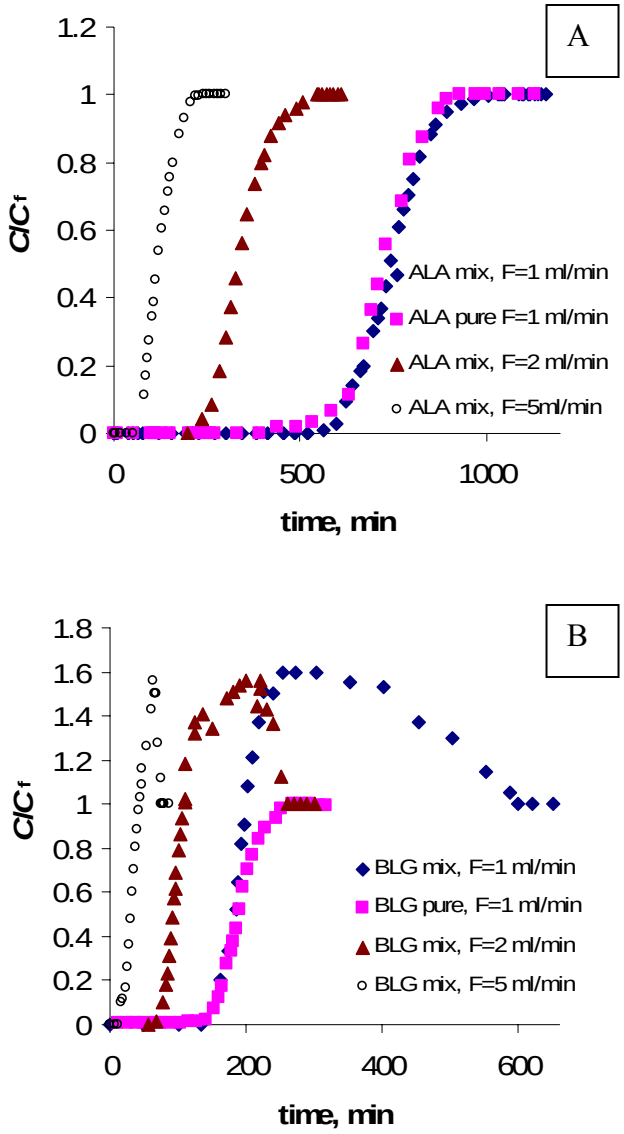

Figure 7.7 Adsorption profile of ALA (A) and BLG (B) when a binary mixture containing ALA and BLG at feed concentrations of 1.5 and 3 mg/ml, respectively was applied onto a 5-ml bed of SP Sepharose FF bed at pH 3.7 and flow rates of 1, 2 and 5 ml/min (corresponding to linear velocities of 30, 60 and 150 cm/h, respectively). The figure also shows the profiles obtained with pure ALA (a) and BLG (b) at a flow rate of 1ml/min.

From both figure and table, it can be deduced for both ALA and BLG that the slopes as well as the plateaus of the breakthrough curves at the three employed linear velocities are nearly the same. Thus, the linear velocity had no effect either on the steepness of the curves or their maximum values of C/C_f. For ALA, the maximum value

of C/C_f was 1 as expected; while for BLG, it peaked at a value of 1.6 at each of the three linear velocities used for reasons that were discussed earlier. As expected, the value of $t_{1/2}$ for both proteins decreased with an increase in linear velocity. Values of $t_{1/2}$ were 38, 93 and 190 min for BLG and 150, 330 and 725 min for ALA at linear velocities of 150, 60 and 30 cm/h, respectively. For both proteins, increasing the linear velocity by a factor of (n) decreased $t_{1/2}$ by a factor of approximately ($1/n$). It is also notable that the $t_{1/2}$ values at linear velocity of 30 cm/h in the 5-ml column (Table 7.2) are five times those obtained during single-component experiments using a 1-ml column at 158 cm/h (Table 7.1). By comparing the adsorption dynamic data of the pure protein with its corresponding data obtained when in binary mixture at a linear velocity of 30 cm/h (Table 7.2), it can be seen that for ALA, the two sets of data are nearly identical. However for BLG, the maximum C/C_f value when in mixture was about 1.6 times its value of 1.0 when pure. In addition, the slope of the pure BLG breakthrough curve was approximately half that of BLG in mixture. From the above study of the effects of linear velocity, it may be inferred that a linear velocity of 150 cm/h is probably the most favourable as it requires the least time required for separation. Furthermore, some overlapping between ALA and BLG breakthrough curves was observed at 60 cm/h (Figure 7.7) and overlapping increased further with increasing the linear velocity to 150 cm/h. Clearly at 30 cm/h, no overlapping was encountered and the two proteins were completely separated (Figure 7.7, also refer to Figure 7.4). The slight decrease in the degree of separation that occurs at 60 cm/h might not justify opting for the significantly longer operational times that would be required at 30 cm/h compared to operation at 60 cm/h.

In Figures 7.8A and 7.8B, C/C_f is plotted as a function of the amount of adsorbate applied to the bed ($F \cdot C_f \cdot t$). The result is breakthrough curves pertaining to ALA and BLG when a binary mixture of both proteins was applied to a 5-ml SP Sepharose FF bed at pH 3.7, with feed concentrations of ALA and BLG of 1.5 and 3 mg/ml, respectively, and flow rates of 1, 2 and 5 ml/min (corresponding to linear velocities of 30, 60 and 150 cm/h, respectively). The curves are shown to be sharper at lower flow rates. Hence, in order to use the maximum amount of the adsorption capacity of the bed before breakthrough occurs, low flow rates would be preferred. Thus, to achieve a reasonable compromise between reducing operational time and maximising the dynamic capacity of the adsorbent

as well as minimising the overlapping of the breakthrough curves, a flow rate of 2 ml/min corresponding to a linear velocity of 60 cm/h would be an optimal choice.

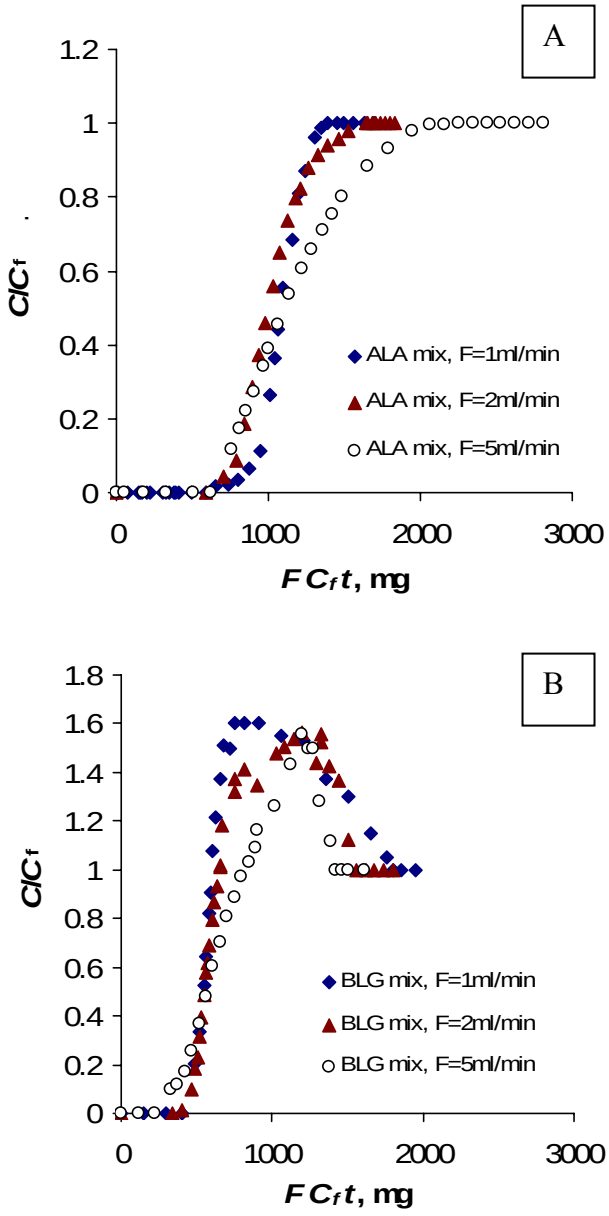

Figure 7.8 Effect of flow rate on the two-component adsorption profiles of ALA (A) and BLG (B) plotted as a function of the amount of protein applied to the bed.

7.4 Conclusions

Single-component packed-bed experiments were performed on the adsorption of pure ALA and BLG to the cation exchanger SP Sepharose FF at pH 3.7. For packed-bed

studies using a 1-ml column and a linear velocity of 158 cm/h, $t_{1/2}$ of ALA was four times longer than that of BLG, probably due to its lower concentration, as well as its smaller size (half that of BLG) which allows for more accessibility to finer pores and hence a more tortuous path.

The packed-bed adsorption and elution of a mixture of ALA and BLG were then investigated under the above conditions but using a 5-ml column. BLG broke through first, and its concentration in the outlet exceeded its feed value by about 60% before declining to the feed value, followed by the breakthrough of ALA. ALA displaced and eluted all the BLG from the column in a pure form. Pure ALA could then be eluted with good recovery. This process was optimised with regard to linear velocity as well as adsorption capacity and an optimum linear velocity of 60 cm/h was chosen.

In summary, a novel method based on selective adsorption of proteins was established to separate ALA and BLG from their pure binary mixture. Evidence of the competitive nature of adsorption observed in binary mixtures can be used to develop a facile separation process for the two proteins from whey. The process promises to have both environmental as well as economical merits because it enables obtaining almost all the BLG present in the two-component system by simple displacement during the loading period, while ALA was subsequently eluted by simple isocratic elution without the need to use salt.

8 Purification of the two major whey proteins using selective adsorption

8.1 Introduction

Several attempts have been made to separate and purify the different components of whey using ion-exchange adsorption techniques. A few adsorption studies involving whey proteins have been performed on ion-exchange membranes. Weinbrenner and Etzel (1994) studied the competitive adsorption of α-lactalbumin and bovine serum albumin to a sulphopropyl ion-exchange membrane. Goodall *et al.* (2008) constructed rennet whey breakthrough curves to show that ALA and BSA were displaced from the strong and weak anion exchange membranes by BLG. The limitation of this method was the low protein binding capacities observed.

Regarding column chromatography studies, a number of workers used anion-exchange chromatography to separate whey proteins. Flashner *et al.* (1983) separated β-lactoglobulin on a polyethyleneimine (PEI)-silica gel anion exchange column using linear gradient elution with potassium phosphate (0.025-0.50 M) at pH 6.80. Colby *et al.* (1996) studied the effect of compression on the scale-up of a commercial packed-bed ion-exchange process to manufacture a whey growth factor extract using lactoperoxidase and lactoferrin as model substances. Vogt and Freitag (1997) investigated the suitability of anion-exchange and hydroxyapatite displacement chromatography for the processing of technical dairy whey. Lan *et al.* (2002) employed a liquid–solid circulating fluidized bed ion-exchange extraction system for continuous protein recovery from cheese whey. Pedersen *et al.* (2003) developed a consistent set of chromatographic data, including isotherms and transport properties, for the adsorption of whey proteins onto several anion exchangers.

Others performed a combination of cation- and anion-exchange steps to purify these proteins. Gerberding and Byers (1998) described a preparative ion-exchange chromatographic process for the separation and recovery of the four major proteins [α-lactalbumin, β-lactoglobulin, bovine serum albumin and immunoglobulin G (IgG)] and lactose from sweet dairy whey. In that work, it was found that an anion-exchange step

was most effective in separating β-lactoglobulin from the whey feed mixture of pH 5.8 while a cation-exchange step was used to further recover the IgG. The low recovery and incomplete separation observed made the process impractical for commercial application. Ye *et al.* (2000) used cation- exchange chromatography to recover lactoperoxidase and lactoferrin by applying salt-gradient elution using 0-0.55 M NaCl in 50 mM Tris-HCl, pH 6.5. The effluent was adjusted to pH 8.5 and passed through an anion exchange column to recover α-lactalbumin and β-lactoglobulin. α-lactalbumin was eluted using 0-0.15 M NaCl in 50 mM Tris-HCl, pH 8.5. Next the buffer irrigating the column was adjusted to pH 6.8, and the β-lactoglobulin was eluted using 0-0.2 M NaCl in 50 mM Tris-HCl, pH 6.8.

Less work has been done on the cation-exchange chromatography of whey proteins. Hahn *et al.* (1998) developed a fractionation scheme for IgG, lactoferrin and lactoperoxidase based on the cation exchangers S-HyperD F, S Sepharose FF, Fractogel EMD-S 650 (S) and Macro-Prep High S. They investigated the binding capacities for IgG and the different elution behaviours observed when sequential step gradients with NaCl buffers were applied. Lozano *et al.* (2008) employed cation-exchange chromatography only as a final purification step after isolating BLG from bovine whey using precipitation. Doultani *et al.* (2004) developed a cation-exchange column chromatography process that used selective elution to fractionate proteins from whey. Three different elution procedures were used as follows: (a) a single elution buffer to obtain whey protein isolate (WPI); (b) two elution buffers to obtain α-lactalbumin and WPI depleted in α-lactalbumin (ALA); and (c) four elution buffers to obtain ALA, WPI depleted in ALA, lactoperoxidase and lactoferrin.

It is now clear that very little work has been done on the cation-exchange adsorption of the two major whey proteins, β-lactoglobulin and α-lactalbumin. In addition, all of the column-chromatography whey purification studies reported in previous literature were based on selective elution rather than selective adsorption.

In the previous chapter, it was shown that it is possible to separate ALA and BLG from a pure binary mixture of both proteins when adsorbed simultaneously as cations onto a 5-ml column of SP Sepharose FF at pH 3.7 at feedstock concentrations of 1.5 and 3 mg/ml, respectively. The optimal flow rate for the process was found to be 2 ml/min

which is equivalent to a linear velocity 60 cm/h. This work is now further extended to whey where the adsorption of proteins from solutions of whey isolate and whey concentrate powders is investigated under the previously developed adsorption conditions. The aim is to study the characteristics of adsorption of proteins from whey as opposed to pure protein systems, and to hence develop a facile separation process to separate the two major whey proteins and produce them with the highest possible yield and purity. As in the previous chapter, the method by which the two major proteins are separated is based on selective adsorption rather than selective elution, a technique which to the best of the author's knowledge has not been adopted elsewhere for column-chromatography purification of whey proteins.

8.2 Preliminary work on whey isolate

Being the purest of available whey powders with regard to total protein content, whey isolate, with a total protein weight percentage of 90%, was first chosen for this study. A concentration of 4.5 mg/ml of this variety of whey was prepared by dissolving the powder in an acetate buffer of pH 3.7, and was used to simulate real whey feedstocks. It should be noted that the 4.5 mg/ml concentration employed was the same as the total (ALA+BLG) concentration (C_{AB}) that was previously used in pure mixtures. Analysis of this mixture on an FPLC chromatography system using size exclusion (Figure 8.1) showed that it contains BLG and ALA, with concentrations of 2.3 and 0.9 mg/ml, respectively.

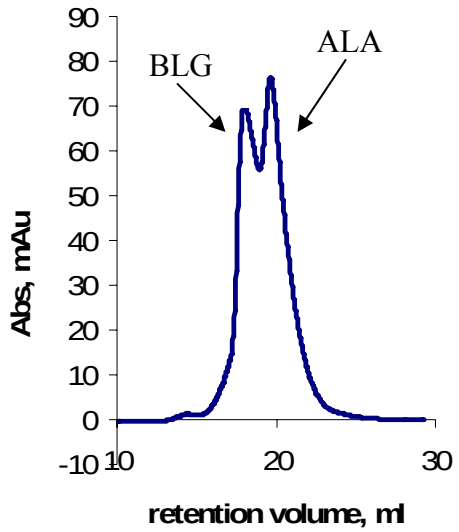

Figure 8.1 Analysis of 4.5 mg/ml of whey isolate using size-exclusion chromatography.

Table 8.1 shows the whey isolate composition according to the manufacturer's specifications, the FPLC analyses and the SDS estimates.

Table 8.1 Whey isolate composition.

	Manufacturer's specifications	SDS estimates	Gel filtration Analyses
total proteins	90%	—	—
BLG*	47%	62%	57%
ALA*	17%	21%	35%

*BLG, ALA percentages are taken on the basis of total proteins in the whey mixture.

A comparison of the protein composition results for the original whey isolate as determined by SDS gel electrophoresis (62% BLG and 21% ALA) with those determined by gel filtration (57% BLG and 35% ALA), showed a significant discrepancy regarding the percentage of ALA present. This could be due to the presumed presence of 26% (w/w) of glycomacropeptides (GMP) in the sweet whey isolate mixture, as indicated by the providing manufacturer. GMP is a peptide fragment produced by enzymatic cleavage of

κ-casein by chymosin during the making of sweet-based cheese (not commonly present in the acidic varieties). It is highly soluble in water and thus remains in the whey fraction after coagulation of milk (Zydney, 1998). According to a previous study of GMP by gel chromatography (Kawasaki *et al.*, 1993), the molecular weight of GMP aggregate was pH dependent, with a range from 20 to 50 kDa at pH 7 and from 10 to 30 kDa at pH 3.5. Although the theoretical molecular weight for monomeric GMP is 7 kDa (Kinsella and Whitehead, 1989; Xu *et al.*, 2000), the apparent molecular weight from 15% SDS polyacrylamide electrophoresis was found to be 20 to 24 kDa (Li and Mine, 2004). Thus, GMP would be expected to run in the same position as BLG in the SDS-PAGE (pH 7.0) analysis, and co-elute with ALA as one peak in the gel filtration (pH 3.7).

In view of the above, it was concluded that BLG would be better quantified by gel filtration than by SDS electrophoresis, and vice versa for ALA. This would translate to whey isolate having a composition of 57% BLG and 21% ALA and, in turn, a BLG to ALA ratio, *R*, of 2.6:1.0. This corresponds to BLG and ALA concentrations of 2.30 and 0.90 mg/ml, respectively in the 4.5 mg/ml solutions employed.

To investigate the behaviour of whey isolate, in presence of GMP, on the adsorption column, a whey solution at a concentration of 4.5 mg/ml corresponding to C_{AB} of 3.20 mg/ml was applied onto a SP Sepharose FF column at pH 3.7 and flow rate 2 ml/min. The relevant BLG and ALA adsorption profiles are depicted in Figure 8.2. It should be noted that there is absolutely no evidence for the presence of GMP with regard to the breakthrough profiles. The presence of GMP in preparations of ALA and BLG is reported to add more value to these proteins. GMP has been examined for improved lipid digestion, protection against influenza, prevention of tartar-adhesion to teeth and hence improvement of teeth decay (Maubois and Ollivier, 1997). It also exhibits various biological activities (Abd El-Salam *et al.*, 1996; Dziuba and Minkiewicz, 1996), such as suppression of gastric secretion, promotion of bifido-bacterial growth, binding of cholera and *Escherichia coli* enterotoxin, inhibition of viral and bacterial adhesion to intestinal walls, and modulation of immune system (Brody, 2000). It would therefore be beneficial for some industrial food and pharmaceutical applications to keep the GMP in the produced ALA and BLG fractions.

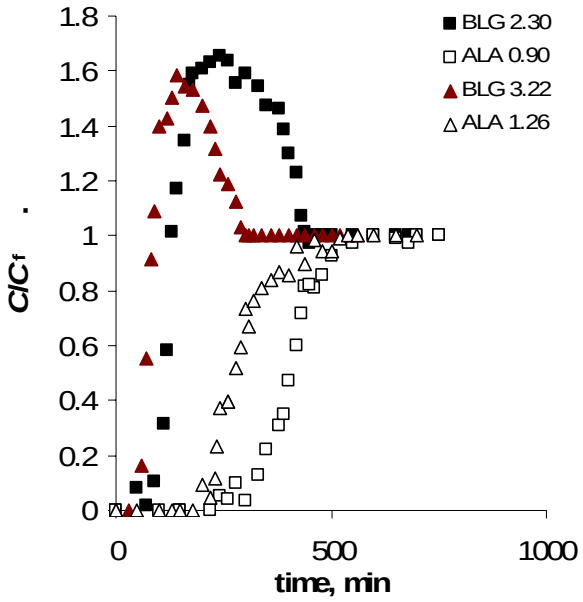

Figure 8.2 Packed-bed adsorption profiles for BLG and ALA when whey isolate solutions of 4.5 and 6.3 mg/ml concentration were applied onto a 5-ml SP Sepharose FF column at pH 3.7 and flow rate 2 ml/min.

As in the pure binary mixtures, studied earlier in Chapter 7, the BLG breakthrough started before that of ALA and its maximum outlet concentration exceeded that of its feedstock concentration by approximately 1.6 times. This implies the ability of ALA to displace some of the adsorbed BLG which was driven off the column indicating the interplay of competitive adsorption between the two proteins. Nevertheless, the ALA breakthrough began when the BLG concentration was at its maximum. It is to be recalled that for the binary mixtures at a flow rate of 2 ml/min, the ALA breakthrough occurred just before the BLG concentration had fallen back to its feedstock value and there was insignificant overlapping between the ALA and BLG curves. This difference in behaviour could be attributed either to the difference between R (BLG to ALA mass ratio) in the pure binary mixtures (3:1.5) and that found in whey isolate (2.6:1.0); or to the difference between C_{AB} in the whey isolate (3.20 mg/ml) from that of binary mixtures (4.50 mg/ml). A loss in both protein recovery and purity using feedstocks of whey isolate would thus be expected, as a result of this overlapping of the ALA and BLG breakthrough curves. To study the effect of total concentration, the initial whey concentration was raised by a factor of 1.4 so as to obtain an initial whey concentration of

6.3 mg/ml that corresponds to C_{AB} of approximately 4.5 mg/ml as in pure mixtures. This increased the steepness of the ALA and BLG breakthrough curves, but no significant change regarding their relative positions was realised (Figure 8.2). Thus, no improvement of separation was achieved, which denotes that the BLG to ALA ratio, rather than the total concentration, might possibly be the key factor. This will be investigated later on.

An additional adsorption experiment was performed on the 4.5 mg/ml whey isolate to determine the recovery and purity of ALA and BLG produced after separation. The experiment was terminated this time at the start of the breakthrough of ALA, when the BLG concentration had reached its maximum, i.e. at a time of 250 min. The column effluent collected up to this point was pooled and analysed on an FPLC system using size exclusion. The analysed fraction was found to contain mostly BLG with a recovery of 84% of the amount fed to the column. The column was then eluted with 0.1M Tris-HCl buffer at pH 9.0 and the eluted fraction was also analysed using gel filtration. This fraction contained mainly ALA along with some BLG, with an ALA recovery of 72% of the amount fed.

The purity of the two collected fractions was determined using SDS-PAGE gel electrophoresis and the relevant patterns are shown in Figure 8.3. The first lane on the left presents the molecular mass marker, the second lane is the whey isolate starting material, the third is the flow through-fraction and the last lane is the eluted fraction. In the original whey isolate, 62% of BLG and 21% of ALA were determined. On the other hand, 95% purity of BLG was achieved in the flow through-fraction whereas in the eluted fraction, purities of 42% for ALA and 37% for BLG were obtained.

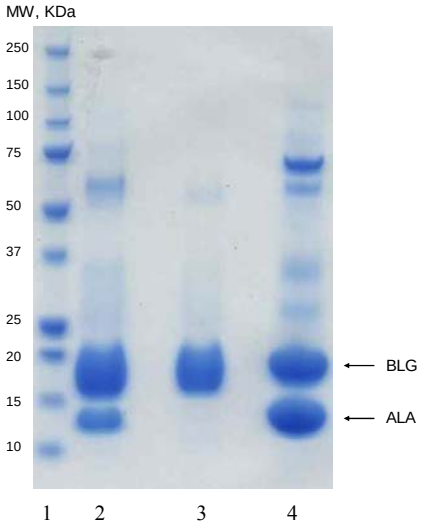

Figure 8.3 Electrophoretic patterns pertaining to whey isolate, lane 1: molecular mass marker; lane 2: whey isolate starting material; lane 3: flow-through-fraction; lane 4: eluted fraction.

The fact that GMP did not show up in the breakthrough curves nor in the SDS or size-exclusion analyses substantiates the supposition that it is camouflaged with either ALA or BLG. If one were to continue working with whey isolate, one should embark on a potentially laborious project whereby GMP is either quantified or removed. Both approaches proved to be unwieldy and unsuccessful as the following literature works attest. Several methods have been attempted such as TCA (1,1,1-trichloroethane) pretreatment (Morr and Seo, 1988), ethanol precipitation (Saito *et al.*, 1991), and ultrafiltration (Kawasaki *et al.*, 1993; Chu *et al*., 1996). Li and Mine (2004) investigated the three previous methods and the highest recovery of GMP, obtained using ultrafiltration was only 33.9%. Accordingly and in order to focus on the separation of the two relevant proteins ALA and BLG and to avoid any further complications, it was decided not to conduct further experiments with the sweet whey isolate but instead focus on the use of acid-based whey concentrate variety which is normally devoid of GMP.

8.3 Whey concentrate studies

A solution of whey proteins was prepared by dissolving whey concentrate powder in acetate buffer of pH 3.7 at a concentration of 4.5 mg/ml, and this was a convenient and

reproducible way to simulate native whey feedstocks. The concentration of 4.5 mg/ml was chosen initially in order that the situation might be directly comparable to the total (ALA+BLG) concentration (C_{AB}) that is normally present in native whey. It is to be noted that a total protein concentration of 4.5 mg/ml was also used when studying pure binary mixtures. Analysis of the whey concentrate solution on an FPLC system using size-exclusion (Figure 8.4) showed that it contains BLG with the higher molecular weight (first peak), and ALA at concentrations of 1.90 and 0.73 mg/ml, respectively, and hence a C_{AB} of 2.63 mg/ml and a BLG to ALA mass ratio (R) of 2.6.

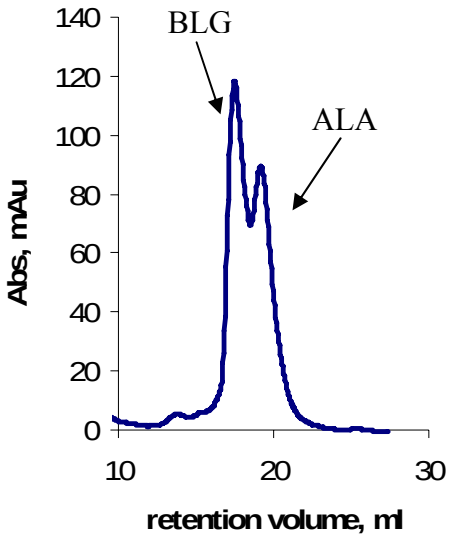

Figure 8.4 Analysis of 4.5 mg/ml of whey concentrate using size-exclusion chromatography.

According to the manufacturer's specifications, the whey concentrate powder contains 80% by wt total proteins of which 20% is ALA and 60% is BLG. FPLC analyses and SDS estimates gave comparable results (Table 8.2).

Table 8.2 Whey concentrate composition.

	Manufacturer's specifications	SDS Estimates	Gel filtration analyses
total proteins	80%	—	—
BLG*	60%	54%	53%
ALA*	20%	21%	20%

*BLG, ALA percentages are taken on the basis of total proteins in the whey mixture.

Figure 8.5 depicts the adsorption profiles pertaining to ALA and BLG when a 4.5 mg/ml whey concentrate mixture was applied to a 5-ml column at a flow rate of 2 ml/min and pH 3.7.

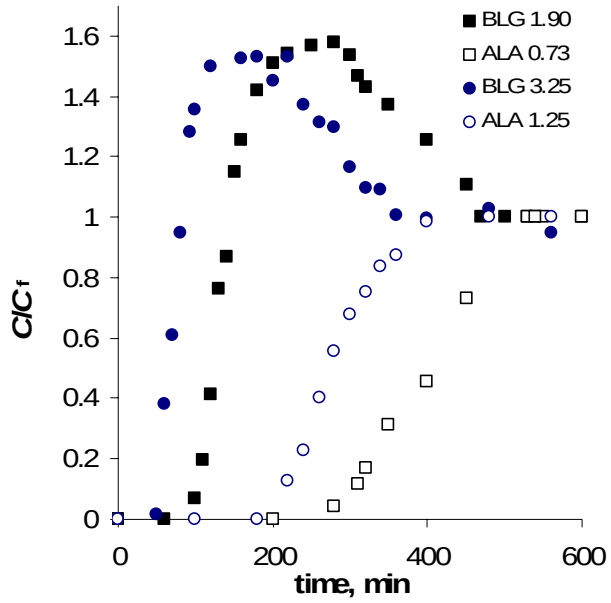

Figure 8.5 Packed-bed adsorption profiles for BLG and ALA when whey concentrate solutions of respectively 4.5 and 7.6 mg/ml concentrations were applied onto an SP Sepharose FF column at pH 3.7 and flow rate 2 ml/min.

As can be seen from the figure, BLG breakthrough preceded that of ALA and its maximum outlet concentration reached approximately 1.6 times its feedstock concentration. This demonstrates the ability of ALA to displace some of the adsorbed BLG which was subsequently desorbed from the column causing the BLG effluent

concentration to exceed that of the feed, a phenomenon indicating the presence of some form of competitive adsorption between the two proteins. Furthermore, ALA breakthrough was observed to begin at the point when the BLG concentration in the effluent had reached a maximum and hence overlapping between the breakthrough curves of the two proteins occurred. This overlapping of the breakthrough curves has a significant detrimental effect on the degree of separation that can be achieved as will be discussed later in detail. It should be noted that in the previous work on pure binary mixtures (Chapter 7), no significant overlapping was observed. In an attempt to reduce the degree of overlapping, several adsorption trials were performed under modified operating conditions including different total concentrations (C_{AB}), BLG to ALA mass ratios (R), and flow rates (F).

In the above experiment, as a result of the whey concentrate powder containing other compounds in addition to ALA and BLG, the total concentrations of these two proteins (C_{AB} = 2.63 mg/ml) was less than that used in the previous work on pure binary mixtures where the total feed concentration was 4.5 mg/ml. The concentration of whey concentrate used as feedstock was therefore increased to 7.6 mg/ml so as to yield concentrations of ALA and BLG of 1.25 and 3.25 mg/ml, respectively thus giving a total concentration of ALA + BLG (C_{AB}) of 4.5 mg/ml. As shown in Figure 8.5, the increase in C_{AB} improved the sharpness of both breakthrough curves, but had no effect on the position of ALA breakthrough with respect to that of BLG and hence overlapping still persisted. The $t_{1/2}$ values for both proteins (the times at which the breakthrough curve had risen to half the feed concentrations) decreased with increasing C_{AB} (Table 8.3). The decrease amounted to roughly 44% and 32% for BLG and ALA, respectively as compared to the values obtained with the 2.63 mg/ml solution of whey concentrate.

Table 8.3 Effect of C_{AB} on the $t_{1/2}$ values of ALA and BLG for whey concentrate.

C_{AB}, mg/ml	2.63	4.5
$t_{1/2\ ALA}$, min	410	280
$t_{1/2\ BLG}$, min	135	75

In conclusion, increasing C_{AB} has no effect on the degree of separation but rather on the operational time. Thus, a C_{AB} of 4.5 mg/ml corresponding to a whey powder concentration of 7.6 mg/ml will be employed in all of the forthcoming studies.

In the next experiment, the flow rate was reduced from 2 to 1 ml/min (Figure 8.6). It is to be noted that in the previous studies on pure binary mixtures (Chapter 7), it was found that overlapping was reduced and in turn separation was improved by decreasing the flow rate. A similar improvement was not observed for whey concentrate solutions. As can be seen from Figure 8.6, roughly the same degree of overlapping occurred at the lower flow rate.

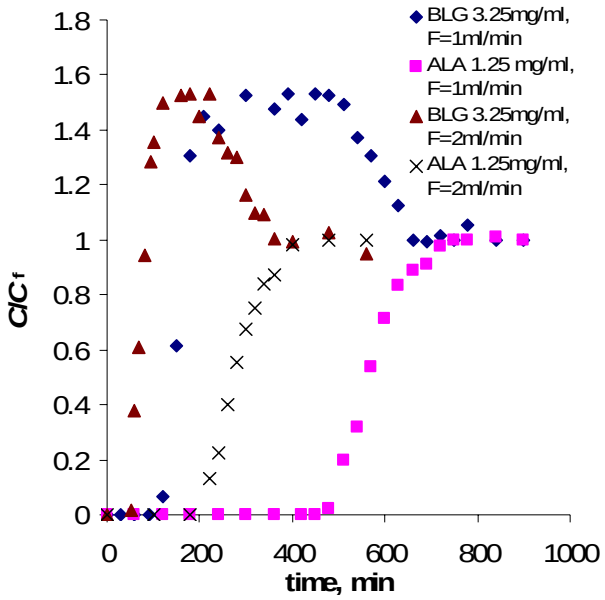

Figure 8.6 Packed-bed adsorption profiles for 3.25 mg/ml BLG and 1.25 mg/ml ALA when 7.6 mg/ml whey concentrate was applied onto an SP Sepharose FF column at pH 3.7 and flow rates of 1 and 2 ml/min.

Finally, the ratio *R* of the concentrations of BLG to ALA was adjusted by adding pure ALA solution to a 7.6 mg/ml whey concentrate solution such that the final concentrations of BLG and ALA in the whey-ALA mixture were 3.0 and 1.5 mg/ml, respectively. The value of *R* would thus be reduced to 2.0 as in the pure binary mixtures used previously. The relevant BLG and ALA adsorption profiles at a flow rate of 1 ml/min are shown in Figure 8.7.

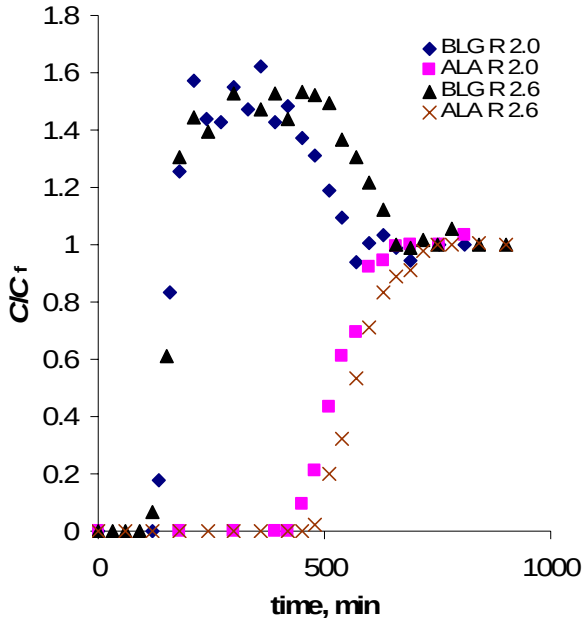

Figure 8.7 Packed-bed adsorption profiles for a solution containing 3.0 mg/ml BLG and 1.5 mg/ml ALA (created by adding pure ALA to a 7.6 mg/ml solution of whey concentrate) was applied onto an SP Sepharose FF column at pH 3.7 and flow rate of 1 ml/min. The profiles pertaining to 7.6 mg/ml whey concentrate (without addition of pure ALA) are also shown.

It can be seen that $t_{1/2}$ for ALA decreased with the decrease in R, while that for BLG did not change significantly. Even though the value of R in the whey mixture was adjusted to be equal to that in the solution of the pure proteins, it was still not possible to obtain the same degree of separation previously achieved using a pure protein mixture. However, increasing the value of R to 4.0 enhanced the separation as will be shown in later experiments (see the second stage in the consecutive two-stage process, Figure 8.13). The above experimental findings would be expected by examining the characteristics of Eq. 8.1:

$$q_m = \left(\frac{C_f * t_{1/2} * F}{V_L} \right) \qquad \textbf{(8.1)}$$

where V_L is the volume of the column, F is the flow rate, C_f is the feed concentration of the protein and q_m is the maximum binding capacity of the adsorbent. The left-hand side of the equation should strictly be q^* which is an estimate of the capacity of the adsorbent

in equilibrium with the feed. However in case of ALA and BLG proteins, the values of K_d are very small compared to the feed concentrations of these proteins, C_f, (Table 5.1) and therefore the values of q^* for each protein are essentially equal to q_m. It should also be noted that this simplified relation applies only to symmetrical breakthrough curves. However, it suffices for the qualitative reasoning discussed hereafter:

- increasing the total concentration, C_{AB}, increases the individual concentrations of ALA and BLG and thus decreases their breakthrough times ($t_{1/2}$) by about the same degree. As a result, overlapping and hence separation were not affected.
- decreasing the flow rate, F, increases $t_{1/2}$ values for both proteins by roughly the same degree and thus has no significant effect on improving the separation.
- increasing the ratio of BLG to ALA, R, increases the concentration of BLG at the expense of the concentration of ALA. This, in turn, decreases the $t_{1/2}$ of BLG relative to that of ALA and thus reduces overlapping between the breakthrough curves of the two proteins and consequently improves separation.

Thus, it can be concluded that modifying the operating conditions (total concentration and flow rate) so as to be comparable with those used previously for pure mixtures did not improve the degree of separation. This is probably a result of the complex nature of whey in which there are additional compounds present. Moreover, of the three operating conditions investigated, R was found to be the key factor dictating the degree of separation achieved; increasing R improved the separation. However, increasing R requires adding pure BLG to the whey feedstock and this would not be feasible in a large-scale process designed for the economic isolation of whey proteins. Therefore, in the following experiments whey concentrate will be used without any additions of pure BLG.

In what follows, the aim is to establish an optimal process for the separation and purification of ALA and BLG from whey concentrate, such that the adsorption of proteins from a 7.6 mg/ml solution of whey concentrate at a flow rate of 2 ml/min is performed on the 5-ml column.

An adsorption experiment was conducted and the loading of the feedstock was terminated at the ALA breakthrough point (also the BLG maximum), i.e. 180 min (Figure 8.5). Analysing the column effluent collected up to this point using size exclusion

revealed that this fraction contained mostly BLG with a recovery of 80% of the amount of BLG that had been fed to the column (Figure 8.8). The column was then eluted with 0.1M Tris-HCl buffer at pH 9.0. The eluted fraction was analysed using gel filtration and was found to contain mainly ALA with a recovery of 84% of that in the feedstock, along with some BLG.

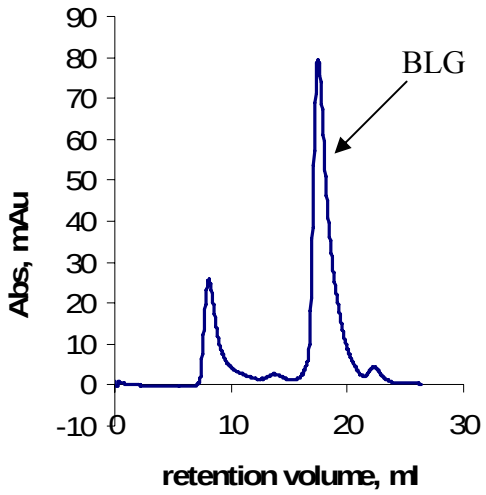

Figure 8.8 Analytical size-exclusion chromatography on Superdex 200 for the flow-through fraction, collected up to the start of the ALA breakthrough, for 7.6 mg/ml whey concentrate.

The purity of the produced ALA and BLG eluted fractions was determined using SDS-PAGE gel electrophoresis. Figure 8.9 shows the electrophoretic patterns pertaining to these fractions. Lanes 1, 2, 3 and 4 from the left present the molecular mass marker, whey concentrate starting material, flow through-fraction and eluted fraction. The purity of BLG in the obtained flow through-fraction was 95%, while the composition of the eluted fraction was 32% ALA and 38% BLG. The higher molecular-weight bands also present are those of bovine serum albumin (BSA) and immunoglobulin G (Ig G). It is to be mentioned here that when this experiment was performed at a flow rate of 1 ml/min, rather than 2 ml/min, and the ALA fraction was analysed using SDS electrophoresis, 44% purity of ALA was obtained. Nevertheless, the improvement in ALA purity with the lower flow rate was not enough to justify operating at such a longer time.

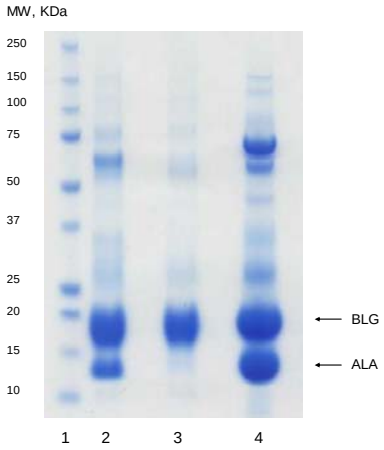

Figure 8.9 Electrophoretic patterns pertaining to 7.6 mg/ml whey concentrate, lane 1: molecular mass marker; lane 2: whey concentrate starting material; lane 3: BLG flowthrough fraction; lane 4: ALA eluted fraction.

In light of the above study, it can be deduced that:

- the purity of ALA in the eluted fraction drops as a result of the overlapping that starts at the ALA breakthrough point, corresponding to BLG maximum, and ends when BLG breakthrough reaches a plateau at its inlet concentration (i.e. at $C/C_f = 1.0$).

- overlapping also affects the recovery of BLG in the flow-through fraction as some of it (20%) was yet to be eluted from the column by the competitive adsorption of ALA at the point of terminating the application of feedstock.

- in spite of the similarity in the shapes of the ALA and BLG breakthrough curves between pure and whey mixtures, it was not possible to attain the same degree of separation obtained in the mixtures of pure proteins due to the complex nature of whey as well as its different BLG to ALA ratio.

To obtain an ALA fraction free of BLG, the loading of feedstock was terminated at the point where the concentration of BLG in the effluent falls back down to its initial value, i.e. $C/C_f = 1$, and that occurred at 420 minutes (Figure 8.5). Two fractions were collected, a BLG flow-through fraction (stream 2, Figure 8.16) collected up to 180 min (which contains BLG), followed by an ALA-BLG flow-through fraction (stream 4, Figure 8.16) collected between 180 and 420 min (which contains a mixture of both ALA and BLG). With this strategy, all BLG is removed from the column and is collected as an effluent in these two fractions. ALA together with other whey impurities are left on the column. To obtain an eluted fraction that contains ALA with minimal co-eluted

impurities (ALA eluted fraction) the column was eluted consecutively with buffers containing 0.1 M solutions of sodium acetate (pH 5.2), Tris-HCl (pH 7.0), and finally Tris-HCl (pH 9.0). The BLG flow-through fraction was found to contain mostly BLG with a recovery of 40% of the applied thereof as estimated by size exclusion chromatography analysis. The recoveries of ALA in the fractions eluted at pH 5.2 and pH 7.0 eluted fractions (streams 3 and 3′, respectively, Figure 8.16) as calculated from size-exclusion analysis (Figure 8.10), were 30% and 15%, respectively. No significant amount of ALA was recovered when the column was further eluted at pH 9.0.

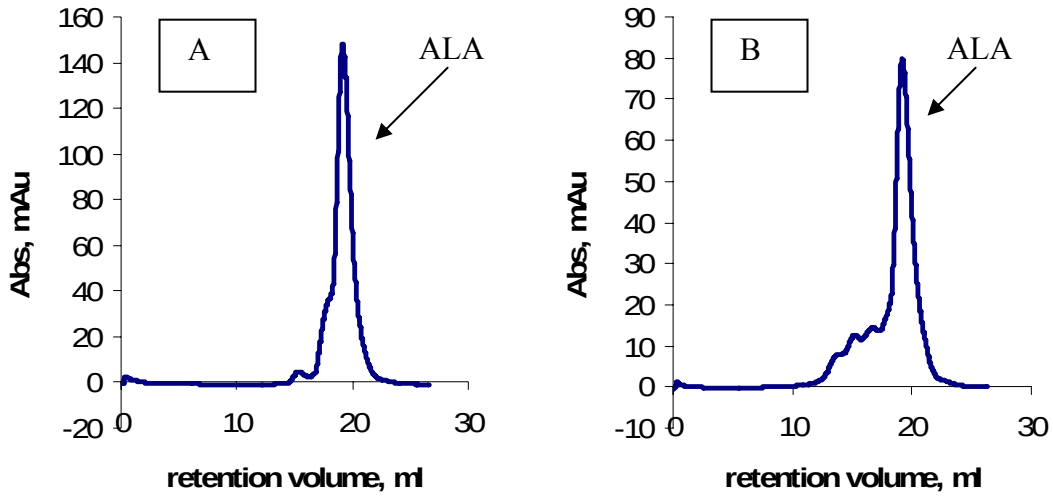

Figure 8.10 Size-exclusion analysis on Superdex 200 for pH 5.2 (A) and pH 7.0 (B) eluted fractions pertaining to 7.6 mg/ml whey concentrate when the prolonged adsorption experiment (one-stage process) was performed.

The SDS analysis (Figure 8.11) of the BLG flow-through fraction yielded a BLG purity of 95%, whereas the purities of ALA in the peaks eluted at pH 5.2 and pH 7.0 were respectively 54% and 60%. The ALA-BLG flow-through fraction contained a mixture of BLG and ALA in the ratio of 5:1.

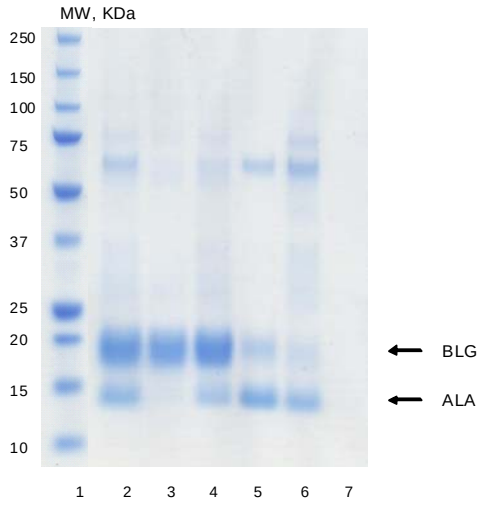

Figure 8.11 Electrophoretic patterns for the ALA and BLG fractions produced after the adsorption and elution of 7.6 mg/ml whey concentrate during the one-stage process, lane 1: molecular mass marker; lane 2: whey concentrate starting material; lane 3: BLG flow-through fraction; lane 4: ALA-BLG flow-through fraction; lane 5: pH 5.2 eluted fraction; lane 6: pH 7.0 eluted fraction; lane 7: pH 9.0 eluted fraction. Samples were diluted 10 times.

As can be seen in Figure 8.11, each of the electrophoretic patterns for the pH 5.2 and pH 7.0 eluted fractions shows the presence of a lower molecular mass band that corresponds to the molecular mass of ALA, and another band that corresponds to the molecular mass of BLG comprising roughly 30% and 15% of the total amount of protein eluted at the respective pH values of 5.2 and 7.0. These fractions also contain other higher bands that represent the higher molecular-weight proteins present in whey concentrate such as bovine serum albumin and immunoglobulin G. A mass balance, performed on the amounts of BLG in both the feed and effluent fractions, showed that almost no BLG was left on the column and that practically none should appear in the eluted fractions. It can thus be inferred that the significant band that runs in the SDS gel electrophoresis analysis with an apparent molecular mass similar to that of BLG is in fact unlikely to be BLG. This might probably be some of the higher molecular weight compounds that had degraded to lower molecular weights at the employed pH values.

To improve the overall recoveries of both proteins, as well as to take advantage of the high *R* in the ALA-BLG flow-through fraction produced during the process (5:1), a consecutive two-stage approach was introduced as follows (see Figure 8.16). The ALA-

BLG fraction was mixed with an equal volume of fresh whey concentrate feedstock (streams 4 and 5, respectively, Figure 8.16). The mixture now containing BLG and ALA in the ratio of 4:1, as estimated by SDS analysis (Figure 8.12), was fed to the column at 2 ml/min and the resulting adsorption profiles for BLG and ALA are shown in Figure 8.13.

As in the first stage, two fractions were collected during the loading period. The first fraction (stream 6, Figure 8.16) was collected up to the start of the ALA breakthrough, while the second fraction (stream 8, Figure 8.16) was collected up to the point where BLG dropped to its inlet concentration ($C/C_f = 1$). The first fraction was found to contain almost pure BLG with a purity of 95% as estimated using SDS gel electrophoresis shown in Figure 8.12. The electrophoretic pattern of the second fraction showed that it contained 86% BLG together with 5% ALA. Therefore this BLG-rich fraction from the second stage required no further processing unlike the situation during the first stage of operation where the amount of ALA present in the equivalent flow-through fraction was substantially higher. It should be noted here that the degree of separation was enhanced by virtue of the higher BLG to ALA ratio now present in the feedstock used in the second stage (4:1), which was the result of the addition of ALA-BLG flowthrough fraction from the first stage to the solution of whey concentrate. In other words, increasing the ratio of BLG to ALA improved the separation as was mentioned earlier. Noteworthy here is the fact that when the protein recovery of the second stage was calculated on the basis of its feed alone, it turned out to increase proportionally with R relative to the first stage. It is clear that the second stage was introduced as an alternative for adding BLG from the beginning in order to raise R.

After collecting the second flow-through fraction, the application of feedstock was terminated and the column was eluted consecutively with 0.1 M sodium acetate buffer (pH 5.2) followed by 0.1 M Tris-HCl buffer (pH 7.0) (streams 7 and 7′, respectively, Figure 8.16). The purities of ALA in the two eluted fractions were estimated to be 54% and 60%, respectively using SDS gel electrophoresis. These values were the same as those for the equivalent fractions collected in the first stage.

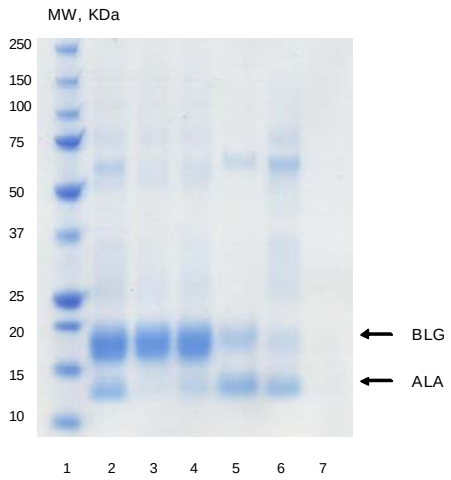

Figure 8.12 Electrophoretic patterns for the ALA and BLG fractions produced after the adsorption and elution of 7.6 mg/ml whey concentrate during the second stage of the consecutive two-stage process, lane 1: molecular mass marker; lane 2: whey concentrate starting material; lane 3: BLG flow-through fraction; lane 4: ALA-BLG flow-through fraction; lane 5: pH 5.2 eluted fraction; lane 6: pH 7.0 eluted fraction; lane 7: pH 9.0 eluted fraction. Samples were diluted 10 times.

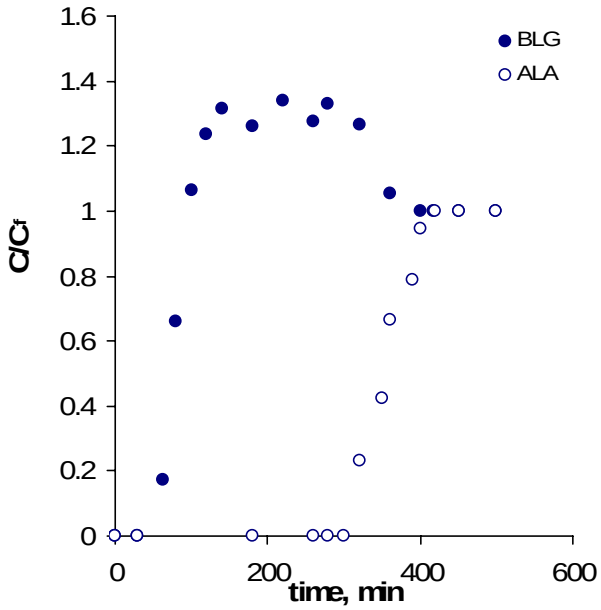

Figure 8.13 Packed-bed adsorption profiles for BLG and ALA when a (1:1 v/v) mixture of 7.6 mg/ml whey concentrate feedstock added to the ALA-BLG flow-through fraction (from the first stage of the consecutive two-stage process) was applied onto an SP Sepharose FF column at pH 3.7 and flow rate 2 ml/min.

The above results showed that the presence of other higher molecular-weight proteins in the eluted fractions lowers the purity of ALA therein. Hence, it was assumed that this purity could be improved by further purification of the eluted fractions using size-exclusion chromatography. To verify this assumption, a 0.2 ml sample of each of the fractions eluted at pH 5.2 and pH 7.0, produced from the first stage of the previous experiment, were applied to a Superdex 200 gel-filtration column and the peaks containing ALA were collected. Each of these peaks was further analysed on the same column (Figure 8.14), as well as on an SDS electrophoresis gel (Figure 8.15). The results showed that fractions containing ALA of at least 85-90% purity could be achieved by this additional step. It is therefore recommended that a subsequent size-exclusion chromatography process be used as an intermediate purification or a final polishing step, in order to increase the purity of ALA in the eluted fractions.

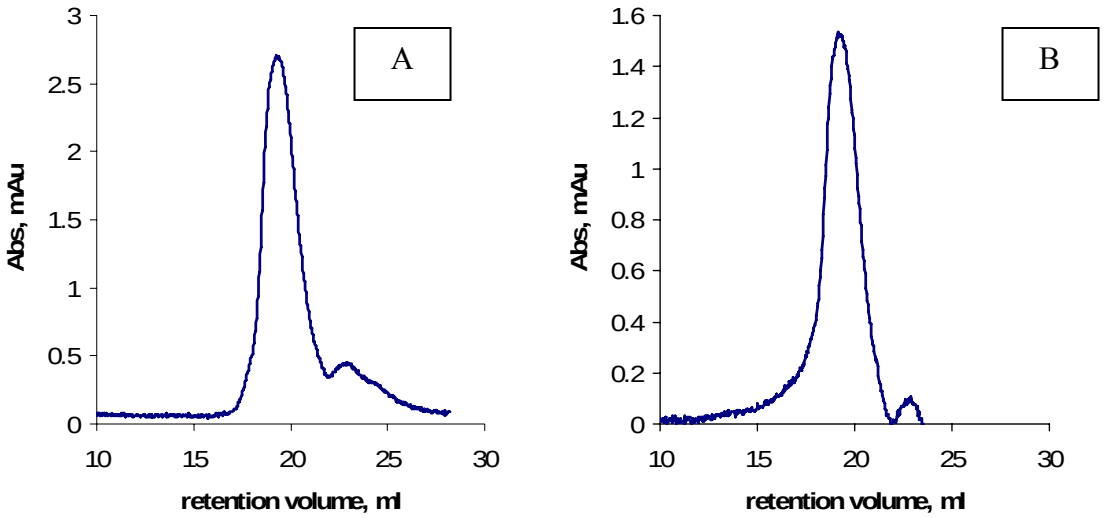

Figure 8.14 Size-exclusion analysis on Superdex 200 for the eluted ALA fractions that were collected from the first stage of the consecutive two-stage process and then further purified on a Superdex 200 size-exclusion column, (A) ALA fraction collected in the pH 5.2 eluate; (B) ALA fraction collected in the pH 7.0 eluate.

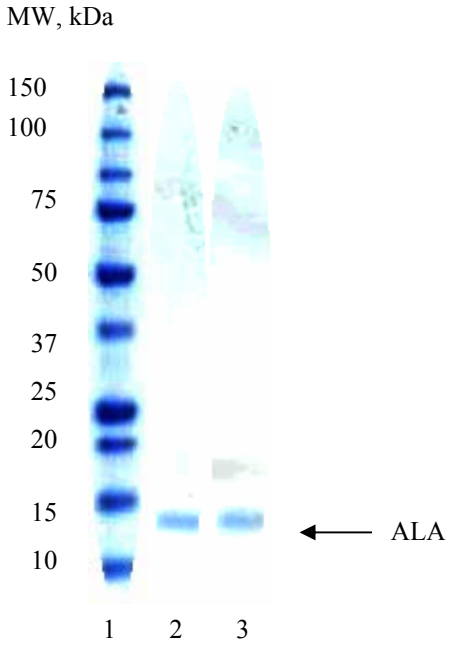

Figure 8.15 Electrophoretic patterns for the collected ALA peaks shown in Figure 8.14, lane 1: molecular mass marker; lane 2: ALA fraction collected from pH 5.2 eluate; lane 3: ALA fraction collected from pH 7.0 eluate. In this experiment, each well was loaded with 14 μl of sample.

A schematic diagram of the consecutive two-stage process is depicted in Figure 8.16. About 78% of the BLG applied in the two feed streams (1 and 5) was recovered in the two flow-through fractions obtained (streams 2 and 6). In the first stage, 27% was recovered, whereas 51% was recovered in the second stage. A further 20% of BLG fed to the process was recovered in the BLG (+ALA) flow-through fraction obtained from the second stage (stream 8). Therefore, a total of 98% (78%+20%) of BLG was recovered using this process. As for ALA, 33% of the amount fed to the process was recovered in the two eluted fractions obtained from the first stage (streams 3, 3′), in addition to a further 34% recovered in the two eluted fractions obtained from the second stage (streams 7, 7′). Hence, a 67% overall recovery of ALA was obtained in this process.

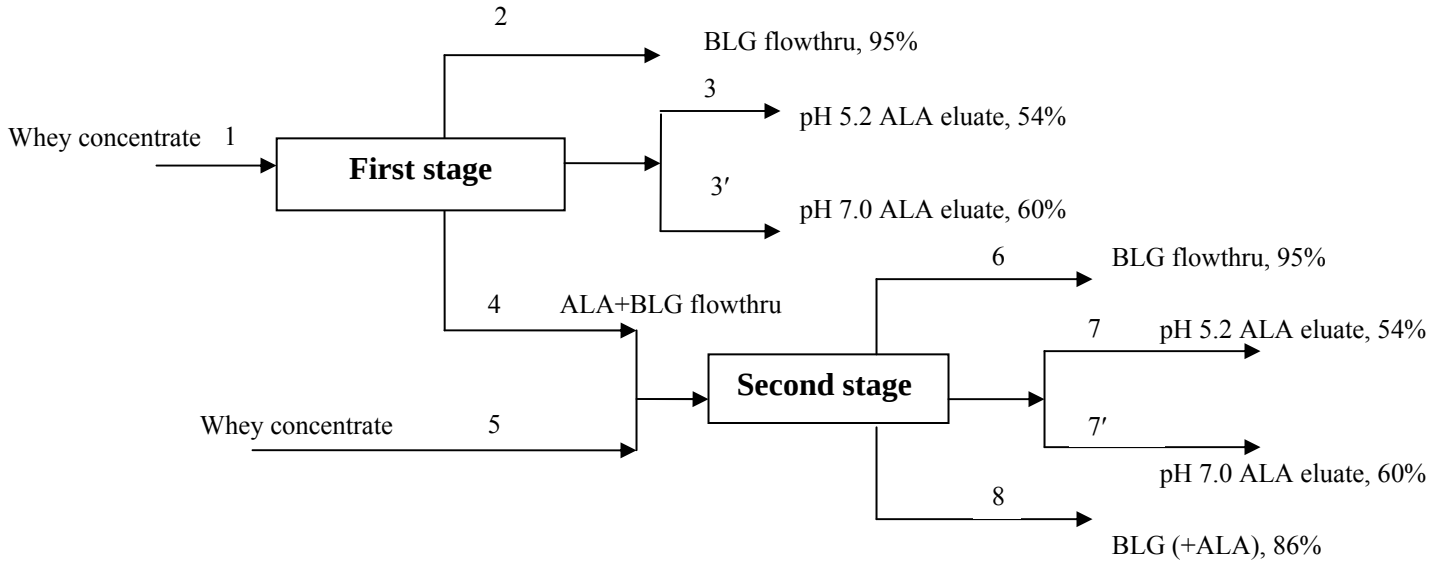

Figure 8.16 Flow diagram of the consecutive two-stage process.

A summary of the recoveries and purities of ALA and BLG obtained from the consecutive two-stage process is presented in Table 8.4.

Table 8.4 Recoveries and purities of ALA and BLG for the consecutive two-stage process.

Protein	Stream number*	recovery (%)	Purity (%)
	Stage 1		
BLG	**2**	**27**	**95**
	3	**22**	**54**
ALA	**3′**	**11**	**60**
	3+3′	**33**	
	Stage 2		
BLG	**6**	**51**	**95**
	8	**20**	**86**
	7	**26**	**54**
ALA	**7′**	**8**	**60**
	7+7′	**34**	
	Overall process		
	2+6	**78**	**95**
BLG	**8**	**20**	**86**
	2+6+8	**98**	
	3+7	**48**	**54**
ALA	**3′+7′**	**19**	**60**
	3+3′+7+7′	**67**	

* see flow diagram (Figure 8.16).

8.4 Conclusions

The cation-exchange adsorption of whey concentrate mixtures was studied at pH 3.7 using SP Sepharose FF with the aim of separating ALA and BLG from these mixtures. BLG breakthrough occurred first, and its concentration in the outlet exceeded its feed value by about a factor of 1.5 before declining to the feed value, followed by the breakthrough of ALA. ALA was able to displace and drive BLG off the column and therefore BLG was collected in a pure form. Substantially pure ALA could then be eluted from the column. This evidence of competitive adsorption was used to establish a consecutive two-stage novel process for separating ALA and BLG from whey concentrate mixtures. In both stages, the application of feedstock was terminated at the point where BLG reached its inlet concentration (at C/C_f=1). In both stages, two fractions were collected during the loading period; a fraction containing almost pure BLG was collected up to the start of the ALA breakthrough, followed by a second fraction containing both ALA and BLG. This second fraction from the first stage was mixed with whey concentrate solution to form the feedstock for the second stage. In the second stage, the second fraction contained BLG at sufficiently high purity as to require no further processing. At the termination of feedstock application during each stage of operation, the column which then had almost no adsorbed BLG remaining was eluted to obtain substantially purified ALA. The flow-through and eluted fractions were analysed using size-exclusion as well as SDS gel electrophoresis to estimate purities. In the second stage, the breakthrough as well as the analysis profiles were very similar to those of the first stage, but the ALA-BLG flowthrough fraction from the second stage was found to contain mostly BLG with 86% purity. The overall recoveries of BLG and ALA from the consecutive two-stage process were found to be 98% and 67%, respectively, showing increases of about 2.5 times and 1.5 times over the one-stage process. The 98% recovery of BLG is the sum of the two BLG flowthrough fractions collected in stages one and two (78%) and the ALA-BLG flowthrough fraction of the second stage (20%). Thus 78% of the recovered BLG had a purity of 95%, whereas the remaining 20% had a purity of 86%. The purity of ALA in the pH 5.2 and pH 7.0 eluted fractions in the two stages was 54% and 60%, respectively. A size-exclusion polishing step has been shown to be suitable for improving the purity of ALA present in the eluted fractions.

To sum up, a novel consecutive two-stage process was developed to isolate ALA and BLG from whey concentrate solutions. The novelty of the process comes from the fact that it is based on selective adsorption of whey proteins rather than selective elution. The latter has been used by many other workers in previous literature. The selective adsorption technique also makes the process simple and viable for separation as mostly all the BLG was recovered during the loading step. ALA, on the other hand, was recovered using simple consecutive elution by varying the pH. No salt addition was required for elution which is an additional economical as well as an environmental merit to the process.

9 Simulation of the breakthrough curves for the adsorption of whey proteins

9.1 Introduction

A few studies have been made on the modelling of whey protein adsorption. James (1994) investigated both the single and binary adsorption/desorption equilibrium and dynamics of lactoferrin and lactoperoxidase, purified from raw whey solutions, using three different Sepharose cation exchangers. Carrere *et al.* (1996) studied the recovery of alpha-lactalbumin and beta-lactoglobulin from sweet whey protein by a fluidized ion exchange chromatographic process. They lumped both components as one entity in the pore-diffusion adsorption model as well as in a subsequent lumped kinetic elution model. By means of the pore-diffusion model, Conrado *et al.* (2005) described, the operating parameters related to the use of a hydrophobic resin (Streamline Phenyl) for the recovery of alpha-lactalbumin from cow's milk whey in an expanded-bed adsorption mode of operation.

As evident from the confocal laser scanning microscopy (CLSM) and packed-bed experiments in Chapters 6 and 7, the more weakly adsorbed protein (ALA) was able to displace the more strongly adsorbed one (BLG), a result that has also been encountered by some authors on other systems (Hubbuch *et al.*, 2003). In order to account for this, the previous equilibrium, kinetic, and packed-bed results were relied upon in order to propose the following explanation. The faster BLG was envisaged to be electrokinetically transferred at first and exchanged for the neutralising Na^+ ions. The locus of this adsorption is assumed to be the diffuse part of the electric double layer. In complexation notation, the adsorbed BLG is an outer-sphere complex separated from the surface by at least one layer thick of the solvent. The displacement occurs later when the lagging (diffusing) ALA manages to catch up with the adsorbed BLG whereupon the mass action redistribution must entail expulsion of some of the adsorbed BLG (an exchange of BLG for ALA) in order to maintain electroneutrality. The importance of this articulation will become evident later in the text.

In this chapter, the intention is to use various models of the adsorption process to simulate the breakthrough curves obtained from our previous packed-bed studies both for pure proteins, either alone or in mixture, and for these proteins when present in whey concentrate. Being the simplest of models as the name implies, the simple kinetic model will be first examined and appropriate correction factors for the isotherm and kinetic parameters will be introduced when necessary. The model has been used by various workers to simulate protein breakthrough curves (Cowan *et al.*, 1989; Skidmore *et al.*, 1990; Conrado *et al.*, 2005; Aboudzadeh *et al.*, 2006). However, the approach of introducing correction factors was not adopted. In addition, the possibility of using a more sophisticated pore and diffusion model will be investigated.

9.2 Single-component systems

In this section, simulation of the packed-bed adsorption of either 3 mg/ml pure BLG or 1.5 mg/ml pure ALA onto a 5-ml column of SP Sepharose at pH 3.7 and linear velocity of 60 cm/h (flow rate of 2 ml/min) is studied. Kinetic studies preceded this work (Chapter 6) where batch uptake profiles for ALA and BLG were predicted using both the simple kinetic model and the pore diffusion model. For both proteins, the former model gave better fit to the experimental data. Therefore the simple kinetic model will be used throughout this study. In order to theoretically predict the breakthrough curve for BLG, values of the equilibrium isotherm parameters determined from batch experiments (q_m = 113.6 mg/ml and K_d = 0.008 mg/ml) (Chapter 5), as well as the forward kinetic rate-constant for adsorption within medium-size adsorbent particles ($k_1 = 35*10^{-3}$ $mlmg^{-1}min^{-1}$) obtained from batch uptake experiments (Chapter 6), were used to solve the simple kinetic model for packed-bed adsorption (Eq. 3.26 and 3.27). The model solves for C as a function of both time and position along the height of packed bed (x). The theoretical breakthrough curve so obtained was constructed as a solid curve (Figure 9.1A) and compared to its corresponding experimental profile.

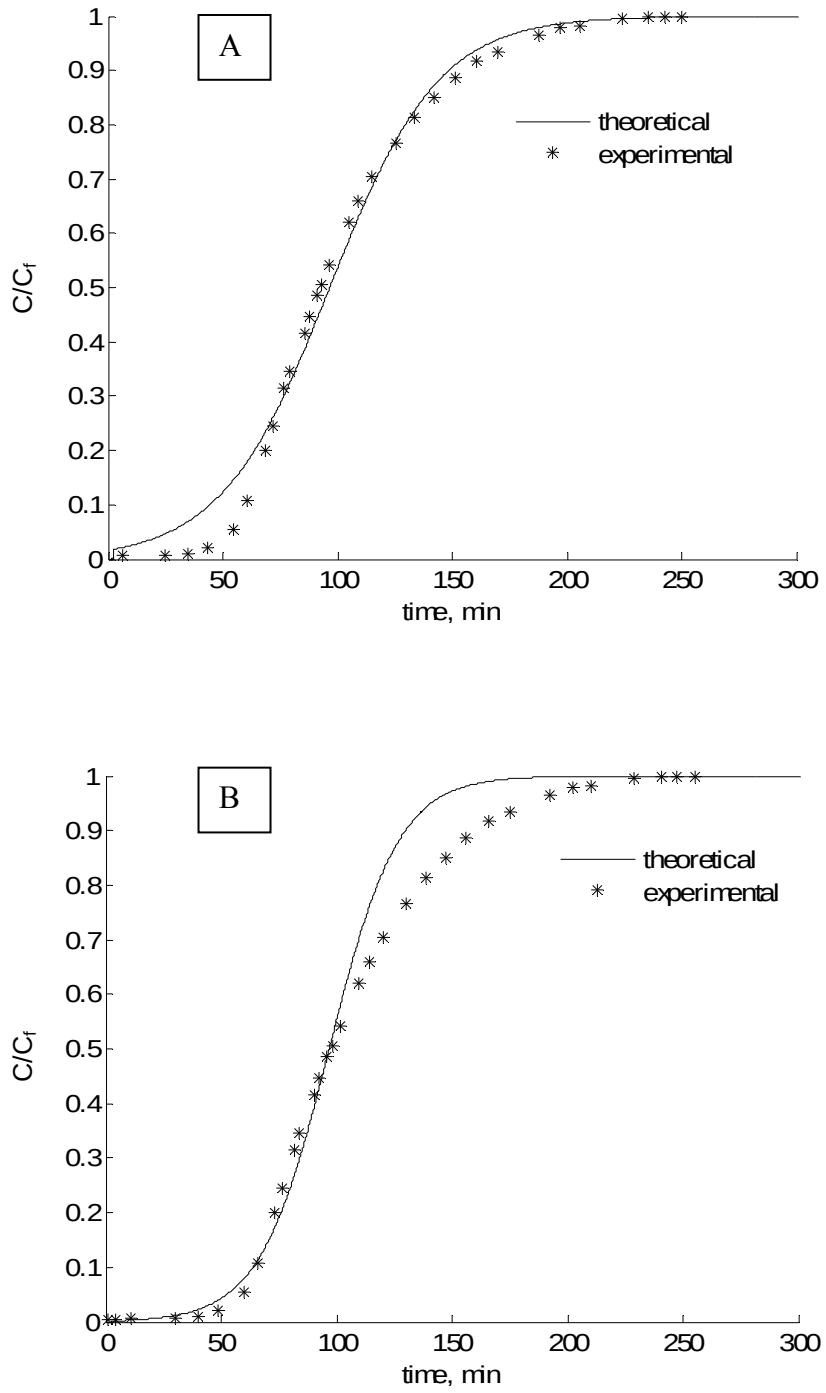

Figure 9.1 Predicted and experimental breakthrough curves for the adsorption of BLG onto a 5-ml packed-bed of SP Sepharose FF at pH 3.7, feed concentration of 3 mg/ml, flow rate of 2 ml/min, and temperature 20°C, using k_1=35*10^{-3}mlmg^{-1}min^{-1}(A), and k_1=55*10^{-3}mlmg^{-1}min^{-1}(B). Agreement between predicted and experimental results was within accuracy of 10%.

As can be seen from the figure, the experimental adsorption profile (discrete points) in its early stage (before reaching $t_{1/2}$) yields a sharp and symmetrical breakthrough curve that is steeper than its corresponding theoretical curve. Both curves nearly have the same $t_{1/2}$ as well as the same equilibrium position (curve plateau), but the time corresponding to 5% of the maximum capacity of the adsorbent or the so called 'breakthrough time' is under-predicted by the model. In addition, the model well predicts the later stage of the breakthrough curve (after reaching $t_{1/2}$). As accurate prediction of the early stage of the breakthrough curve is more important from a practical point of view, the value of k_1 was increased from $35*10^{-3}$ to $55*10^{-3}$ $mlmg^{-1}min^{-1}$, in order to get a better fit to the experimental data (Figure 9.1B). The modified value of k_1 corresponds to adsorption within the smallest particles of the adsorbent, as was determined from the relevant profiles of adsorbed protein as visualised using CLSM techniques (Figure 6.24A). Hence, the early stage of the breakthrough curve is better predicted using the value of the rate constant corresponding to adsorption within the smallest particles, while the later stage of the curve could be predicted using the value of the rate constant corresponding to adsorption within the medium-size particles. This could be due to difference in the nature of packed beds as opposed to batch adsorption systems. During the packing process, the adsorbent suspension is allowed to sediment and the supernatant liquid is subsequently removed from the top of the column. The larger particles are therefore expected to settle predominantly towards the bottom of the column while the smaller particles aggregate towards the top. During operation in a downflow mode (as was the case here), the protein solution will be expected to come in contact first with the smaller particles. Therefore, the rate of adsorption in the packed bed at the beginning of feedstock application was more controlled by adsorption to the smaller particles rather than to the larger ones. Apparently, with time the smaller particles became completely saturated first and hence the adsorption was then governed by the rate of adsorption to the larger particles.

The experimental and theoretical profiles for 1.5 mg/ml pure ALA are depicted in Figure 9.2.

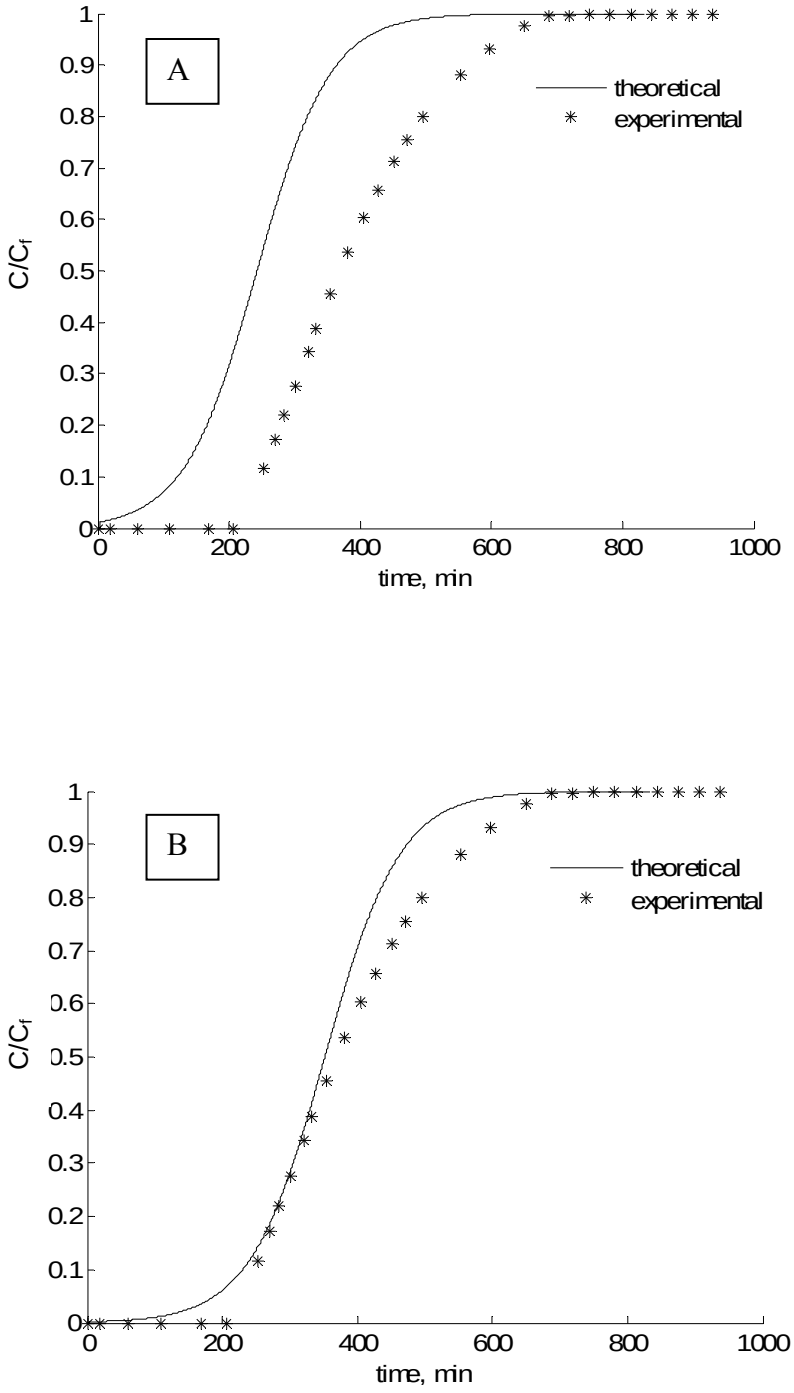

Figure 9.2 Predicted and experimental breakthrough curves for the adsorption of ALA onto a 5-ml packed-bed of SP Sepharose FF at pH 3.7, feed concentration of 1.5 mg/ml, flow rate of 2 ml/min, and temperature 20^{o}C, using k_1=30*10^{-3}mlmg^{-1}min^{-1} and the equilibrium batch isotherm parameters (A), and after increasing q_m 1.5 times (B).

The theoretical profile was predicted using the relevant equilibrium isotherm parameters (q_m = 147.0 mg/ml and K_d = 0.029 mg/ml) obtained in Chapter 5, and the kinetic rate constant for adsorption within the medium-size particles ($k_1 = 30*10^{-3}$ $mlmg^{-1}min^{-1}$) obtained in Chapter 6. As can be seen in Figure 9.2A, the predicted value for $t_{1/2}$ is lower by about one-third of its actual value. This, in turn, indicates that the predicted amount of protein adsorbed onto the bed, q, is underestimated by the model by a factor of two-thirds according to Eq. 4.2. This implies that additional adsorption processes are occurring in the packed-bed (relative to the batch system). These could be a result of the segregation of the different sizes of adsorbent beads in packed beds, a phenomenon that does not occur in batch systems, as well as the continuous feed at a constant inlet concentration in packed bed operation which might have resulted in ALA, being small in size, becoming more accessible to finer pores (additional adsorption sites). If one is to assume that additional adsorption sites are available for ALA within the packed-bed, q_m can be modified to account for this by increasing its value by a factor of 1.5. With this modification, good agreement between predicted and actual results was attained in the early stage of the breakthrough curve using the value of the rate constant that corresponds to adsorption within the medium-size particles (Figure 9.2B). Unlike BLG, the adsorption in the early stage appears to be governed by the transport within the medium-size particles not the smallest ones. This is understandable in light of the fact that the largest amount of ALA was adsorbed within the medium-size particles as was implied from the profiles of adsorbed ALA obtained using CLSM techniques (Figure 6.24B).

Survey of the literature (Aboudzadeh *et al.*, 2006; Yun *et al.*, 2005; Tong *et al.*, 2003; Chen *et al.*, 2003; Avci *et al.*, 2000; Skidmore *et al.*, 1990) showed that the alternative use of a pore diffusion model to model packed bed adsorption does not significantly affect the $t_{1/2}$ value and thus it is not expected to resolve the discrepancy observed.

9.3 Two-component systems

As was highlighted previously in the 'Introduction' to this chapter, it has been postulated that the transport mechanism is different for the two proteins under consideration; while BLG is electrokinetically transported, ALA is governed by a slower diffusion process. Strictly speaking, the author realises that the simple kinetic model is not suited for such a situation. However, in the absence of a compatible model accounting for these two mechanisms, it was decided to continue to work with the simple model to see whether introducing appropriate correction factors to the system parameters can improve the agreement between experimental results and theoretical simulations as was the case with the single-component systems.

For the two-component system, an attempt was made to predict the individual breakthrough profiles for BLG and ALA when a mixture of both proteins was adsorbed onto SP Sepharose FF at the reference whey conditions (i.e. feed concentrations of 3 mg/ml and 1.5 mg/ml for BLG and ALA, respectively) and at the optimum flow rate of 2 ml/min. The simple kinetic model for two-component systems with competition between species was solved (Eq. 3.32, 3.33, 3.34, and 3.35).

The following two-component simulation results will first deal with pure binary mixtures and will be extended thereafter to whey concentrate.

9.3.1 Pure binary mixture

The adsorption profiles for ALA and BLG in the two-component system are shown in Figure 9.3. It was not possible to predict the shapes of the individual breakthrough curves of ALA and BLG using the single-component equilibrium isotherm parameters obtained in Chapter 5. As shown in the figure, the BLG overshoot could only be predicted when the value of K_d for BLG was increased by a factor of 600 (i.e. was more than 150 times higher than that of ALA), while the value of q_m for the same protein was augmented 3.5 times (i.e. was 2.7 times larger than that of ALA). The apparent (modified) values of q_m and K_d will be referred to as q'_m and K'_d, respectively.

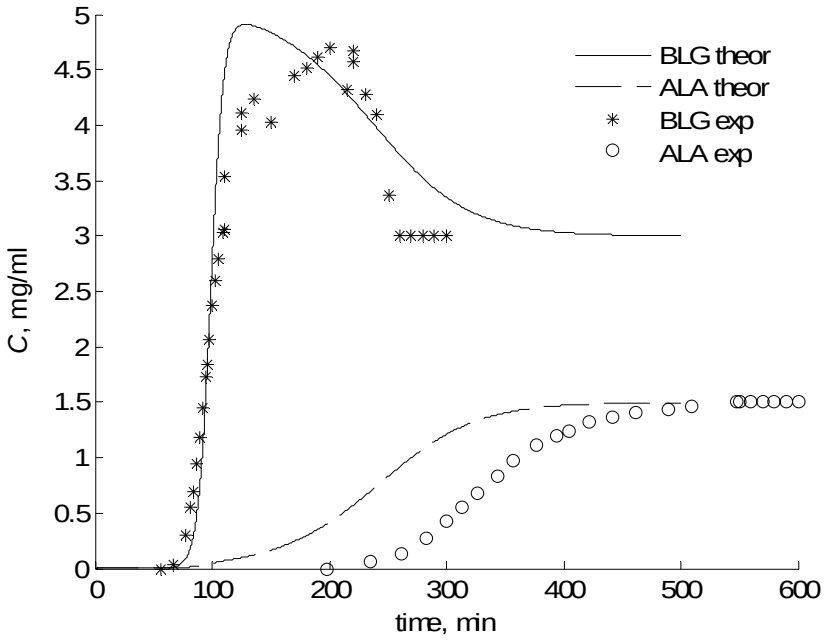

Figure 9.3 Experimental and predicted profiles for the packed-bed adsorption of a mixture of BLG and ALA onto SP Sepharose FF at pH 3.7, flow rate of 2 ml/min and feed concentrations of 3 and 1.5 mg/ml, respectively. The theoretical profiles were predicted after modifying BLG isotherm parameters such that q'_m = 3.5 (q_m) and K'_d = 600 (K_d).

Both the value of $t_{1/2}$ and the maximum value of the overshoot for BLG were well predicted by the simple kinetic model under the modified conditions. This could be understandable in light of the fact that theoretically and from the electrokinetic point of view, the strongly-bound protein BLG (with lower K_d) should displace the weakly-bound ALA, provided that the transport of both proteins is not limited by mass transfer resistances (or the mass transfer rate limitation is the same for both proteins). However in the situation under consideration, ALA was able to displace BLG, in spite of the apparent lower affinity of the former to the adsorbent, as was evidenced from both the packed-bed and also from the two-component, batch CLSM results. The reason for this could be attributed to the difference in transport mechanisms of the two proteins; BLG being governed by a fast electrokinetic transport mechanism, whilst ALA being controlled by a diffusional one. As a result, the transport of ALA was slower, and hence it managed to displace the BLG that had already been adsorbed in the diffuse layer as was explained in

detail in chapter 6 (Section 6.3.2). It is also to be noted that the predicted ALA breakthrough profile (Figure 9.3) was not in agreement with its experimental counterpart and $t_{1/2}$ was underestimated by the model as was encountered with the single-component ALA results. If the q_m for ALA were to be modified as in the single-component system by increasing it 1.5 times, a good fit to the ALA breakthrough curve would be obtained (Figure 9.4). The value of q_m for BLG would, however, need to be slightly modified such that the apparent (modified) q_m (q'_m) is 3.0 times (rather than 3.5 times) higher than the original q_m obtained from batch experiments. In addition, the overshoot was not as accurately described as in Figure 9.3.

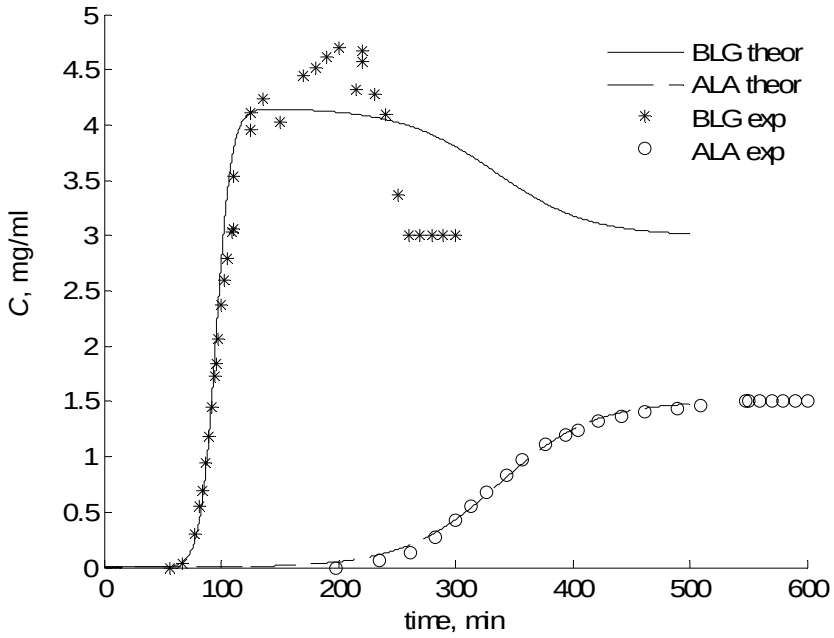

Figure 9.4 Experimental and predicted profiles for the packed-bed adsorption of a mixture of BLG and ALA onto SP Sepharose FF at pH 3.7, flow rate of 2 ml/min and feed concentrations of 3 and 1.5 mg/ml, respectively. The theoretical profiles were predicted after modifying the isotherm parameters such that for BLG: q'_m = 3.0 (q_m) and K'_d = 600 (K_d), and for ALA: q'_m = 1.5 (q_m). Agreement between predicted and experimental results is within accuracy of 10-15%.

9.3.2 Whey concentrate

To simulate the novel whey concentrate separation process developed in Chapter 8, the relevant breakthrough curves of ALA and BLG for stages one and two of the process were predicted by the simple kinetic model using the fore-cited modified equilibrium isotherm parameters for both proteins, as well as the corresponding kinetic rate constants (obtained in section 9.3.1). The theoretical profiles along with their experimental counterparts are depicted in Figure 9.5. For the first stage of the process (Figure 9.5A), as was the case with the pure binary mixture, the BLG overshoot could only be predicted when the value of K_d for BLG was increased 600 times (i.e. was more than 150 times higher than that of ALA), while the value of q_m for the same protein was augmented 3.5 times (i.e. was 2.7 times larger than that of ALA). Unlike the pure binary mixture, the model, under the previously employed conditions, overestimated the value of $t_{1/2}$ for BLG but fairly predicted that of ALA in both stages of the process. The model was also able to predict the maximum overshoot value of BLG.

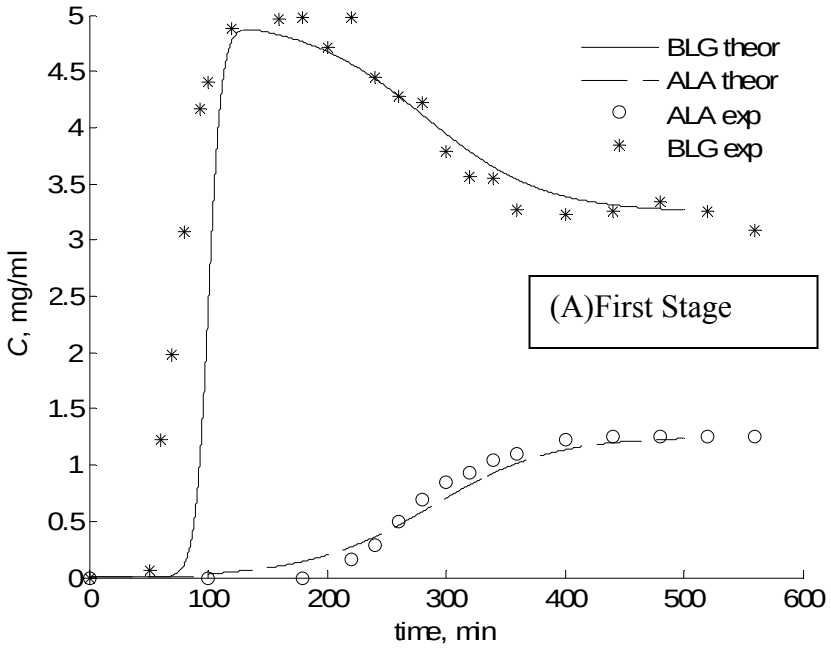

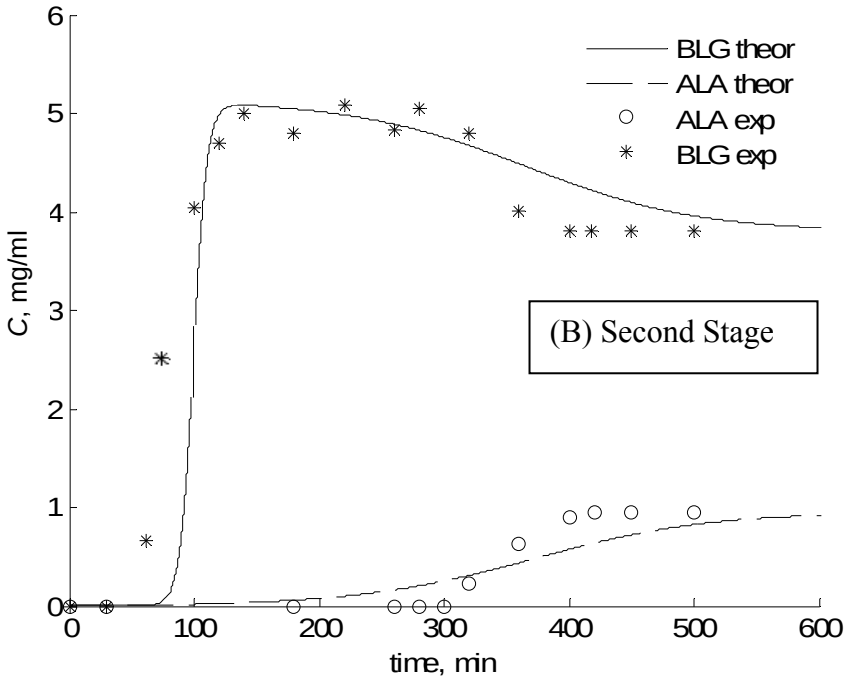

Figure 9.5 Experimental and predicted profiles for the packed-bed adsorption of BLG and ALA during the first (A) and second (B) stages of the whey purification process. The theoretical profiles were predicted after modifying the isotherm parameters such that for BLG: q'_m = 3.5 (q_m) and K'_d = 600 (K_d).

To obtain a better fit for the ALA breakthrough curve in the second stage, k_1 was increased three times from $30*10^{-3}$ $mlmg^{-1}min^{-1}$ to $90*10^{-3}$ $mlmg^{-1}min^{-1}$ (Figure 9.6). Furthermore, a better fit for the early part of the BLG breakthrough curve could be obtained by decreasing the value of either q_m, K_d or k_1 (data not shown). As a result, the value of $t_{1/2}$ was decreased but unfortunately that also decreased the maximum value of the overshoot. Therefore, it was not possible to obtain a good fit for both $t_{1/2}$ and the overshoot maximum value at the same time, as they are interrelated.

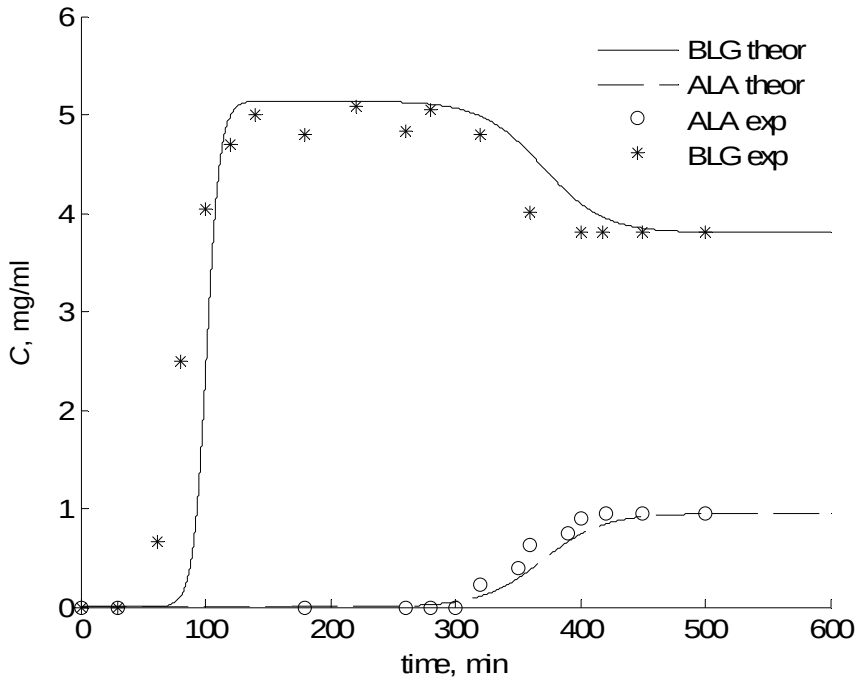

Figure 9.6 Experimental and predicted profiles for the packed-bed adsorption of BLG and ALA during the second stage of the whey purification process. The theoretical breakthrough curve for ALA was predicted using a modified value for k_1 ($90*10^{-3}$ $mlmg^{-1}min^{-1}$). Agreement between predicted and experimental results is within accuracy of 5-10%.

The corrected and the original experimental values of the isotherm parameters and the forward kinetic rate constant for the adsorption of ALA and BLG from single-, two-

component and whey concentrate mixtures are summarised in Table 9.1. The values pertaining to the two individual stages of the whey purification process are also included.

Table 9.1 Original and corrected values of the isotherm parameters and the rate constant for the adsorption of ALA and BLG from single-, two-component and whey concentrate mixtures. The values pertaining to the two stages of the whey purification process are included.

	ALA			BLG		
	K_d	q_m	k_1*10^3	K_d	q_m	k_1*10^3
Original	0.029	147	30	0.008	113.6	35
Corrected (single)	0.029	147*1.5	30	0.008	113.6	55
Corrected (two-component)	0.029	147*1.5	30	0.008*600	113.6*3.0	35
Corrected (whey, 1st stage)	0.029	147	30	0.008*600	113.6*3.5	35
Corrected (whey, 2nd stage)	0.029	147	90	0.008*600	113.6*3.5	35

9.4 Conclusions

The single-component breakthrough curve of pure BLG was well predicted by the simple kinetic model using Langmuir isotherm parameters obtained from batch uptake experiments. This model, however, could only accurately predict the breakthrough of ALA when q_m was increased by a factor of 1.5 which implies the occurrence of additional adsorption processes occurring during adsorption in a packed bed compared to batch uptake. That the two proteins differ in their mechanism of adsorption is reflected in the nature of the correction factor involved, the factor needing correction was associated with k_1 for BLG and with q_m for ALA.

Agreement between experimental and theoretical two-component breakthrough curves for mixtures of pure ALA and BLG could only be obtained using the simple

model after correcting the Langmuir isotherm parameters. K_d for BLG needed to be increased by a factor of 600, while q_m was augmented by a factor of 3.0. In addition, the q_m value for ALA needed to be increased by a factor of 1.5 as was encountered in the single-component systems. It is evident that the enormous factor of 600 is not merely a correcting one but rather an inversion factor because what is needed here is to significantly reverse the relative values of the two dissociation constants. With K_d for ALA greater than that of BLG, it is ALA that should have been displaced according to the simple kinetic model; the opposite was found in practice.

For adsorption of whey concentrate mixtures, the simple kinetic model accurately predicted the individual breakthrough curves for ALA and BLG after correcting the Langmuir isotherm parameters for BLG using the same factors as proved necessary for pure mixtures. The value of q_m for ALA, however, needed no correction.

In summary, the batch experiments did not necessarily produce parameters that could be used to obtain accurate simulations of pure single-component breakthrough curves, let alone multi-component adsorption. Packed-bed experiments with the individual pure proteins did not yield information that would predict what would happen with mixtures of the two proteins. However, work with the mixture of the two pure proteins gave a good expectation of what would happen with whey concentrate.

The results obtained herewith should be beneficial to the theoretician who wants to combine the electrokinetic and diffusion transport mechanisms while taking into account the additional adsorption processes in a model befitting the present case. Until then, the simulation conducted herein might find applicability to situations not far from that adopted here, i.e. when the operating conditions like the flow rate and volume of the column are varied.

10 Overall conclusions and outlook

The present studies on the cation-exchange adsorption of pure ALA and BLG onto SP Sepharose FF, both in single- and two-component systems, elucidated the nature of the adsorption process and yielded information that was later exploited in developing the whey concentrate purification process. These studies included batch, batch uptake and packed-bed experiments to study the equilibrium, kinetics and dynamics of adsorption.

Single-component batch experiments were useful in determining the Langmuir isotherm parameters, q_m and K_d, for ALA and BLG at different pH values. The pK_d versus pH relation proved to be linear for both proteins and its extrapolation to pK_d = 0 gave the pI for each protein. The q_m versus pH relation enabled the determination of the optimum working pH of 3.7, at which the adsorption of both proteins was maximised. At this pH, K_d for ALA (K_d = 0.029 mg/ml) was found to be approximately four times larger than that of BLG (K_d = 0.008 mg/ml) which implies stronger binding for BLG. The value of q_m for ALA (q_m = 147.0 mg/ml), on the other hand, was about 30% higher than that of BLG (q_m = 113.6 mg/ml) which indicates higher accessibility of ALA to adsorption sites probably due to its smaller size.

In single-component traditional batch uptake experiments, the adsorption profiles of ALA and BLG were better described by the simple kinetic model rather than by the pore diffusion model. Therefore, the rate constants for both proteins were determined using the former model and were estimated to be $30*10^{-3}$ $mlmg^{-1}min^{-1}$ and $35*10^{-3}$ $mlmg^{-1}min^{-1}$, respectively. In the two-component system, the individual batch uptake profiles for the two proteins showed no evidence for competitive adsorption. The values of the rate constants for ALA and BLG respectively dropped by 50% and 33% of their corresponding values in the single-component systems. In both single- and two-component systems, it was found that BLG was adsorbed faster than ALA as was judged from the values of the rate constants of both proteins. The value of k_1 for BLG was 17% and 55% higher than that of ALA in single- and two-component systems, respectively.

The confocal laser scanning microscopy (CLSM) experiments were helpful in further understanding the adsorption process, as they permitted direct visualisation of the protein adsorption at the bead level, and hence determining the location of the adsorption

sites for both proteins. In the single-component systems, the different behaviour of ALA and BLG with regard to their penetration within the adsorbent beads suggested that the two proteins have different transport mechanisms governing their adsorption; ALA being characterised by a pore-diffusional transport whereas BLG characterised by an electrokinetically-based secondary transport that is non-diffusive. BLG penetrated fast into the adsorbent beads and gradually filled them in a shell-wise fashion, while adsorption of ALA was mostly confined to the outer shells of the adsorbent, with some ALA molecules penetrating in an uneven manner into the innermost region. The two-component system results showed that ALA was able to displace BLG in spite of the lower affinity of the former protein to the adsorbent. For both single- and two-component systems, CLSM results, *F*-*t* curves, were compared both qualitatively and quantitatively to their counterparts, *q*-*t* curves, obtained in traditional experiments by indirect measurements of the protein concentration in the fluid phase. A novel quantitative approach was undertaken by modifying the simple kinetic rate model traditionally used to determine the kinetic rate constant, k_1, for batch uptake experiments, in order to describe batch uptake kinetics based on CLSM data. The CLSM method successfully reproduced the value of the rate constant for BLG, but failed to do so with ALA probably because the mass transfer properties of the protein were altered as a result of its conjugation to the dye.

Single-component packed-bed experiments using 1-ml columns at a linear velocity of 158 cm/h and initial concentrations of 3 mg/ml for BLG and 1.5 mg/ml for ALA, showed that the breakthrough time value, $t_{1/2}$, for ALA was four times longer than that of BLG, probably due to its lower concentration, as well as its smaller size (half that of BLG) which allows for more accessibility to finer pores. The difference in the breakthrough time values of both proteins suggested the feasibility of using this adsorbent to separate the two proteins when present in a mixture. However, it was not possible to separate ALA from BLG in the two-component system during the adsorption stage using a 1-ml column, perhaps due to insufficient adsorption capacity under the employed chromatography conditions. The behaviour of each of the two proteins in the mixture was very much similar to that when applied to the column as single components. In other

words, there was no clear evidence for a degree of competition between the two proteins with regard to binding to adsorption sites under the employed conditions.

Subsequent two-component packed-bed experiments with 5-ml columns at the above concentrations and a linear velocity of 30 cm/h showed evidence of competitive adsorption. BLG broke through first, and its concentration in the outlet exceeded its feed value by about 1.6 times before declining to the feed value, followed by the breakthrough of ALA. ALA displaced and eluted all the BLG from the column in a pure form. The remaining ALA could be eluted thereafter at high purity and with 91% recovery. The fact that ALA displaced BLG in spite of the lower affinity of the former to the adsorbent supported the CLSM results obtained earlier. This process was optimised with regard to linear velocity as well as adsorption capacity and an optimum linear velocity of 60 cm/h was chosen. Evidence of the competitive nature of adsorption observed in binary mixtures was used to develop a facile separation process for ALA and BLG from whey concentrate.

Adsorption of aqueous solutions of whey concentrate powders was performed using a 5-ml column and at a linear velocity of 60 cm/h. The characteristics of adsorption were studied in light of the results of the pure systems. As was the case with pure binary mixtures, BLG breakthrough occurred first, and its concentration in the outlet exceeded its feed value by about 1.5 fold before declining to the feed value, followed by the breakthrough of ALA. ALA was able to displace and drive BLG off the column and therefore BLG was collected in a pure form. Substantially pure ALA could then be eluted from the column. With whey concentrate mixtures, however, a lower degree of separation was obtained relative to the pure binary mixtures. This was a result of the substantial overlapping that occurred between the individual breakthrough curves of ALA and BLG when adsorbed from whey concentrate. Furthermore, it was found that modifying the operating conditions (total concentration and flow rate) so as to be comparable with those used previously for pure mixtures did not improve the degree of separation. This is probably a result of the complex nature of whey in which there are additional compounds present. Moreover, of the three operating conditions investigated (variation of total concentration, flow rate and ratio of BLG to ALA), the ratio, R, was found to be the key factor dictating the degree of separation achieved; increasing R improved the separation.

However, increasing R requires adding pure BLG to the whey feedstock and this would not be feasible in a large-scale process designed for the economic isolation of whey proteins.

Making use of the strong competitive adsorption between the two proteins, a novel consecutive two-stage separation process was developed to separate ALA and BLG from whey concentrate mixtures. Almost all of the BLG in the feed was recovered, with 78% being recovered at 95% purity in the first stage and a further 20% at 86% purity in the second. In addition, 67% of ALA was recovered; 48% at 54% purity followed by 19% at 60% purity in both the first and second stages. In both stages, the application of feedstock was terminated at the point where BLG reached its inlet concentration (at C/C_f=1). In both stages, two fractions were collected during the loading period; a fraction containing almost pure BLG was collected up to the start of the ALA breakthrough, followed by a second fraction containing both ALA and BLG. This second fraction from the first stage was mixed with whey concentrate solution to form the feedstock for the second stage. In the second stage, the second fraction contained BLG at sufficiently high purity as to require no further processing. At the termination of feedstock application during each stage of operation, the column which then had almost no adsorbed BLG remaining was eluted to obtain substantially purified ALA. The novelty of the process stems from the fact that it is based on selective adsorption of whey proteins rather than selective elution. The latter has been used by many other workers in previous literature. The selective adsorption technique also makes the process simple and viable for separation as mostly all the BLG was recovered during the loading step. ALA, on the other hand, was recovered using simple consecutive elution by varying the pH. No salt addition was required for elution which is an additional economical as well as an environmental merit to the process.

The simple lumped kinetic model was used to simulate the single and two-component breakthrough curves for the adsorption of ALA and BLG onto a 5-ml column and at a linear velocity of 60 cm/h. When compared to equivalent experimental results, the model accurately predicted the single-component BLG adsorption profiles using the Langmuir isotherm parameters, q_m and K_d, obtained in batch experiments. The breakthrough curve for ALA, however, was well predicted only after increasing q_m which

indicates the occurrence of additional adsorption processes in the packed-bed relative to the batch system. An overshoot of the concentration of BLG in the bed exit stream observed experimentally in the two-component system, was only predicted after correcting the two isotherm parameters in order to account for the unexpected finding that the weakly-bound ALA was able to displace the strongly-bound BLG. The correction factors employed for the pure binary mixture were used to simulate the breakthrough curves of the two proteins in experiments conducted with whey concentrate in each of the two stages of the novel consecutive two-stage separation process, and there was agreement between the experimental and theoretical results. These considerations should be helpful in developing a model compatible with the mechanisms of adsorption that were proposed for these two proteins in light of the CLSM and packed-bed results.

Concerning the unexpected result that the more weakly adsorbed protein (ALA) was able to displace the more strongly adsorbed one (BLG), the author proposed the following. The faster BLG was envisaged to be electrokinetically transferred at first and exchanged for the neutralising Na^+ ions. The locus of this adsorption is assumed to be the diffuse part of the electric double layer. In complexation notation, the adsorbed BLG is an outer-sphere complex separated from the surface by at least one layer thick of the solvent. The displacement occurs later when the lagging (diffusing) ALA manages to catch up with the adsorbed BLG whereupon the mass action redistribution must entail expulsion of some of the adsorbed BLG (an exchange of BLG for ALA) in order to maintain electroneutrality. Therefore, the widespread notion that the more-strongly adsorbed (lower K_d) protein would be expected to displace the weaker one needs to be reconsidered. It is only when the mass transfer resistances are not rate-limiting (or the mass transfer rate limitation is the same for both proteins) that we can expect this notion to hold under similar experimental conditions for the two proteins.

Outlook

The logical approach of studying the characteristics of adsorption in pure systems before extending the study to real mixtures can be adopted for other protein systems. In order to study the adsorption in pure systems, the proteins under consideration should be highly soluble in the buffer solution. Therefore in the present study, the adsorption was investigated at pH values below the pIs of both proteins where the two proteins are soluble and act as cations. Alternatively, the anion-exchange adsorption can be studied at a pH value above the pI range between both proteins. It is to be noted that ALA has limited solubility in that pH range. However, an alternative approach can be adopted if the sole purpose of the study is to separate ALA and BLG from whey without studying the pure system. The adsorption can be performed on either a cation- or an anion-exchanger at a pH lying between the pI values of the two proteins. In this case, one protein will be a cation and the other an anion. That protein with a charge opposite to that of the adsorbent will thus be adsorbed, while the other protein having the same charge as that of the adsorbent will therefore be driven off the column. A third approach is to conduct the adsorption at the pI of one of the two proteins. Thus, one protein will have a net zero charge and could hence be easily eluted off the column. Nevertheless, even at its pI, the protein could still bind to the ion-exchanger by virtue of forces other than the electrostatic (coloumbic) ones, such as asymmetrical charge distribution or hydrogen-bonding. However, this should not be discouraging since the extent of such adsorption might not be sizable. Even if it was, this protein will be weakly bound to the adsorbent, relative to the other protein, and thus could be easily separated by elution.

The present work focuses on studying the adsorption of ALA and BLG at the whey conditions. In future work, the physico-chemical properties for ALA and BLG particularly in the binary system can be studied under various conditions of initial concentration and BLG to ALA ratio. As evident from the present study, the BLG to ALA ratio plays a key role in the separation process. Therefore, its effect on the competitive adsorption between the two proteins and hence on their separation can be further investigated.

Using the q_m versus pH and the K_d versus pH relations obtained from batch experiments in delineating the pI of ALA and BLG is a promising method that can be

generalised to other protein systems. To verify the general applicability of this method, batch experiments can be performed under different values of ionic strength and at a larger range of pH values covering the cation- and anion exchange regions of the adsorbent. It is to be realized that the method is based on the electrochemical rather than the electro-kinetic (zeta) potential.

Confocal laser scanning microscopy could be a useful technique in understanding the events underlying the separation and in elucidating the nature of adsorption provided the labelling of the protein does not affect its mass transfer properties. Thus, the effect of dye conjugation on altering the mass transfer properties of the protein needs to be further investigated. This could be done by conducting gradient elution experiments with labelled and unlabelled proteins and comparing their retention factors in order to study the criteria affecting the mass transfer alteration such as size and structure of the protein. This should also facilitate the task of constructing a suitable model for the process.

The novel two-stage process developed for whey concentrate purification on a small lab-scale can be scaled up by increasing the column height first and then gradually increasing the column diameter. The volumetric flow rate and sample load will be increased accordingly. The linear flow rate, sample concentration and ratio of sample to adsorbent will be kept the same. The same type of adsorbent used for the small scale should be suitable for the large scale due to its good flow characteristics. However, different system factors such as less efficient flow distribution, wall effects, and extra column zone spreading that leads to peak broadening and hence less resolution, may affect performance after scale up and will therefore need to be taken into consideration.

An economic assessment of the two-stage process will be required to test its feasibility. The cost of the products is much higher than the cost of the raw material which indicates that the process could have a promising potential. The whey concentrate costs about £ 15 per Kg, while ALA costs about £ $350*10^3$ per Kg and BLG costs about £ $30*10^3$ per Kg. In addition, the cost of SP Sepharose FF is low compared to other commercially available adsorbents, and it is anticipated that the column could be reused for many cycles of operation (however the precise number would have to be determined under process conditions), while the cost of buffers should not be high as they are used in very low concentrations. From the technical point of view, the process provides products

with relatively high yields and purities as compared to the other separation processes cited in literature. Therefore, it is worth a protein manufacturer taking a greater interest in this novel process.

Final remark

The objectives that were set out for investigation as outlined in the Introduction have been fully achieved. It is believed therefore that this dissertation makes a significant contribution to knowledge regarding the isolation of proteins from whey.

11 References

Abd El-Salam, M.H.; El-Shibiny, S.; Buchheim, W., Characteristics and potential uses of the casein macropeptide, *Int. Dairy J.* 6 (1996) 327-341.

Aboudzadeh, M.R.; Jiawen, Z.; Bin, W., Modeling of protein adsorption to DEAE sepharose FF: Comparison of data with model simulation, *Korean Journal of Chemical Engineering* 23(2006) 1, 124-130.

Amersham Biosciences, Ion exchange chromatography, principles and methods (2001).

Amersham Biosciences, Ion exchange chromatography and chromatofocusing (2004).

Arnold, F.H.; Blanch, H.W.; Wilke, C.R., Analysis of affinity separations, *Journal of Chemical Engineering* 30 (1985) B9–B23.

Arve, B.H.; Liapis, A.I., Biospecific adsorption in fixed and periodic countercurrent beds, *Journal of Biotechnology and Bioengineering* 32 (1988) 616–27.

Avcı, A.K.; Camurdan, M.C.; Kutlu, O.U., Quantitative description of protein adsorption by frontal analysis, *Process Biochemistry Journal* 36 (2000) 141-148.

Belter, P.A.; Cussler, E.L.; Hu, W.S., Bioseparations: Downstream processing for biotechnology, Wiley-Interscience (1988).

Beszedits, S.; Netzer, A., Protein recovery from food-processing wastewaters, *Food Technology* 37(1983) 8, 160.

Bohart, G.S.; Adams, E.Q., Some aspects of the behavior of charcoal with respect to chlorine, *Journal of American Chemical Society* 42 (1920) 523.

Bonnerjea, J.; Oh, S.; Hoare, M.; and Dunnil, P., Protein purification-The right step at the right time, *Journal of Biotechnology* 4 (1986) 954.

Bottomley, R.C.; Evans, M.T.A.; Parkinson, C.J., Whey proteins, Harris P., editor. Food Gels. New York: Elsevier (1990) 435.

Bottomley, R.C.; Storer, A.C.; Trayer, I.P., A new method of quantitative affinity chromatography and its application to the study of myosin, *Journal of Biochemistry* 159 (1976) 667-676.

Boushaba, R.; Kaminski, C.F.; Slater, N.K.H., Dual fluorescence confocal imaging of the accessibility and binding of $F(ab')_2$ to an EBA resin with various immobilized antigen densities, *Process Biochemistry* 42 (2007) 812–819.

Brody, E.P., Biological activities of bovine glycomacropeptide, *Br. J. Nutr.* (2000) 84 (Suppl.1) S39–S46.

Bromley, E.H.C.; Krebs, M.R.H.; Donald, A.M, Aggregation across the length scales in beta-lactoglobulin, *Faraday Discussions* 128 (2005) 13–27.

Bruce, L.J.; Chase, H.A., The combined use of in-bed monitoring and an adsorption model to anticipate breakthrough during expanded bed adsorption, *Journal of Chemical Engineering Science* 57 (2002) 3085-3093.

Cabilio, N.R.; Omanovic, S.; Roscoe, S.G., Electrochemical studies of the effect of temperature and pH on the adsorption of alpha-lactalbumin at Pt, *Langmuir* 16 (2000) 22, 8480-8488.

Cano, T.; Offringa, N.; Willson, R.C., Competitive ion-exchange adsorption of proteins: Competitive isotherms with controlled competitor concentration, *Journal of Chromatography A* 1079 (2005) 116-126.

Cano, T.; Offringa, N.; Willson, R.C., The effectiveness of three multi-component binding models in describing the binary competitive equilibrium adsorption of two cytochrome b5 mutants, *Journal of Chromatography A* 1144 (2007) 197-202.

Carrere, H.; Bascoul, A.; Floquet, P.; Wilhelm, A.M.; Delmas, H., Whey proteins extraction by fluidized ion exchange chromatography: simplified modeling and economical optimization, *Chemical Engineering Journal and Biochemical Engineering Journal* 64 (1996) 3, 307-317.

Carta, G.; Ubiera, A.R.; Pabst, T.M., Protein mass transfer kinetics in ion exchange media : Measurements and Interpretations, *Chem. Eng. Technol.* 28 (2005) 1252-1264.

Cayot, P.; Lorient, D., Structure function relationships of whey proteins. Food proteins and their applications, S. Damodaran and A. Paraf (1997) 225-256, Marcel Dekker, New York.

Chaiken, I.; Wilcheck, M.; Parikh, I., Affinity chromatography and biological recognition, Academic Press, New York (1984).

Chaplin, L.C., Hydrophobic interaction fast protein liquid chromatography of milk proteins, *Journal of Chromatography A* 363 (1986) 2, 329-335.

Chase, H.A., Prediction of the performance of preparative affinity chromatography, *Journal of Chromatography* 297 (1984) 179–202.

Chen, W.D.; Dong, X.Y.; Sun, Y., Analysis of diffusion models for protein adsorption to porous anion-exchange adsorbent, *Journal of Chromatography A* 962 (2002) 1-2, 29-40.

Chen, W.D.; Dong, X.Y.; Bai, S.; Sun, Y., Dependence of pore diffusivity of protein on adsorption density in anion-exchange adsorbent, *Biochemical Engineering Journal* 14 (2003) 45.

Chu, L.; Macleod, A.; Ozimek, L., Isolation of glycomacropeptide from sodium caseinate hydrolysate solution by ultrafiltration, *Milchwissenschaft* 51 (1996) 303–306.

Coetzee, J.W.; Petersen, F.W., A simplified resistance model for reversible multicomponent ion exchange, *Hydrometallurgy* 76 (2005) 19-24.

Colby, C.B.; O'Neill, B.K.; Vaugham, F.; Middelberg, A.P., Simulation of Compression effects during scaleup of a commercial ion-exchange process, *Journal of Biotechnology Progress* 12 (1996) 662.

Colowick, S.P.; Kaplan, N.O., In: Methods in Enzymology (Jakoby, W.B., ed.) Academic Press, Inc., Orlando, FL, 104, part C (1984).

Conrado, LS; Veredas, V; Nobrega, ES; Santana, CC, Concentration of α-lactalbumin from cow milk whey through expanded bed adsorption using a hydrophobic resin, *Brazilian Journal of Chemical Engineering*, 22 (2005) 4, 501-509.

Cowan, G.H.; Gosling, I.S.; Sweetenham, W.P., Modelling methods to aid the design and optimization of batch stirred-tank and packed-bed column adsorption and chromatography units, *Journal of Chromatography* 484 (1989) 187-210.

Craig, L.C., J. Biol. Chem., 155 (1944) 519, cited in Guichon, G., and Lin, B., Modeling for preparative chromatography, Academic Press (2003).

Cuatrecasas, P.; Wilcheck, M.; Anfinsen, C.B.; Selective enzyme purification by affinity chromatography, *Proc. Natl. Academic Science* 61 (1968) 636.

Dechow, F., Separation and purification techniques in biotechnology (1989), Noyes publications, Chapter 3.

De Vault, D., The theory of chromatography, *Journal of American Chemical Society* 65 (1943) 4, 532.

de Wit, J.N., Nutritional and functional characteristics of whey proteins in food products, *Journal of Dairy Science* 81 (1998) 597–602.

Doultani, S.; Turhan, K.N.; Etzel, M.R., Fractionation of proteins from whey using cation exchange chromatography, *Process Biochemistry* 39 (2004) 1737-1743.

Dybing, S.T.; Smith, D.E., The ability of phosphates or kappa-carrageenan to coagulate whey proteins and the possible uses of such coagula in cheese manufacture, *Cultured Dairy Production Journal* (1991) 4-12.

Dziennik, S.R.; Belcher, E.B.; Barker, G.A.; DeBergalis, M.J.; Fernandez, S.E.; Lenhoff, A.M., Non diffusive mechanisms enhance protein uptake rates in ion exchange particles, *Proc. Nat. Acad. Sci.* U.S.A. 100 (2003) 420-425.

Dziuba, J.; Minkiewicz, P., Influence of glycosylation on micelle-stabilizing ability and biological properties of C terminal fragment of cow's casein, *Int. Dairy J.* 6 (1996) 1017-1044.

Eigel, W. N.; Butler, J. E.; Ernstrom, C. A.; Farrell, H. M.; Harwalkar, V. R.; Jenness, R.; and Whitney, R. McL., Nomenclature of proteins of cows milk, *Journal of Dairy Science* 67 (1984) 1599.

Etzel, M.R., Isolating beta-lactoglobulin and alpha-lactalbumin by eluting from a cation-exchanger without sodium chloride, US patent 5986063, 1999.

Farrell, H.M.; Bede, M.J.; Enyeart, J.A.; Binding of *p*-nitrophenyl phosphate and other aromatic compounds by β-LG, *Journal of Dairy Science* 70 (1987) 252–258.

Finette, G.M.S.; Mao, Q.M.; Hearn, M.T.W., Examination of protein adsorption in fluidized bed and packed bed columns at different temperatures using frontal chromatographic methods, *Journal of Biotechnology and Bioengineering* 58 (1998) 35–46.

Flashner**,** M.; Ramsden, H.; Crane, L.J., Separation of proteins by high-performance anion-exchange chromatography, *Journal of Analytical Biochemistry* 135 (1983) 2, 340-344.

Fox, P.F., The milk protein system, *Developments in Dairy Chemistry*. In: P.F. Fox, Editor, *Functional Milk Proteins* Vol. 4, Applied Science, London (1989).

Galisteo, F.; Norde W., Adsorption of lysozyme and alpha-lactalbumin on poly(styrenesulphonate) latices 1. Adsorption and Desorption behavior, *Colloids and Surfaces B: Biointerfaces* 4 (1995) 375-387.

Gallant, S.R., Modeling ion-exchange adsorption of proteins in a spherical particle, *Journal of Chromatography A* 1028 (2004) 189-195.

Gambero, A.; Kubota, LT; Gushikem, Y.; Airoldi, C.; Granjeiro, JM; Taga, EM; and Alcantara, E.F.C., Use of chemically-modified silica with β-diketoamine groups for separation of α-lactalbumin from bovine milk whey by affinity chromatography, *Journal of Colloid and Interface Science* 185 (1997) 2, 313-316.

Ganjam, L.S.; Thornton, W.H.; Marshall, R.T.; MacDonald, R.S., Antiproliferative effects of yoghurt fractions obtained by membrane dialysis on cultured mammalian intestinal cells, *Journal of Dairy Science* 80 (1997), 2325–2339.

Garke, G.; Hartmann, R.; Papamichael, N.; Deckwer, W.D.; Anspach, F.B., The influence of protein size on adsorption kinetics and equilibria in ion-exchange chromatography, *Separation Science and Technology* 34 (1999) 2521-2538.

Gerberding, S.J.; Byers, C.H., Preparative ion-exchange chromatography of proteins from dairy whey, *Journal of Chromatography A* 808 (1998) 141-151.

Goodall, S.; Grandison, A.S.; Jauregi, P.J.; Price, J., Selective separation of the major whey proteins using ion exchange membranes, *Journal of Dairy Science* 91 (2008) 1-10.

Graves, D.J.; Wu, Y.T., Methods in Enzymology (Jakoby, W.B., ed.) Academic Press, Inc., Orlando, FL 84 (1974) 150.

Grimes, B.A.; Liapis, A.I., The interplay of diffusional and electrophoretic transport mechanisms of charged solutes in the liquid film surrounding charged non-porous adsorbent particles employed in finite bath adsorption systems, *J. Colloid Interf. Sci.* 248 (2002) 504-520.

Guiochon, G.; Golshan-Shirazi, S.; and Jaulmes, A., Computer simulation of the propagation of a large-concentration band in liquid chromatography, *Journal of Analytical Chemistry* 60 (1988) 1856.

Gurgel, PV; Carbonell, RG; Swaisgood HE., Fractionation of whey proteins with a hexapeptide ligand affinity resin, *Bioseparation* 9 (2000) 385–92.

Hahn, R.; Deinhofer, K; Machold, C; Jungbauer, A, Hydrophobic interaction chromatography of proteins: II. Binding capacity, recovery and mass transfer properties, *Journal of Chromatography B* 790 (2003) 1-2, 99-114.

Hahn, R.P.; Schulz, M.; Schaupp, C.; Jungbauer, A., Bovine whey fractionation based on cation-exchange chromatography, *Journal of Chromatography A* 795 (1998) 277-287.

Harinarayan, C.; Mueller, J.; Ljunglöf, A.; Farhner, R.; Van Alstine, J.; van Reis, R., An exclusion mechanism in ion exchange chromatography, *Journal of Biotechnology and Bioengineering* 95 (2006) 775-787.

Harrison, R.G.; Todd, P.; Rudge, S.R.; Petrides, D.P., *Bioseparations science and engineering*, Oxford University Press (2003).

Hortsmann, B.J.; Chase, H.A., Rate-limiting mass transfer in immunosorbents: Characterisation of the adsorption of paraquat-protein conjugates to anti-paraquat Sepharose 4B, *Bioseparation* (1998) 7, 145-157.

Hubbuch, J.; Linden, T.; Knieps, E.; Thömmes, J.; Kula, M.R., Dynamics of protein uptake within the adsorbent particle during packed bed chromatography, *Journal of Biotechnology and Bioengineering* 80 (2002) 4, 359-368.

Hubbuch, J.; Linden, T.; Knieps, E.; Ljunglöf, A.; Thommes, J.; Kula, M., Mechanism and kinetics of protein transport in chromatographic media studied by confocal laser scanning microscopy, Part I. The interplay of sorbent structure and fluid phase conditions, *Journal of Chromatography A* 1021 (2003) 93-104.

Hubbuch, J.; Linden, T.; Knieps E.; Thommes,, J.; Kula, M., Mechanism and kinetics of protein transport in chromatographic media studied by confocal laser scanning microscopy, Part II. Impact on chromatographic separations, *Journal of Chromatography A* 1021 (2003) 105-115.

Huffman, L.M.; Harper, W.J., Maximizing the value of milk through separation technologies, *Journal of Dairy Science* 82 (1999) 2238–2244.

Jacobson, J.M.; Frenz, J.H.; Horvath, Cs., Measurement of competitive adsorption isotherms by frontal chromatography, ***Ind. Eng. Chem. Res. Des.*** 26 (1987) 43.

James, E.R., The application of multicomponent adsorption theory to an ion exchange chromatography system for recovery of whey proteins, 'Thesis' , University of Queensland, Australia (1994).

Janson, J.; Ryden, L., Protein purification (1998), Wiley-VCH, 2nd edition.

Kawasaki, Y.; Kawakami, H.; Tanimoto, M.; Dosako, S.; Tomizawa, A.; Kotake, M.; Nakajima, I., pH-Dependent molecular weight changes of κ-casein glycomacropeptide and its preparation by ultrafiltration, *Milchwissenschaft* 48 (1993) 191–195.

Kim, Y.; Kuga, S.; Ion-exchange separation of proteins by polyallylamine-grafted cellulose gel, *Journal of Chromatography A* 955 (2002) 191–196.

Kinsella, J.E.; Whitehead, D.M., Proteins in whey: chemical, physical and functional properties. *Adv Food Nut Res* 33 (1989) 343–438.

Konecny P.; Brown, R.J.; Scouten, W.H., Chromatographic purification of immunoglobulin G from bovine milk whey, *Journal of Chromatography A* 673 (1994) 1, 45-53.

Kosikowski, F.V., Whey utilization and whey products, *Journal of Dairy Science* 62 (1979) 1149.

Lan, Q.; Bassi, A.; Zhu, J.X.; Margaritis, A., Continuous protein recovery from whey using liquid-solid circulating fluidized bed ion-exchange extraction, *Journal of Biotechnology and Bioengineering* 78 (2002) 157.

Larson, P.O.; Glad, M.; Hanson, L.; ***et al.***, In: Advances in chromatography, (Giddings, J.C., ed.) Marcel Dekker, New York, 21 (1983).

Levenspiel, O., Chemical reaction engineering, New York, John Wiley and Sons Inc. (1972) 364.

Lewus, R.K.; Carta, G., Binary protein adsorption on gel-composite ion-exchange media, ***AIChE J.*** 45 (1999) 512.

Lewus, R.K.; Carta, G., Protein diffusion in charged polyacrylamide gels- Visualization and analysis, *Journal of Chromatography A* 865 (1999) 155.

Lewus, R.K.; Carta, G., Protein analysis in constrained anionic hydrogels: Diffusion and boundary-layer mass transfer, ***Ind. Eng. Chem. Res.*** 40 (2001) 1548.

Leaver, G., Large scale ion exchange chromatography of animal blood proteins, PhD Thesis**,** University of Wales, Swansea (1984).

Li, E.W.Y.; Mine, Y., Technical Note: Comparison of Chromatographic Profile of Glycomacropeptide from Cheese Whey Isolated Using Different Methods, *Journal of Dairy Science* 87 (2004) 174-177.

Liapis, A.I.; Anspach, B.; Findley, M.E.; Davies, J.; Hearn, M.T.W.; Unger, K.K., Biospecific adsorption of lysozyme onto monoclonal antibody ligand immobilized on nonporous silica particles, *Journal of Biotechnology and Bioengineering* 34 (1989) 467–77.

Liapis, A.I.; Grimes, B.A.; Lacki, K.; Neretnieks, I., Modeling and analysis of the dynamic behavior of mechanisms that result in the development of inner radial humps in the concentration of a single adsorbate in the adsorbed phase of porous adsorbent particles observed in confocal scanning laser microscopy

experiments: diffusional mass transfer and adsorption in the presence of an electrical double layer, *Journal of Chromatography A* 921 (2001) 2, 135.

Lightfoot, E.N., Speeding the design of bioseparations: A heuristic approach to engineering design, *Ind. Eng. Chem. Res.* 38 (1999) 3628-3634.

Linden, T.; Ljunglöf, A.; Hagel, L.; Kula, M.R.; Thommes, J., Visualizing two-component protein diffusion in porous adsorbents by confocal scanning laser microscopy, *Journal of Biotechnology and Bioengineering* 65 (1999) 6, 622-630.

Linden, T.; Ljunglöf, A.; Hagel, L.; Kula, M.R.; Thommes, J., Visualizing patterns of protein uptake to porous media using confocal scanning laser microscopy, *J. Sep. Sci. and Technol.* 37 (2002) 1, 1-32.

Ljunglöf, A., Doctoral thesis, Direct observation of biomolecule adsorption and spatial distribution of functional groups in chromatographic adsorbent particles, Uppsala University (2002) http://www.uu.se/avhandlingar.

Ljunglöf, A.; Hjorth, R.J., Confocal microscopy as a tool for studying protein adsorption to chromatographic matrices, *Journal of Chromatography A* 743 (1996) 75-83.

Ljunglöf, A.; Lacki, K.M.; Mueller, J.; Harinarayan, C.; van Reis, R.; Farhner, R.; Van Alstine, J., Ion exchange chromatography of antibody fragments, *Journal of Biotechnology and Bioengineering* 96 (2006) 515-524.

Ljunglöf, A.; Lacki, K.M.; Mueller, J.; Harinarayan, C.; van Reis, R.; Farhner, R.; Van Alstine, J., Ion-exchange chromatography of antibody fragments, *Journal of Biotechnology and Bioengineering* 96 (2007) 3, 515-524.

Ljunglöf, A.; Thömmes, J., Visualising intra-particle protein transport in porous adsorbents by confocal microscopy, *Journal of Chromatography A* 813 (1998) 387-395.

Lowe, C.R., An introduction to affinity chromatography, Elsevier Biomedical Press, New York (1979).

Lowe, C.R., New developments in downstream processing, *Journal of Biotechnology* 1 (1984) 3-12.

Lozano, J.M.; Giraldo, G.I.; Romero, C.M., An improved method for isolation of β-lactoglobulin, *International Dairy Journal* 18 (2008) 55–63.

Madureira, A.R.; Pereira, C.I.; Gomes, A.M.P.; Pintado, M.E.; Malcata, F.X., Bovine whey proteins-Overview on their main biological properties, *Food Research International* 40 (2007) 10, 1197-1211.

Mao, Q.M.; Johnston, A.; Prince, I.G.; Hearn, M.T.W., High-performance liquid chromatography of amino acids, peptides and proteins, *Journal of Chromatography* 548 (1991) 147–63.

Martin, C.; Iberer, G.; Ubiera, A.; Carta, G., Two-component protein adsorption kinetics in porous ion-exchange media, *Journal of Chromatography A* 1079 (2005) 105-115.

Martin, A.J.P.; James, A.T., Gas-liquid partition chromatography: the separation and micro-estimation of ammonia and the methylamines, *Journal of Biochemistry* 50 (1952) 679.

Martin, A.J.P.; Synge, R.L.M., *Biochemistry Journal*, 35 (1941) 1358, cited in Guichon, G., Review: preparative chromatography, *Journal of Chromatography* 969 (2002) 129.

Mate, J.I.; Krochta, J.M., β-lactoglobulin separation from whey protein isolates on a large scale, *Journal of Food Science* 59 (1994) 1111-1114.

Maubois, J.L.; and Ollivier, G., Extraction of milk proteins. Food Proteins and their Applications, In: S. Damodaran and A.Paraf, (1997) 579-595, Marcel Dekker, New York.

McCreath, G.E.; Owen, R.O.; Nash, D.C.; Chase, H.A., Novel affinity separations based on perfluorocarbon emulsion reactor for continuous affinity separations and its application in the purification of human-serum albumin from blood-plasma, *Journal of Chromatography A* 773 (1997) 73-83.

Melter, L.; Butte, A.; Morbidelli, M., Preparative weak cation-exchange chromatography of monoclonal antibody variants- Single component adsorption, *Journal of Chromatography A* 1200 (2008) 156-165.

Mohan, C., A guide for the preparation and use of buffers in biological systems (2003), MERCK Co.

Morel, F.M.M., Principles of Aquatic Chemistry, John Wiley&Sons, inc., 1983.

Morr, C.V.; Ha, E.Y.W, Off-flavours of whey protein concentrates: A literature review, *International Dairy Journal* 1 (1991) 1.

Morr, C.V.; Ha, E.Y.W, Whey protein concentrates and isolates: processing and functional properties, *Critical Reviews in Food Science and Nutrition* 33 (1993) 431-476.

Morr, C.V.; Seo, A., Fractionation and characterization of glycomacropeptide from caseinate and skim milk hydrolysates, *Journal of Food Science* 53(1988) 80–87.

Nigam, S.C.; Sakoda, A.; Wang, H.Y., Bioproduct recovery from unclarified broths and homogenates using immobilized adsorbents, *Biotechnology Progress* 4 (1988)166.

Nishikawa, A.H., Affinity purification of enzymes, *Journal of Chemical Technology* 5 (1975) 564-571.

Nishikawa, A.H.; Bailon, P.; Ramel, A.H., Quantitative parameters in affinity chromatography, *Adv Expl Med Biol* (1974) 33-42.

Noppe, W; Haezebrouck, P; Hanssens, I; De Cuyper, M., A simplified purification procedure of alpha-lactalbumin from milk using Ca2+ dependent adsorption in hydrophobic expanded bed chromatography, *Bioseparation* 8 (1998) 153–8.

Outinen, M.; Tossavainen, O.; and Syvaoja, E.L., Chromatographic fractionation of alpha lactalbumin and beat lactoglobulin with polystyrenic strongly basic anion exchange resins, *lebensmittel-Wissenschaft und-Technologie* 29 (1996) 4, 340-343.

Owen, R.O.; Chase, H.A., Modeling of the continuous counter-current expanded-bed adsorber for the purification of proteins, *Journal of Chemical Engineering Science* 54 (1999) 3765-3781.

Parikh, I.; Cuatrecasas, P., Affinity chromatography, *Chemical Engineering News* 63 (1985) (34) 17.

Pearce, R.J., Whey protein recovery and whey protein fractionation. In Whey and Lactose Processing, ed.J.G. Zadow, (1992) 271-316, Elsevier Applied Science, New York.

Pedersen, L.; Mollerup, J.; Hansen, E.; Jungbauer, A., Whey Proteins as a model for chromatographic separation of proteins, *Journal of Chromatography B* 790 (2003) 161-173.

Peterson, E.A.; Sobers, H.A., Chromatography of proteins: 1. Cellulose ion exchange adsorbents, *Journal of the American Chemical Society* 78 (1956) 751-755.

Polson, A., Some aspects of diffusion in solution and a definition of a colloidal particle, *Journal of Physical Colloid Chemistry* 54 (1950) 649-652.

Puerta, A.; Jaulmes, A.; De Frutos, M.; Diez-Masa, JC; Vidal-Madjar, C, Adsorption kinetics of beta-lactoglobulin on apolyclonal immunochromatographic support, *Journal of Chromatography A* 953 (2002) 1-2, 17-30.

Russell, S.M.; Belcher, E.B. ; Carta, G., Protein partitioning and transport in supported cationic acrylamide-based hydrogels, *AIChE J.* 49 (2003) 1168-1171.

Russell, S.M.; Carta, G., Multicomponent protein adsorption in supported cationic polyacrylamide hydrogels, *AIChE J.* 51 (2005) 9, 2469-2480.

Ruthven, D.M., Principles of adsorption and adsorption processes, Wiley-Interscience, 1984.

Saito, T.; Yamaji, A.; Itoh, T., New isolation method of GMP from sweet whey, *Journal of Dairy Science* 74 (1991) 2831–2837.

Sawyer, L.; G. Kontopidis, The core lipocalin, bovine beta-lactoglobulin, *Biochim Biophys Acta* 1482 (2000) 136–48.

Scouten, W.H., Affinity Chromatography: Bioselective adsorption on inert matrices, John Wiley&Sons, New York (1981).

Sienkiewicz, T., Nomenclature and some properties of whey proteins, *Nahrung-food* 25 (1981) 4, 329-343.

Skidmore, G.L.; Chase, H.A., Two component protein adsorption to the cation exchanger S Sepharose FF., *Journal of Chromatography* 505 (1990) 329-347.

Skidmore, G.L.; Horstmann, B.J.; Chase, H.A., Modelling single-component protein adsorption to the cation exchanger S Sepharose FF, *Journal of Chromatography* 498 (1990)113–28.

Smithers, G.W.; Ballard, F.J.; Copeland, A.D.; De Silva, K.J.; Dionysius, D.A.; Francis, G.L., Symposium: advances in dairy foods processing and engineering, *Journal of Dairy Science* 79 (1996) 1454-9.

Staby, A.; Sand, M.B.; Hansen, R.G.; Jacobsen, J.H.; Andersen, L.A.; Gerstenberg, M.; Bruus, U.K.; Jensen, I.H., Comparison of chromatographic ion-exchange resins. IV Strong and weak cation-exchange resins and heparin resins, *Journal of Chromatography A* 1069 (2005) 65–77.

Stone, M.C.; Carta, G., Patterns of protein adsorption in chromatographic particles visualized by optical microscopy, *Journal of Chromatography A* 1160 (2007) 206–214.

Strange, E.D.; Malin, E.L.; Van Hekken, D.L.; and Basch, J., Chromatographic and electrophoretic methods used for analysis of milk proteins, *Journal of Chromatography* 624 (1992) 1-2, 81-102.

Swaisgood, H.E.; Huang, X.L.; Catignani, G.L., Characteristics of the products of limited proteolysis of beta-lactoglobulin 650 (1996) 166-177.

Tanford, C., Physical Chemistry of Macromolecules, John Wiley & Sons, inc., 1961.

Teske, C.A.; Schroeder, M.; Simon, R.; Hubbuch, J., Protein labeling-effects in confocal laser scanning microscopy, *J. Phys. Chem. B* 109 (2005) 13811-13817.

Teske, C.A.; von Lieres, E.; Schroder, M.; Ladiwala, A.; Cramer, S.M.; Hubbuch, J., Competitive adsorption of labeled and native protein in confocal laser scanning microscopy, *Journal of Biotechnology and Bioengineering* 95 (2006) 58-66.

Tong, X.D.; Xue, B.; Sun, Y., Modeling of expanded-bed protein adsorption by taking into account the axial particle size distribution, *Biochemical Engineering Journal* 16 (2003) 265-272.

Uhrinova, S.; Smith, M.H.; Jameson, G.B.; Uhrin, D.; Sawyer, L.; Barlow, P.N., Structural changes accompanying ph-induced dissociation of the beta-lactoglobulin dimer, *Journal of Biochemistry* 39 (2000) 3565–74.

Van Deemter, J.J.; Zuiderweg, F.J.; Klinkenberg, A., Longitudinal diffusion and resistance to mass transfer as causes of nonideality in chromatography, *Journal of Chemical Engineering Science* 5 (1956) 271-289.

Velayudhan, A.; Horvath, Cs., Preparative chromatography of proteins-Analysis of the multivalent ion exchange formalism, *Journal of Chromatography* 443 (1988) 13-29.

Vogt, S.; Freitag, R., Comparison of anion-exchange and hydroxyapatite displacement chromatography for the isolation of whey proteins, *Journal of Chromatography A* 760 (1997) 125-137.

Vyas, H.K.; Izco, J.M.; Jimenez-Flores, R, Scale-up of native beta-lactoglobulin affinity separation process, *Journal of Dairy Science* 85 (2002) 7, 1639-1645.

Wahlgren, M.; Arnebrant, T.; Paulson, M., The adsorption from solutions of beta-lactoglobulin mixed with lactoferrin or lysozyme onto silica and methylated silica surfaces, *Journal of Colloid and Interface Science* 158 (1993) 46-53.

Wang, Q.; Swaisgood, H.E., Characteristics of beta-lactoglobulin binding to the all-trans-retinal moiety covalently immobilized on CeliteTM., *Journal of Dairy Science* 76 (1993)1895–901.

Weinbrenner, W.F.; Etzel, M.R., Competitive adsorption of alpha-lactalbumin and bovine serum albumin to sulfopropyl ion exchange membrane, *Journal of Chromatography A* 662 (1994) 414-419.

Weiss, J., J. Chem. Soc. p.297, 1943, cited in Guichon, G. and Lin, B., Modeling for preparative chromatography, Academic Press (2003).

Wicke, E.; Kolloid, Z., 90 (1940) 156, cited in Guichon, G. and Lin, B., Modeling for preparative chromatography, Academic Press (2003).

Wicke, E.; Kolloid, Z., 86 (1939) 295, cited in Guichon, G. and Lin, B., Modeling for preparative chromatography, Academic Press (2003).

Wilson, J.N., A theory of chromatography, *Journal of American Chemical Society* 62 (1940) 6, 1583.

Wong, D.W.S.; Camirand, W.M.; Pavlath, A.E., Structures and functionalities of milk proteins, *Critical Reviews in food science and nutrition* 36 (1996) 807-844.

Xu, Y.; Sleigh, R.; Hourigan, J.; Johnson, R., Separation of bovine immunoglobulin G and glycomacropeptide from dairy whey, *Process Biochemistry* 36 (2000) 5, 393-399.

Ye, Xiuyun; Yoshida, Shigeru; Ng, T. B., Isolation of lactoperoxidase, lactoferrin, α-lactalbumin, β-lactoglobulin B and β-lactoglobulin A from bovine rennet whey using ion exchange chromatography, *International Journal of Biochemistry & Cell Biology* 32 (2000) 11-12, 1143-1150.

Yun, J.; Lin, D.Q.; Yao, S.J., Predictive modeling of protein adsorption along the bed height by taking into account the axial non-uniform liquid dispersion and particle classification in expanded beds, *Journal of Chromatography A* 1095 (2005) 16-26.

Zall, R.R., Trends in whey fractionation and utilization , A global perspective, *Journal of Dairy Science* 67 (1984) 2621-2629.

Zhang, X.; Grimes, B.A.; Wang, J.C.; Lacki, K.M.; Liapis, A.J., Analysis and parametric sensitivity of the behavior of overshoots in the concentration of a charged adsorbate in the adsorbed phase of charged adsorbent particles: practical implications for separations of charged solutes, *J. Colloid Interf. Sci.* 273 (2004a) 22-38.

Zydney, Andrew L., Protein separations using membrane filtration: new opportunities for whey fractionation, *International Dairy Journal* 8 (1998) 243-250.

12 Appendix

% **Solving the simple kinetic-rate constant model for single-component packed-bed adsorption**

```
function [u1,u2,x]=simpmodel
clear;
close all;
% defining input parameters
% height of packed-bed, x in m
x= 0.023;
% forward-rate constant, k1 in mlmg-1min-1
k1=1.7*10^-3;
% maximum adsorption capacity for the resin, qm in mg/ml
qm=120;
% dissociation constant for the ion-exchanger protein interaction, kd in mg/ml
kd=0.019;
% Flowrate in ml/min
F=1;
% diameter of packed-bed in cm
d=1;
% velocity in m/s (=F/area*conversion factor)
v=(F*(4/pi)/d^2)*0.01/60;
% initial bulk concentration, C0 in mg/ml
C0=1;
m = 0;
x = linspace(0,x,50);
%  time in seconds
t = (0:120:24000);
sol = pdepe(m,@pdex4pde,@pdex4ic,@pdex4bc,x,t);
u1 = sol(:,:,1);
u2 = sol(:,:,2);
figure(1);
hold on
plot(t,u1(:,end),'r')
title('Concentration as a function of time');
ylabel('C, mg/ml');
xlabel('Time,sec ');
figure (2);
plot(t,u2(:,end))
title('Amount adsorbed as a function of time');
ylabel('q, mg/ml');
xlabel('Time, sec');
% defining the boundary condition
function [c,f,s] = pdex4pde(x,t,u,dudx)
```

```
c = [1; 1];
f = [0; 0] .* dudx;
y= k1*(u(1)*(qm-u(2))-(kd*u(2)));
s = [-(v)*dudx(1)-y; y];
end
% defining the initial condition
function u0 = pdex4ic(x)
if x==0
   u0= [C0;0];
else
   u0= [0;0];
end
end
function [pl,ql,pr,qr] = pdex4bc(xl,ul,xr,ur,t)
pl = [ul(1)-C0; 0];
ql = [0; 1];
pr = [0; 0];
qr = [1; 1];
end
end
```

% **Solving the simple kinetic-rate constant model for single-component batch uptake adsorption**

```
function dy=beta (t,y)
% defining the initial condition
dy = zeros(2,1);
%v=volume of settled resin, ml
v=1;
%V=volume of solution, ml
V=14;
%Kd= dissociation constant, mgml^-1
Kd=0.008;
%qm=maximum resin capacity, mg/ml
qm=113.6;
%k1= adsorption rate constant,mlmg^-1min^-1
K1=30*10^-3;
% dc/dt=-dq/dt
dy(1) = [-K1*y(1)*(qm-y(2))+K1*Kd*y(2)]*(v/V);
%dq/dt=k1C(qm-q)-k2q
dy(2)= [K1*y(1)*(qm-y(2))-K1*Kd*y(2)];
```

% **Script of the program**

```
close all
clear all
clc
```

```
%t=time, min
t=150
%C0=initial concentration, mg/ml
C0=4
[t,y] = ode45(@beta,[0 t],[C0 0]);
figure(1)
plot (t, y(:,1),'b')
hold
figure(2)
plot (t, y(:,2),'k')
% Experimental results
t=[0
0.183
0.55
0.75
1.033
1.383
1.783
3
3.583
4.533
5.533
7.5
12.15
15.933
18.033
24.467
32.367
40.567]
C= [4
3.91
3.61
3.37
3.126
2.788
2.509
2.3
1.77
1.44
1.3
1
0.626
0.372
0.146
0.059
0.048
```

```
0.064]
figure(1)
plot(t,C,'*')
```

% **Solving the simple kinetic-rate constant model for two-component packed-bed adsorption**

Read Input data file

```
function outputs = read_input_data()
%Contains problem set up statements

%Flag for testing numerical dispersion/diffusion - when 0 it turns off any absorption
test_flag=1;

%%Flow data
% outputs.flow = 4.3e-4;        %Metres per second
F=2;
% diameter of packed-bed in cm
d=1.6;
% velocity in m/s (=F/area*conversion factor)
outputs.flow = (F*(4/pi)/d^2)*0.01/60;
outputs.length = 2.5e-2;     %Metres
outputs.node_number = 300;    %number

%Vector of inputs

outputs.C0(1) =3.0;
outputs.C0(2)=1.5;          %mg/ml


%Vector of binding constants

outputs.qm (1) = 113.6*3.0;   %mg/ml
outputs.qm (2) = 147*1.5;

%Vector of kds

outputs.kd (1) = 0.008*600;  %mg/ml
outputs.kd (2) = 0.029;

%Vector rate constants btw binder and material in solution

outputs.k1 (1) = test_flag*35e-3/60;   %ml . mg^-1 . s^-1
outputs.k1 (2) = test_flag*30e-3/60;
```

```
outputs.max_steptime = 5;     %seconds
outputs.solver_time = 20000;  %seconds
outputs.mu = 1/6;     %Upwinding parameter

% area = pi()*outputs.d^2*0.25;
% outputs.flow = ((outputs.vol_flow*1e-6)/60)/area;

outputs.display_step_size = 10;

end
```

ODE statement file

```
function dC=ode_statements(t,c)


%The ODE statements


%Initialise global variables
global M C b time_steps k1 kd qm v dx old_q new_q sim_nodes mu qsum;


num_comps=max(size(kd));
new_q=0;


%Let's have a go at a competitive binding scenario where kd1 is a function
%of c2



%Calculate the value of q based on delta t between now and previously. If
%yet_to_ityerate is 1 then iteration not started!
%Determine whether time_steps is empty or not
ts_not_initialised=length(time_steps);


if t==0
   %This is the first iteration
```

```
    %DEBUG DEBUG DEBUG
        q=c.*0;
    %q=linspace(1,10,10)';
    %DEBUG DEBUG DEBUG

    new_q=q;
    %Added
    %old_q=q;
else
    %Work out last time step
    %Care needed at the front end since time_steps will still be empty at
    %the first *proper* iteration.

    if ts_not_initialised==1 && t>0
        time_steps=[0 t];
        old_q=c.*0;
        dt=t;
    else
        dt=t-time_steps(1,end);
    end
%Loop through all components
    for j=1:num_comps
        %Work out current, updated vector of q - simple forward time step
        %new_q=old_q(:,end).*(1-k1*dt.*c-k1*dt*kd)+k1*qm*dt.*c;
        %Loop to add up individual old q components but first extract the q
        %and c for the component j in the outer loop
        current_start=(j-1)*sim_nodes+1;
        current_stop=sim_nodes*j;
        current_q=old_q(current_start:current_stop,end);
        current_c=c(current_start:current_stop,1);
```

```
      additive_term=0;
          for i=1:num_comps
        start_node=(i-1)*sim_nodes+1;
        stop_node=sim_nodes*i;

        %Perform addition
        additive_term=additive_term+old_q(start_node:stop_node,end)./qm(i);
      end
      sum_term=k1(j)*qm(j).*current_c.*additive_term;

      %       if length(time_steps)<2
      new_q(current_start:current_stop,1)=dt*(-
k1(j)*kd(j).*current_q+k1(j)*qm(j).*current_c-sum_term)+current_q;

      %Now, BC states that first value of new_q is always zero
      new_q(current_start,1)=0;

      %       else
  %                                                  new_q(current_start:current_stop,1)=((-
k1(j)*kd(j).*current_q+k1(j)*qm(j).*current_c-sum_term)-
eta.*old_q(current_start:current_stop,end-1)+lambda.*current_q)./(lambda-eta);
      %       end


   end
end
%Now we have a new vector 'q' for the current timestep.

%Populate sparse matrix and BC vector. Start from 2 to deal with boundary
%condition at l=0 where C=C0
for j=1:num_comps
```

```
%Removing end BC - sim_nodes-1 --> sim_nodes-0
for i=2:(sim_nodes-0)

        %Define current index in matrix and vectors and the current q
    %subvector
    index=(j-1)*sim_nodes+i;
    start_q=(j-1)*sim_nodes+1;
    stop_q=sim_nodes*j;

    %Extract current q and c (for flux correction of current time step)
    current_q=new_q(start_q:stop_q,1);
    current_c=c(start_q:stop_q,1);
%Extract additive term for q at point i for all components
    q_sum=0;
    for k=1:num_comps
       start_temp_q=(k-1)*sim_nodes+1;
       stop_temp_q=sim_nodes*k;
       current_temp_q=new_q(start_temp_q:stop_temp_q,1);
       q_sum=q_sum+current_temp_q(i)/qm(k);
    end

    %Interrogate value of q_sum for sanity check
%       disp('Q sum is currently:');
%       disp(num2str(q_sum));

    %Put into global for viewing later
    %qsum=[qsum q_sum];

    %If this is wrong STOP!
    if q_sum>1 || q_sum<0
       break
```

```
end

%van Leer giving difficulties. Trying generalised 4-point, upwind
%biased scheme instead. This applies between nodes 3 and
%sim_nodes-1

%Evalulate all constants
alpha=(-v/dx)*(0.5-mu);
beta=-3*mu*v/dx;
gamma=(-v/dx)*(-0.5-3*mu);
delta=(-v/dx)*mu;

%Populate main matrix M as per pg 214 of Chu et al.
if i>=3 && i<sim_nodes
   %Populate matrix for general case
   M(index,index+1)=alpha;
   M(index,index)=beta-k1(j)*qm(j)+k1(j)*qm(j)*q_sum;
   M(index,index-1)=gamma;
   M(index,index-2)=delta;

elseif i==2
   %For sim_node 2 - do normal upwinding
   %M(index,index+1)=alpha;
   M(index,index)=-(v/dx)-k1(j)*qm(j)+k1(j)*qm(j)*q_sum;
   M(index,index-1)=(v/dx);

%      elseif i==1
%          %For sim_node 1
%          M(index,index+1)=alpha;
%          M(index,index)=beta-k1(j)*qm(j)+k1(j)*qm(j)*q_sum;
```

```
        elseif i==sim_nodes
            %For last node also do normal upwinding
            M(index,index)=-(v/dx)-k1(j)*qm(j)+k1(j)*qm(j)*q_sum;
            M(index,index-1)=v/dx;
                end
              %Populate BC vector
        b(index,1)=k1(j)*kd(j)*current_q(i);
    end
%Define linear relationship for ode solver to solve
dC=M*c+b;
end
```

Pde solution file

```
function output=pde_solution(input_data)
clear global M C b time_steps k1 kd qm v dx old_q sim_nodes
global M C b time_steps k1 kd qm v dx old_q sim_nodes mu qsum ;

time_steps=0;

%Unpack required data to start with
sim_nodes=input_data.node_number;
length=input_data.length;
C0=input_data.C0;
kd=input_data.kd;
qm=input_data.qm;
k1=input_data.k1;
solution_time=input_data.solver_time;
v=input_data.flow;
mu=input_data.mu;
max_step_time=input_data.max_steptime;
```

```
%Work out node spacing
dx=length/(sim_nodes-1);

%Interrogate number of components
num_comp=max(size(kd));

%Work out total number of nodes in each vector and matrix as number of
%components*number of nodes required
nodes=num_comp*sim_nodes;

%Prepare blank concentraion vector and sparse matrix
C=zeros(nodes,1);
%C=ones(nodes,1)*1e-1;
M=spalloc(nodes,nodes,2*nodes);
b=zeros(nodes,1);

%Populate Jacobian pattern to ease ode15s' job a bit
jac_patt=M;
for i=3:nodes-1
   jac_patt(i,i+1)=1;
   jac_patt(i,i)=1;
   jac_patt(i,i-1)=1;
   jac_patt(i,i-2)=1;
end
jac_patt(1,1)=1;
jac_patt(1,2)=1;
jac_patt(2,1)=1;
jac_patt(2,2)=1;
jac_patt(2,3)=1;
jac_patt(nodes,nodes)=1;
```

```
jac_patt(nodes,nodes-1)=1;
jac_patt(nodes,nodes-2)=1;

%Turn off divide by zero errors
%s=warning('off','MATLAB:divideByZero')

options=odeset('OutputFcn',@query_solver,'JPattern',jac_patt,'MaxStep',max_step_time);

%Define time span vector
time_span=[0 solution_time];
%Populate initial conditions
initial_conds=zeros(nodes,1);
%initial_conds=ones(nodes,1)*1e-1;
for i=1:num_comp
   initial_conds((sim_nodes*(i-1))+1,1)=C0(i);
end
%Call our ODE solver
[T C]=ode15s(@ode_statements,time_span,initial_conds,options);
output.concs=C;
output.time=T;
output.q=old_q;

end
```

Query solver file

```
function status=query_solver(t,y,flag)

global time_steps old_q new_q

%Put current version of q and time into the old q for next iteration
old_q=[old_q new_q];

%First time around, time_steps is the time span which screws things up.
```

```
%This has length 2, so examine and correct
 if length(t)==2
    %time_steps=t(1);
    %Don't damn well touch it!!!
 else
   time_steps=[time_steps t];
 end
status=0;

disp(num2str(t));

%Return status value

end
```

Main program file

```
%*****************************************
%Solve concentration profile for adsorption in a column
%
%
%*****************************************

clear;
clc;


%Read in initialisation data
input_data=read_input_data();

%Solve PDE
pde_solution=pde_solution(input_data);

%Display results
display_results(pde_solution, input_data);
```

Display results file

```
function display_results(results, input_data)

step=input_data.display_step_size;
time_size=length(results.time);
q=results.q';
num_comps=max(size(input_data.kd));
sim_nodes=input_data.node_number;
```

```
%Plot the final breakthrough curve
for i=1:num_comps
   break_through(:,i)=results.concs(:,(i*sim_nodes));
end
figure;
plot(results.time*2.5/60,break_through/3);

hold

% experimental results
tB = [55.787
67.307
77.547
82.027
83.947
86.507
89.067
91.627
94.187
95.467
97.387
100.587
103.147
105.707
109.547
110.187
110.5
125.5
125.5
135.5
150.5
170.5
180.5
190.5
200.5
220.5
220.5
215.5
230.5
240.5
250.5
260.5
270
280
290
```

```
300]
CB=[0
0.012
0.099
0.183
0.233
0.314
0.395
0.485
0.575
0.615
0.687
0.793
0.866
0.933
1.011
1.021
1.181
1.321
1.37
1.411
1.344
1.481
1.507
1.537
1.564
1.557
1.524
1.441
1.427
1.367
1.124
1
1
1
1
1]
plot (tB, CB*3, '*')

tA = [197.867
234.987
261.867
282.347
299.627
313.067
326.507
```

```
343.787
357.227
377.067
394.347
404.587
421.227
441.707
462.187
489.067
509.547
547.307
550
560
570
580
590
600
610]
CA= [0
0.041938688
0.084486705
0.185036124
0.285677711
0.371080969
0.457326533
0.560210858
0.647867095
0.7376483
0.797687624
0.824073078
0.880507637
0.91469403
0.938488558
0.959541109
0.978233153
1
1
1
1
1
1
1
1]
plot (tA, CA*1.5, 'o')

end
```